Quarterly Reviews of Biophysics **31**, 1 (1998), pp. 41–106. Printed in the United Kingdom

^{13}C-NMR, MS and metabolic flux balancing in biotechnology research

THOMAS SZYPERSKI

Institut für Molekularbiologie und Biophysik, Eidgenössische Technische Hochschule Hönggerberg, CH-8093 Zürich, Switzerland

Dedicated to my wife Susanne

Abbreviations: ATP, adenosine 5′-triphosphate; BIRD, bilinear rotational decoupling; BDF, biosynthetically-directed fractional; CoA, coenzyme A; COSY, correlation spectroscopy; CP, cross polarization; ct, constant-time; DCP, double CP; DEPT, distorsionless enhancement by polarization transfer; DOSY, diffusion-ordered spectroscopy; DQ, double-quantum; GC, gas chromatography; HMBC, heteronuclear multiple bond correlation; HMQC, heteronuclear multiple-quantum correlation; HSQC, heteronuclear single-quantum correlation; IE, isotope enrichment; INADEQUATE, incredible natural abundance double-quantum experiment; INEPT, insensitive nuclei enhanced by polarization transfer; IRMS, isotope ratio mass spectrometry; isotopomer, isotope isomer; $^{n}J_{XY}$, *n*-bond scalar coupling between nuclei X and Y; MAS, magic angle spinning; MCA, metabolic control analysis; MID, mass isotopomer distribution; MFB, metabolic flux balancing; MS, mass spectrometry; NAD(P)H, nicotinamide adenine dinucleotide (phosphate); NMR, nuclear magnetic resonance; PFG, pulsed-field gradient; PPP, pentose phosphate pathway; REDOR, rotational echo double resonance; SQ, single-quantum; TCA, tricarboxylic acid; TOCSY, total correlation spectroscopy; TQ, triple-quantum; [U-^{13}C], uniformly ^{13}C-labelled. Abbreviations for additional metabolites are given in the legend of Fig. 9.

1. INTRODUCTION

The European Federation of Biotechnology defines biotechnology as 'the integration of natural sciences and engineering sciences in order to achieve the application of organisms, cells, parts thereof and molecular analogues for products and services'. Biotechnology thus focuses on the industrial exploitation of biological systems and is based on their unique expertise in specific molecular recognition and catalysis. The enormous potential for drug synthesis, design of biomedical diagnostics, large-scale production of biochemicals including fuels, food production, degradation of resistant wastes and extraction of raw materials will very likely make biotechnology, along with electronics and material sciences, one of the key technologies of the 21st century. From the chemical engineer's point of view, the living system participating in a biotechnological process is the central unit that catalyses chemical reactions. It exhibits a complex dependence on the bioprocess parameters, and the engineer focuses on these parameters to achieve optimal control (Hamer, 1985; Bailey & Ollis, 1986). For the natural scientist, the living system itself is in the centre of interest, so that attempts to optimize a bioprocess aim at its appropriate redesign by genetic manipulations. The increase in penicillin production by strain improvement based on random mutagenesis, which was pursued from 1940 to the mid 1970s, represents an early contribution of life scientists to improve a bioprocess that is of utmost medical importance (Hardy & Oliver, 1985).

Nowadays, recombinant DNA technology offers a large arsenal of approaches for the rational redesign of an organism's genome. However, even when the environmental conditions are well defined, we are far from understanding how the genomic programme determines the living organism (Palsson, 1997; Strohman, 1997). Although future complete knowledge of a genome's DNA sequence (Fodor, 1997; Rowen *et al*. 1997) will engender further understanding of this process, it will clearly not suffice to unravel all principles governing the most complex phenomenon of life. Hence, the phenotype resulting from a rationally modified genotype will remain, at best, difficult to predict. This holds, in particular, when cellular metabolism, i.e. the molecular machine that produces, converts or degrades chemical compounds in a biotechnological process, becomes the target for redesign.

Taking stock of our current understanding of cellular metabolism, we recognize a decreasing completeness of knowledge when considering, (i) the structure of the metabolic networks, (ii) the three-dimensional structure (Hendrickson & Wüthrich, 1991–7) and dynamics (e.g. Bennett & Huber, 1983) of biological macromolecules involved in metabolism, (iii) the mechanisms of enzymatic reactions (Fersht, 1985; Warshel, 1997) and transport processes (Krämer, 1996),

(iv) the *in vivo* thermodynamics (Jones, 1979; Mavrovouniotis, 1990; Pissarra & Nielsen, 1997) and kinetics (Liao & Lightfoot, 1988) of biochemical reactions, (v) the efficiency of cellular adenosine 5′-triphosphate (ATP) production by chemiosmotic processes (Nicholls & Ferguson, 1992) and (vi) the control and regulation of metabolism. The metabolic networks, which are defined by the chemical nature of the metabolites, the stoichiometry for their interconversion and the biochemical pathways, are well known for many organisms of biotechnological interest. In fact, the central carbon metabolism of eucaryotes and eubacteria represents settled text-book knowledge (e.g. Gottschalk, 1986; Stryer, 1994), and many experimental techniques are available to unravel as yet unknown pathways efficiently. In contrast, *in vivo* control and regulation of metabolic networks appears to be a largely unexplored field for experimental research. This is due both to our deficiencies in the empirical description of the living systems alluded to in points (ii)–(v) and to relatively recent, far-reaching conceptual advances.

One of the early paradigms of metabolic regulation, i.e. the central role of a few rate limiting reaction steps being catalysed by allosteric enzymes, that provided a basis for attempts to manipulate cellular metabolism during several decades (Fell, 1997), has recently been challenged by the new view of 'multisite modulation' (Fell, 1992; Fell & Thomas, 1995). This view has been fostered by the results obtained from metabolic control analysis (MCA) (Kacser & Burns, 1973; 1979; Heinrich & Rappoport, 1974) and biochemical systems theory (Savageau, 1969, 1970), which are two mathematically related approaches (Savageau *et al*. 1987). Accordingly, the regulation of biochemical reaction rates, designated 'metabolic fluxes', is usually distributed throughout the enzymes of the network so that more than a single enzyme exerts significant control for a given pathway, and the balanced distribution of regulation over several enzymes may well shift with a change in metabolic state (Quant, 1993; Fell & Thomas, 1995). Moreover, a formal description of a bioreaction network using differential equations predicts a complex non-linear, possibly chaotic behaviour that may manifest itself in the form of spatial and temporal periodic patterns of metabolite concentrations, for example in energy metabolism (Sel'kov, 1979; Reich & Sel'kov, 1981) or in cell-free glycolysis *in vitro* (Hess, 1997). The action of a metabolic network thus appears as a non-linear dissipative process of holistic nature. Consequently, regulation can hardly be tackled appropriately by a purely reductionistic approach, i.e. a thorough analysis of the network components alone does not suffice to guide successfully rational network redesign. Instead, this must primarily be accomplished at the system's level, which, in view of the large number of unknowns, requires powerful analytical methods to assess experimentally the network response to manipulations in a non-invasive manner.

The rational redesign of cellular metabolism in order to optimize living systems for biotechnological applications has been coined 'metabolic engineering' (Bailey, 1991; Lessard, 1996). Such modification of the bioreaction network aims at a redirection of carbon and energy fluxes to achieve increased production, conversion or degradation of biotechnological target compounds (Stephanopoulos & Vallino, 1991; Cameron & Tong, 1993). These objectives are often closely

related to those of 'biochemical engineering' which comprises efforts to manipulate cells for medical and pharmaceutical research (Zabriskie, 1996). Clearly, metabolic engineering depends on the elucidation of the bioreaction network to direct the introduction of a specific genetic manipulation. This may include (i) a thorough compilation of available experimental data about the network components, (ii) the identification of 'critical nodes' (Stephanopoulos & Sinskey, 1993) in the network, i.e. those branching points at which flux partitioning will have a major effect on product yield, and the determination of their rigidity, i.e. their inherent resistance to changes in metabolic flux, (iii) an estimation of *in vivo* fluxes, i.e. the characterization of a cell's metabolic state for a defined set of environmental parameters, and (iv) a theoretical description of the network considering, for example, MCA (e.g. Hatzimanikatis & Bailey, 1996, 1997; Westerhoff & Kell, 1996). Obviously, methods for unravelling the structure of metabolic networks and for determining *in vivo* fluxes play an important role for metabolic engineering. The fluxes represent a final, balanced manifestation of all components of the living system that influence metabolism, and they are, in conjunction with the metabolite pool sizes, key observables that link the experimental knowledge about the network components and the theoretical description. Moreover, assessment of the fluxes under varying experimental conditions supports the identification of critical nodes and their rigidity. This may in turn suggest a focus for network redesign, for example, by introducing biochemical bypasses, or by amplifying or deregulating important enzymes (e.g. Eggeling *et al.* 1997; Hatzimanikatis *et al.* 1998).

Radioactive (e.g. DiStefano, 1980; Wolfe, 1992) and stable isotope labelling experiments (e.g. London, 1988; Cerdan & Seelig, 1990; Gadian, 1995) have a long tradition in non-invasive exploration of biosynthetic pathways and have been used to derive either biochemical reaction rate constants, or ratios of fluxes through pathways diverging from a common node. Among the vast number of labelling protocols using stable isotopes (e.g. ^{2}H, ^{13}C, ^{15}N, ^{17}O, ^{19}F, ^{31}P; see Lundberg *et al.* 1990), those based on ^{13}C have a predominant role in metabolic research, since they provide the core information about the organic chemistry of life. In contrast to ^{14}C tracer labelling experiments, site-specific information can be obtained without chemical degradation of metabolites by recording ^{13}C nuclear magnetic resonance (NMR) or mass spectra. ^{13}C-labelling experiments also offer the unique possibility to monitor the formation and breakage of covalent bonds within the bioreaction network *via* observation of ^{13}C–^{13}C spin–spin scalar or dipolar couplings in NMR spectra. An alternative, currently widely used method for estimating *in vivo* fluxes is metabolic flux balancing, which combines the stoichiometry of the reactions constituting the bioreaction network, measurement of uptake and secretion rates, biosynthetic requirements for biomass production and quasi steady-state mass balances on metabolic intermediates (e.g. Holms, 1986; Vallino & Stephanopoulos, 1990; Varma & Palsson, 1994; for a review discussing other approaches to estimate fluxes, see Eggeling *et al.* 1996). This article primarily considers ^{13}C-labelling protocols that are of interest for biotechnological research and can potentially be applied in conjunction with flux

balancing (e.g. Marx *et al.* 1996; Szyperski *et al.* 1996*a*; Sauer *et al.* 1997). In particular, the vast number of radioactive tracer experiments and studies performed with stable isotopes other than ^{13}C will not be discussed. Moreover, recently published review articles and monographs will be referenced throughout to accomplish an appropriately tuned balance between conciseness and comprehensiveness.

2. ANALYSIS OF ^{13}C-LABELLED METABOLITES

The introduction of ^{13}C-labelled molecules into a bioreaction network yields non-randomly ^{13}C-labelled metabolites. The determination of atom specific enrichments and the elucidation of the relative abundances of isotope isomers (isotopomers) in a metabolite's pool are at the heart of all metabolic studies. Currently, two experimental approaches are available to achieve this goal: NMR spectroscopy and mass spectrometry (MS). The merits of both approaches are discussed in this chapter, and a survey of applications is provided in the following chapters.

2.1 *NMR spectroscopy*

2.1.1 *NMR assignment of metabolites*

Employment of ^{13}C-NMR spectroscopy for metabolic studies requires the knowledge of both the covalent structure of the metabolites and the corresponding unambiguous ^{13}C (and often also ^{1}H) resonance assignments. NMR spectroscopy is an extraordinarily powerful tool to unravel the covalent structures of organic molecules, and is routinely used in conjunction with other spectroscopic techniques for that purpose (e.g. Hull, 1987; Hesse *et al.* 1995). Hence, the desired resonance assignments are often obtained when the metabolite's configuration is determined. The assignment may thus be decoupled from the actual metabolic study, i.e. it can be performed with a sample whose ^{13}C enrichment differs from that encountered for the biosynthetically labelled metabolite. In particular, the assignment may be accomplished at natural ^{13}C isotope abundance. Moreover, biosynthetically labelled metabolites are quite generally represented by an ensemble of different ^{13}C isotopomers for which the ^{13}C isotope abundance at a given atom position may in principle vary between 1·1 % (natural abundance) and 100 %. Hence, NMR techniques designed for both ^{13}C-labelled and non-enriched molecules, i.e. molecules labelled with ^{13}C at natural isotope abundance, are of interest and are surveyed. Since ample literature is available (e.g. Ernst *et al.* 1987; Homans, 1989), recent developments promising to have impact for future metabolic studies are emphasized.

2.1.1.1 *Carbon–proton correlation NMR spectroscopy*

Among the large number of heteronuclear NMR schemes, two-dimensional (2D) [^{13}C,^{1}H]-correlation spectroscopy ([^{13}C,^{1}H]-COSY) tailored to link carbon chemical shifts with the resonances of directly attached protons *via* large one-bond scalar couplings ($\sim$ 100–200 Hz), $^{1}\mathcal{J}_{CH}$, represents the most straightforward

https://doi.org/10.1017/S0033583598003412 Published online by Cambridge University Press

approach to connect ^{1}H and ^{13}C resonance assignments (for a compilation of $^{1}\mathcal{J}_{CH}$ values see Hansen, 1981). Provided that the ^{1}H chemical shift dispersion is sufficient, ^{1}H assignments can then be unambiguously transferred to ^{13}C (e.g. Mendz *et al*. 1997). Such mapping of the ^{1}H onto the ^{13}C chemical shifts recruits homonuclear ^{1}H resonance assignment techniques (e.g. Kessler *et al*. 1988) to derive the desired ^{13}C assignments. Since ^{1}H-NMR spectroscopy is the most sensitive, this is an attractive approach for smaller non-enriched metabolites, that may be complemented by $^{13}CH_n$ multiplicity edited spectroscopy (e.g. Ernst *et al*. 1987; Parella *et al*. 1997), for example using maximum-quantum [^{1}H, ^{1}H]-COSY (e.g. Liu *et al*. 1995). 2D [^{13}C,^{1}H]-COSY which is based on both, ^{1}H excitation and detection, offers the highest sensitivity among the various possible schemes and should be employed whenever possible. Neglecting relaxation, such spectroscopy is theoretically eight times more sensitive than 2D [^{13}C,^{1}H]-COSY schemes using ^{1}H excitation and ^{13}C detection. Considering that frequency labelling in an indirect dimension decreases the signal-to-noise ratio by $\sqrt{2}$, such 2D [^{13}C,^{1}H]-COSY is about five times more sensitive than one-dimensional (1D) ^{13}C-NMR experiments performed with insensitive nuclei enhanced by polarization transfer (INEPT) or distorsionless enhancement by polarization transfer (DEPT), or nuclear Overhauser enhancement for small molecules (Ernst *et al*. 1987). Potential advantages that may arise in special cases from ^{13}C detection have been outlined by Gemmecker & Kessler (1995). 2D ^{1}H detected [^{13}C,^{1}H]-COSY can be implemented in two fundamentally different ways. In the heteronuclear single-quantum coherence (HSQC) version (Bodenhausen & Ruben, 1980), ^{1}H magnetization is transferred into ^{13}C single-quantum (SQ) coherence, which evolves in the indirect dimension, t_1, and is subsequently transferred back to ^{1}H. In the heteronuclear multiple-quantum coherence (HMQC) version (Müller, 1979), proton–carbon two-spin coherence is generated which evolves according to the carbon chemical shift during t_1, before ^{1}H SQ coherence is regenerated for detection. To achieve optimal sensitivity, the magnetization transfer delays, τ, must be tuned to $\frac{1}{2}{}^{1}\mathcal{J}_{CH}$ in 2D [^{13}C,^{1}H]-COSY (Ernst *et al*. 1987). Consequently, for molecules exhibiting a large range of different $^{1}\mathcal{J}_{CH}$ values (Hansen, 1981) one must choose a compromise value for τ. In these cases, the $\mathcal{J}$-compensated 2D [^{13}C,^{1}H]-COSY offers significant signal enhancement for CH-groups (Torres *et al*. 1993). When recording [^{13}C,^{1}H]-correlation spectra to accomplish resonance assignments, the HSQC and HMQC approaches perform similiarly well, and the HMQC experiment may be extended to three-dimensional (3D) maximum-quantum HMQC to provide CH_n multiplicity editing (Liu *et al*. 1997). However, most important for applications in metabolic studies, ^{1}H–^{1}H scalar couplings are manifested as in-phase splittings in the indirect ^{13}C dimension in HMQC, but not in HSQC spectroscopy. Hence, only the latter experiment ensures unperturbed observation of ^{13}C–^{13}C scalar coupling ($\mathcal{J}_{CC}$) fine structures, which serve to determine relative ^{13}C isotopomer abundances. If the $\mathcal{J}_{CC}$ values are too small to be resolved, the $\mathcal{J}$-scaled 2D [^{13}C,^{1}H]-HSQC experiment becomes attractive (Willker *et al*. 1997). However, in its published implementation, this experiment is prone to artifacts arising from partial decoupling of $\mathcal{J}_{CC}$. This occurs when the chemical shift evolution of scalar-

coupled ^{13}C spins are refocused during $\mathcal{J}$-evolution, which are not both completely inverted by the refocusing 180° pulse (M. Hochuli, T. Szyperski & K. Wüthrich, unpublished results). When assigning a metabolite, it may actually be desirable to decouple completely the one-bond ^{13}C–^{13}C scalar coupling ($^1\mathcal{J}_{CC}$) interactions to enhance spectral resolution. This can be accomplished in constant-time (ct) 2D [^{13}C,^1H]-HSQC spectroscopy, where the ct-delay is set to one or several ^{13}C–^{13}C scalar coupling dephasing/rephasing cycles of duration $1/^1\mathcal{J}_{CC}$ (Santoro & King, 1992; Vuister & Bax; 1992). It is a key feature of this experiment that cross peaks arising from isotopomers with an odd number of passive $^1\mathcal{J}_{CC}$ couplings and those with none or an even number of carbon coupling partners have opposite sign provided that the ct-delay equals an odd multiple of $1/^1\mathcal{J}_{CC}$. This may lead to mutual cancellation of signals arising from different isotopomers (see fig. 2 in Hiroaki *et al*. 1996), so that setting of the ct-delay to even multiples of $1/^1\mathcal{J}_{CC}$ is recommended when spectra are recorded with biosynthetically ^{13}C-labelled metabolites (Szyperski *et al*. 1997). It is also important to note that one has to compromise on the ct-delay if the $^1\mathcal{J}_{CC}$ values (Horak *et al*. 1985; Krivdin & Kalabin, 1989) in the molecule of interest cover a larger range. This leads to signal attenuation for atoms with carbon–carbon couplings deviating significantly from the $^1\mathcal{J}_{CC}$ value used to calculate the duration of the ct-delay.

In order to resolve spectral overlap or to detect quarternary carbons, one may record an HMQC experiment for which the magnetization transfer delay τ is tuned to a long-range scalar coupling $^n\mathcal{J}_{CH}$ ($n > 1$). This scheme has been dubbed heteronuclear multiple bond correlation (HMBC) experiment (Bax & Summers, 1986), and a version using selective pulses has recently been published (Bax *et al*. 1996). Since $^1\mathcal{J}_{CH} \gg {}^n\mathcal{J}_{CH}$, one-bond correlations can effectively be suppressed by introduction of a low pass $\mathcal{J}$-filter (Kogler *et al*. 1983), i.e. one or several 90° carbon pulses are applied at multiples of $\frac{1}{2}\,{}^1\mathcal{J}_{CH}$ after the first 90 ° proton pulse. A major caveat of the HMBC experiment is that ^1H–^1H scalar coupling evolution during the heteronuclear magnetization transfer prevents the possibility of obtaining pure phases in the indirect carbon dimension. However, this can be accomplished in long-range HSQC experiments (Mattila *et al*. 1995; Bax *et al*. 1996), or in a DEPT-based 2D scheme (Hoffman *et al*. 1993) which includes suppression of one-bond correlations but relies on ^{13}C detection. When working with a spectrometer not equipped with a pulsed field gradient accessory, it is of practical interest that long-range HSQC experiments yield high-quality spectra with spin-lock purge pulses only (Otting & Wüthrich, 1988; Mattila *et al*. 1995).

2D ^1H-total correlation spectroscopy (TOCSY) relayed [^{13}C,^1H]-COSY represents a valuable addition for the correlation of ^{13}C chemical shifts with the chemical shifts of non-attached protons *via* ^1H–^1H scalar couplings, i.e. such spectroscopy may provide the information of HMBC except for quaternary carbons. HSQC (Otting & Wüthrich, 1988) and HMQC (Lerner & Bax, 1986) based schemes have been devised, which can be employed for both, ^{13}C-enriched and non-enriched molecules. For the assignment of ^{13}C enriched samples, 2D ^1H-TOCSY relayed ct-[^{13}C,^1H]-HMQC (Zerbe *et al*. 1996) is attractive, since this experiment ensures decoupling of the ^{13}C–^{13}C scalar coupling interaction in the indirect carbon dimension while the ^1H–^1H TOCSY relay is concomitantly

https://doi.org/10.1017/S0033583598003412 Published online by Cambridge University Press

enhanced at shorter mixing times by generation of ^{1}H–^{1}H anti-phase magnetization during the ct-delay. This becomes important when limited sensitivity requires the reduction of magnetization losses during the TOCSY relay. For the determination of the absolute configuration of a chiral metabolite, the measurement of scalar couplings constants is often required. The arsenal of approaches that is currently available has been reviewed by Eberstadt *et al.* (1995), and recent promising developments for ^{13}C-enriched molecules include ^{13}C-resolved in-phase [^{1}H,^{1}H]-COSY (Grzesiek *et al.* 1995; Szyperski *et al.* 1998*a*) and spin-state selective excitation combined with exclusive COSY type techniques (Meissner *et al.* 1997*a*).

Heteronuclear NMR spectroscopy has greatly profited from the development of the pulsed-field gradient (PFG) technology during the last years (Keeler *et al.* 1994; Kay, 1995). This holds, in particular, for [^{13}C,^{1}H]-COSY performed with lowly ^{13}C enriched samples, where the suppression of the large, unwanted signals from ^{12}C bound protons is of paramount importance to obtain spectra free of artifacts, e.g. t_1-noise that arises from imperfect cancellation in phase cycling schemes (Ernst *et al.* 1987). Conventionally, this goal has been achieved by the application of bilinear rotation decoupling (BIRD) pulse clusters (Garbow *et al.* 1982), which have recently also been incorporated in double PFG spin echoes (Mackin & Shaka, 1996). This promises a significant improvement over the original BIRD approach, and appears to be relatively easy to implement. BIRD may also be replaced by PFGs which are used to reject (Bax & Pochapsky, 1992; Wider & Wüthrich, 1993) or to select (e.g. Hurd & John, 1991) coherence transfer pathways. A formalism supporting the design of optimized PFG sequences for pathway selection has recently been developed (Mitschang *et al.* 1995). In conjunction with spin-lock purge pulses (Otting & Wüthrich, 1988), pathway rejection by PFGs usually warrants recording of high-quality 2D [$^{13}C^{1}H$]-COSY spectra at low ^{13}C enrichment with a minimal phase cycle. The small number of phase cycling steps facilitates collection of spectra with a high resolution in the indirect dimension, which is required to make good use of the quite generally favourable carbon chemical shift dispersion. Even better suppression of ^{12}C-bound proton and solvent proton signals can often be achieved by coherence transfer pathway selection. Unfortunately, depending on the actual implementation of the experiment, the sensitivity is then reduced at least by a factor $\sqrt{2}$ (Ross *et al.* 1993). For heteroatoms bound to a single proton, i.e. methine groups, this signal loss may be recovered by combining the pathway selection by PFGs with a sensitivity enhancement scheme (Palmer *et al.* 1991). In fact, this approach (Kay *et al.* 1992) yields equal sensitivity with and without pathway selection for CH-groups (Gavin *et al.* 1996). However, such schemes cannot be used to increase simultaneously the sensitivity for CH, CH2 and CH3 groups (Schleucher *et al.* 1994).

2.1.1.2 *Carbon–carbon correlation NMR spectroscopy*

Carbon–carbon COSY makes use of ^{13}C–^{13}C scalar couplings for magnetization transfer in order to establish connectivities within the carbon skeleton of a

molecule. 2D ^{13}C–^{13}C double-quantum (DQ) COSY, coined the incredible natural abundance DQ experiment (INADEQUATE) (Bax *et al.* 1980), which is based on the use of $^{1}\mathcal{J}_{CC}$, represents one of the most valuable approaches for this purpose. However, when performed at natural ^{13}C isotope abundance (1·1 %), INADEQUATE exhibits limited sensitivity since only about 1 out of 10000 molecules carries the necessary ^{13}C-^{13}C connectivity at a given position. Fortunately, carbon detected INADEQUATE can be performed relatively 'artifact-free' because singly ^{13}C-labelled species are efficiently suppressed by double-quantum filtration, while ^{12}C–^{1}H moieties are not excited. Recent improvements aiming at the sensitivity enhancement of the classical experiment include the use of compensated delays and pulses (Torres *et al.* 1992), consideration of symmetry criteria (Nakazawa *et al.* 1996) and isotopic shifts (Lambert & Buddrus, 1993), and the inclusion of the sensitivity enhancement scheme (Nielsen *et al.* 1995) alluded to in chapter 2.1.1.1 (Palmer *et al.* 1991; Kay *et al.* 1992). For ^{13}C-labelled metabolites, 2D ^{13}C-^{13}C triple-quantum (TQ) COSY has been proposed to observe selectively fully labelled $^{13}C3$ fragments (Beale *et al.* 1987). Although this experiment is of conceptual interest for assigning ^{13}C resonances, it is not feasible for non-enriched molecules for which only about 1 out of 10^6 molecules possesses the required $^{13}C3$ fragment. To further relax the sensitivity limitations of INADEQUATE, a variety of versions using both, excitation and detection of ^{1}H-magnetization have been developed. The detection takes place at the initially excited ^{1}H, so that these schemes belong to the family of 'out-and-back' experiments (Edison *et al.* 1994). Here, the major challenge is the suppression of signals from ^{12}C–H by a factor of more than about 10000 in order to detect properly the protons that are bound to the ^{13}C–^{13}C fragments. In fact, the first 2D ^{13}C–^{13}C TQ and DQ COSY experiments with excitation and detection of ^{1}H-magnetization have been employed for ^{13}C-enriched samples, where the suppression of ^{12}C–H magnetization is not critical (Pratum & Moore, 1993). The suppression requires the application of PFGs for coherence transfer pathway selection, as exemplified in ^{1}H-detected 2D INEPT-INADEQUATE (Weigelt & Otting, 1995*a*) and closely related ^{13}C-relayed 2D [^{13}C, ^{1}H]-HSQC (Weigelt & Otting, 1995*b*). ^{1}H-detected 2D ^{13}C–^{13}C DQ HSQC/HMBC experiments based on $^{1}\mathcal{J}_{CH}$ or $^{n}\mathcal{J}_{CH}$ couplings for INEPT, and $^{1}\mathcal{J}_{CC}$ or $^{n}\mathcal{J}_{CC}$ couplings for ^{13}C–^{13}C DQ generation have been devised by Reif *et al.* (1996). The schemes of Weigelt & Otting (1995*a*) and Reif *et al.* (1996) have subsequently been critically reviewed and extended with DEPT-type experiments by Meissner *et al.* (1997*b*). Recently, a ^{1}H-detected 2D $\mathcal{J}$-resolved INEPT–INADEQUATE that provides $^{1}\mathcal{J}_{CC}$ values in the indirect dimension was published by Zangger & Sterk (1996), and the 2D ^{1}H-detected INEPT–INADEQUATE of Kozinski & Nanz (1996), which uses separate DQ- and $\mathcal{J}$-evolution periods, promises to provide smaller, conformation-dependent $^{n}\mathcal{J}_{CC}$ couplings (Krivdin & Della, 1991). A general disadvantage of ^{1}H detected INADEQUATE stems from the reduced dispersion of proton when compared to carbon chemical shifts, i.e. it may well be that the ^{1}H-detected experiment does not provide the same yield of connectivities due to spectral overlap. Basically, two approaches have been

developed to circumvent this problem. Firstly, a 3D ^{1}H detected ^{13}C,^{13}C correlation experiment comprising both, an indirect ^{13}C SQ and an indirect ^{13}C DQ dimension (Chung *et al.* 1993; Gosser *et al.* 1993) may be recorded, of which an optimized version has recently been published (Saito & Rinaldi, 1996). Secondly, it is possible to combine 2D ^{1}H-detected INADEQUATE with 2D [^{13}C, ^{1}H]-COSY by sophisticated data processing, so that a 2D spectrum with a ^{13}C SQ and a ^{13}C DQ dimension is generated (Pratum, 1995). While the 3D experiment is feasible only for ^{13}C-enriched molecules, the latter approach promises to be of value for metabolites studied at natural ^{13}C abundance (Pratum, 1996).

Instead of using ^{13}C DQ chemical shift evolution, it is possible to select for ^{13}C–^{13}C connectivities by DQ-filtration (Ernst *et al.* 1987). 2D DQ-filtered [^{13}C,^{13}C]-COSY has been implemented to identify $^{13}C_2$ and $^{13}C_3$ fragments in biosynthetically labelled metabolites (Jones & Sanders, 1989). This experiment also allows determination of the relative abundance of groups of isotopomers by analysis of in-phase splittings from passive ^{13}C–^{13}C scalar couplings, which are manifested in the anti-phase COSY cross peaks. However, the same information can be obtained from analysis of the ^{13}C–^{13}C scalar coupling fine structure in ^{1}H-detected 2D [^{13}C–^{1}H]-HSQC (Szyperski *et al.* 1992; Szyperski, 1995) which exhibits much higher sensitivity. Moreover, the anti-phase cross peak pattern is prone to effects arising from mutual cancellation of the multiplet components, since active and passive couplings are often comparably large. However, 2D DQ-filtered [^{13}C,^{13}C]-COSY is the preferred choice for special applications, i.e. when ^{1}H chemical shift degeneracy limits the use of 2D [^{13}C–^{1}H]-HSQC, for example in polysaccharides (Jones & Sanders, 1989), or when connectivities between two quaternary carbons must be assessed.

With ^{1}H-detection, in-phase [^{13}C,^{13}C]-COSY can be implemented. For the assignment of ^{13}C-enriched metabolites, ^{1}H-detected [^{13}C,^{13}C]-COSY ('HCCH-COSY') (Kay *et al.* 1990) and ^{1}H-detected [^{13}C,^{13}C]-TOCSY ('HCCH-TOCSY') (Bax *et al.* 1990), which are most popular for the resonance assignment of ^{13}C-labelled biological macromolecules (Cavanagh *et al.* 1996), represent attractive experiments. In contrast to ^{1}H-detected 'out-and-back' INADEQUATE, these are 'out-and-stay' experiments (Edison *et al.* 1994) in which the magnetization is excited and detected on two different protons, i.e. it is excited on one proton, transferred (i) by INEPT to its attached carbon, (ii) by [^{13}C,^{13}C]-COSY/TOCSY to another carbon, and (iii) by INEPT to the attached proton on which detection takes place. Depending on the nuclei that are chosen for frequency-labelling, various 2D and 3D experiments are possible, e.g. 2D (H)C(C)H-COSY/TOCSY provides ^{13}C-relayed ^{13}C,^{1}H correlation information, and 3D HC(C)H-or 3D (H)CCH-type experiments offer dispersion in an additional indirect proton or carbon dimension. A major drawback of this class of 'out-and-stay' experiments for metabolic studies is that only connectivities with two proton-bound carbons are detectable. Moreover, although the 3D spectra are attractive in view of the good carbon chemical shift dispersion, it is hardly possible to perform these experiments with two highly resolved indirect dimensions within a reasonable

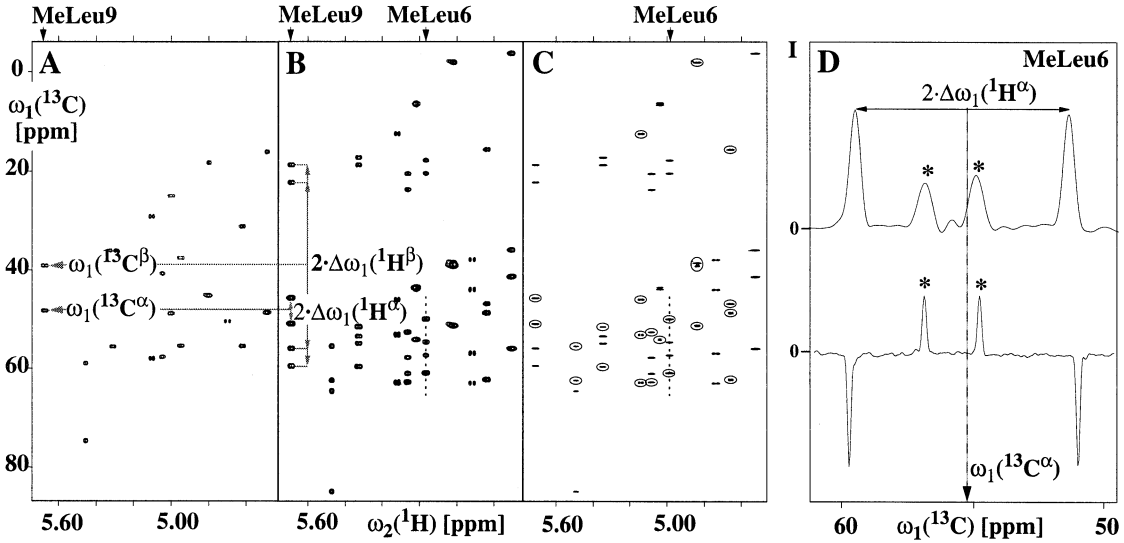

Fig. 1. Reduced dimensionality 2D ct-HC(C)H-COSY spectra recorded with acquisition of central peaks (Szyperski *et al.* 1996*b*) for uniformly ^{13}C-labelled Cyclosporin A. The regions containing the signals detected on the α-protons are shown ($T = 23$ °C; concentration: 10 mM; ^{1}H resonance frequency: 600 MHz; measurement time: 23 min for A and B with ct-delay = $t_{1,max}(^{13}C/^{1}H) = 6{\cdot}6$ ms; and 110 min for C with ct-delay = $t_{1,max}(^{13}C/^{1}H) = 33$ ms; solvent: 100% $CDCl_3$). (A) Subspectrum showing the central peaks. For *N*-methyl-leucine 9 (denoted MeLeu 9) the $^{13}C^{\alpha}$ and $^{13}C^{\beta}$-peaks are individually identified. (B) Subspectrum containing the doublets corresponding to the peaks in (A). The peak positions are at $\omega_1(^{13}C^{\alpha}) \pm \Delta\omega_1$ ($^{1}H^{\alpha}$) and $\omega_1(^{13}C^{\beta}) \pm \Delta\omega_1(^{1}H^{\beta})$, and the in-phase splittings (indicated by arrows) measured on the ^{13}C chemical shift scale in ppm, $2.\Delta\omega_1(^{1}H)$, are equal to $2.\delta\omega(^{1}H){\cdot}[\gamma(^{1}H)/\gamma(^{13}C)]$, where $\delta\omega(^{1}H)$ denotes the chemical difference in ppm with respect to the ^{1}H carrier position and γ(X)-the gyromagnetic ratio of nucleus X. (C) Same as (B), but with a five times longer ct-delay ensuring high resolution (negative peaks are enclosed in circles). (D) Cross sections taken along the broken vertical lines from the two subspectra shown in (B) and (C) at the $^{1}H^{\alpha}$ chemical shift of *N*-methyl-leucine 6 (denoted MeLeu6). The peaks marked with an asterisk correspond to one component each of the two doublets arising from the non-degenerate β protons of MeLeu6. Adapted with permission from Szyperski *et al.* (1997).

measurement time. The reduced-dimensionality approach offers a solution for both problems (Szyperski *et al.* 1997). This approach was introduced with two-spin coherence spectroscopy (Szyperski *et al.* 1993*a*) yielding peak doublets encoding n chemical shifts in a $n-1$ dimensional spectrum. It has subsequently been generalized to arbitrary heteronuclear pulse schemes (Szyperski *et al.* 1993*b*), and was extended by the simultaneous acquisition of central peaks located at the centre of the doublets resulting from projection (Szyperski *et al.* 1996*b*). Firstly, a projected n dimensional spectrum can be acquired with the resolution of an $n-1$ dimensional spectrum (see appendix in Szyperski *et al.* 1998*b*), e.g. 2D ct-HC(C)H-COSY (Szyperski *et al.* 1997) (Fig. 1) can be acquired with about the resolution of 2D ct-(H)C(C)H-COSY (Yu *et al.* 1993). Secondly, quaternary carbons bound to a CH_n moiety are accessible by the observation of central peaks derived from ^{13}C steady-state magnetization, which is suppressed as axial peak magnetization in conventional spectra (Ernst *et al.* 1987).

2.1.1.3 *Diffusion-ordered NMR spectroscopy*

Diffusion-ordered spectroscopy (DOSY) aims at the separation of NMR signals according to the diffusion coefficients, D_i, of the corresponding molecular species i (Morris & Johnson, 1992). In a stimulated echo PFG NMR experiment, the attenuation of the echo amplitude is proportional to $\exp(-D_iK^2)$ where K represents the gradient strength, i.e. gradient duration times gradient amplitude. Recording a series of NMR spectra with increasing K yields a spectrum in which the signals are dispersed by diffusion constants in one dimension (Fig. 2). Along this dimension, the signals exhibit gaussian shapes, and the line widths represent the standard errors obtained from data analysis, e.g. performed by approximate inverse Laplace transformation. Unfortunately, such multiexponential analysis is an ill-conditioned problem (Clayden & Hesler, 1992). Hence, even at a very high signal-to-noise ratio, only diffusion coefficients differing by a factor 2 or more can be resolved (Morris *et al.* 1994), or polydisperse samples with a broad distribution of diffusion coefficients can be analysed (Chen *et al.* 1995). However, much better accuracy can be achieved when a single exponential function can be fitted to the experimental data, so that a single diffusion coefficient is ascribed to every line (Fig. 2). In this case, lines from species with diffusion coefficients differing by less than 20% could be well separated (Barjat *et al.* 1995; Wu *et al.* 1996*a*, *b*). Consequently, 3D DO-[^{1}H,^{1}H]-COSY (Wu *et al.* 1996*b*), 3D DO-[^{1}H,^{1}H]-TOCSY (Jerschow & Müller, 1996) and 2D DO-^{13}C-NMR spectroscopy (Barjat *et al.* 1995) have been implemented to avoid any overlap in the chemical shift dimensions. In the same spirit, several methodological improvements, e.g. the incorporation of longitudinal eddy current delays (Gibbs & Johnson, 1991) and bipolar gradient pulses to reduce effects from eddy-currents (Wider *et al.* 1994; Wu *et al.* 1995), the development of a stop-and-go spinner system that allows for a start of sample spinning during the longitudinal eddy current delay (e.g. Morris *et al.* 1994) and the design of convection compensated pulse schemes (Jerschow & Müller, 1997) aimed at the improvement at the spectral resolution. In spite of its relatively low sensitivity, DOSY promises to be a valuable approach to determine

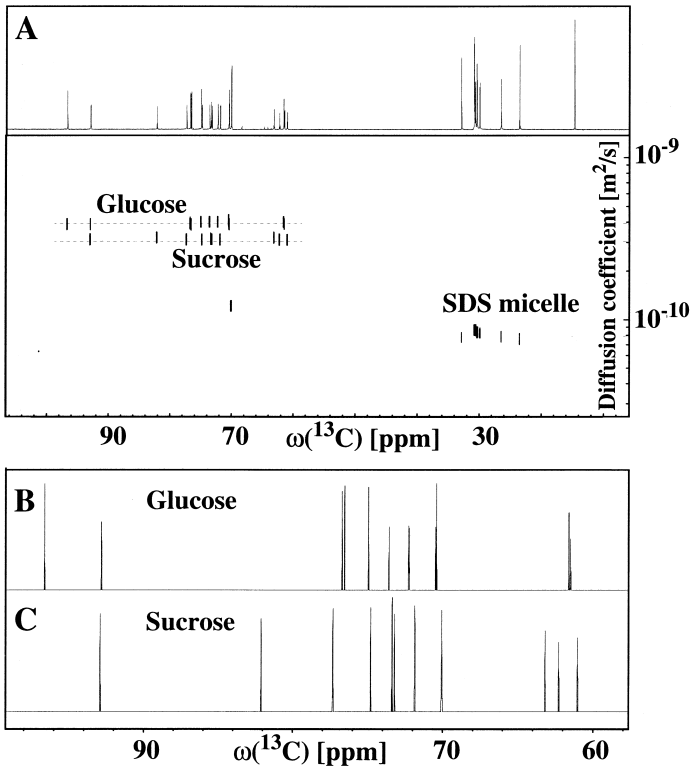

Fig. 2. 2D DO-^{13}C-NMR spectrum recorded with INEPT enhancement for a mixture containing non-enriched glucose, sucrose and sodium dodecyl sulphate (SDS) micelles ($T = 27$ °C; concentration of each component: 500 mM; ^{1}H resonance frequency: 250 MHz; measurement time: 50 hours; solvent: D_2O) (A) Contour plot with the 1D ^{13}C-NMR spectrum shown at the top. The diffusion coefficients are: $3{\cdot}60 \times 10^{-10}$ m^2 s^{-1} (glucose), $2{\cdot}92 \times 10^{-10}$ m^2 s^{-1} (sucrose), 7.78×10^{-11} m^2 s^{-1} (SDS micelles). (B) and (C) show 1D ^{13}C-NMR spectra extracted along the broken horizontal lines from the 2D DO-^{13}C-NMR spectrum of the mixture shown in (A). Adapted with permission from Wu *et al.* (1996*a*).

diffusion coefficients, to separate the NMR signals of mixtures and to investigate intermolecular interactions (e.g. Gozansky & Gorenstein, 1996). In view of future metabolic studies it is of interest that DOSY can be performed with complex physiological mixtures, for example, Barjat *et al.* (1995) have successfully studied a perchloric acid extract of gerbil brain.

2.1.1.4 *Solid-state NMR spectroscopy*

NMR spectroscopy performed with magic angle spinning (MAS) in order to average out dipolar interactions allows the recording of high resolution spectra of solids (Stejskal & Memory, 1994). The techniques required for high-resolution NMR of biological solids (McDowell & Schaefer, 1996) have been rapidly improved over the last years. While only a few of these newer techniques have as yet been employed for metabolic studies, their use will very likely increase in the next few years. The direct detection of ^{13}C spins is usually enhanced with cross-polarization (CP) MAS ^{13}C-NMR spectroscopy (Schaefer & Stejskal, 1976), and

https://doi.org/10.1017/S0033583598003412 Published online by Cambridge University Press

$\mathcal{J}_{CH}$ scalar interactions are suppressed by high-power proton decoupling (Stejskal & Memory, 1994) during ^{13}C detection. Such spectroscopy enjoyed numerous applications with both natural ^{13}C abundance and enriched samples (e.g. Evans *et al*. 1986; Jacob *et al*. 1987). Notably, one of the first applications aimed at the measurement of the abundance of poly(β-hydroxybutyrate), a bacterial storage polymer of high biotechnological interest (Sasikala & Ramana, 1995; Valentin & Dennis, 1997), in lyophilized Pseudomonas cells (Jacob *et al*. 1986). Making use of two consecutive CP transfer steps, this approach can be extended for the detection of dipolar coupled heteronuclei, e.g. ^{13}C–^{15}N spin pairs, to double CP (DCP) MAS ^{13}C-NMR (Schaefer *et al*. 1979), which, however, is relatively insensitive. Moreover, DCP/CP MAS ^{13}C-NMR spectra recorded for ^{13}C-enriched samples usually require the recording of a control experiment with non-enriched samples in order to subtract the background from the natural ^{13}C abundance signals. The detection of dipolar coupled spin pairs is nowadays preferably achieved with recoupling experiments in which rotor-synchronized radio-frequency pulses operating exclusively on the spin coordinates partly compensate for MAS, e.g. rotational echo double resonance (REDOR) (Gullion & Schaefer, 1989*a*, *b*) for heteronuclear spin interactions, and dipolar recovery at the magic angle NMR spectroscopy (DRAMA) (Tycko & Dabbagh, 1990) for homonuclear spin interactions. In particular, REDOR NMR spectroscopy offers better sensitivity than DCP MAS ^{13}C-NMR spectroscopy.

While the resonance assignment in the solid state has traditionally been achieved by through space dipolar correlations (e.g. Fujiwara *et al*. 1995; Sun *et al*. 1997), Baldus & Meier (1996) have recently implemented the first solid state NMR experiment, dubbed total through-bond correlation spectroscopy (TOBSY), relying exclusively on scalar couplings for magnetization transfer. This promises to engender the development of experimental protocols based on $\mathcal{J}$-correlations for the assignment of solid state NMR spectra in the next years. In fact, Lesage *et al*. (1997) have very recently presented the solid-state version of the 2D INADEQUATE experiment, which performed well for natural ^{13}C abundance compounds, and they also reported the successful use of DQ-filtered [^{13}C,^{13}C]-COSY for enriched compounds. In view of the ongoing rapid increase in NMR spectrometer performance, it may thus well be that ^{13}C-resonance assignments of metabolites in solid samples obtained from future labelling experiments will be performed with $\mathcal{J}$-correlation experiments.

2.1.2. *Positional ^{13}C-enrichments from NMR data*

The ^{13}C and ^{1}H resonance assignments of a metabolite provide the basis to determine positional ^{13}C isotope enrichments (IEs), i.e. the number of molecules bearing a ^{13}C spin at a given position divided by the total number of molecules. Several approaches have been developed in order to determine enrichments. (i) The resonance intensity observed in 1D ^{13}C-NMR is compared with the one obtained for a standard sample containing non-enriched metabolite. For an accurate calculation of IEs, ^{13}C-relaxation effects have to be considered (London, 1988), and absolute enrichments are then derived from the separately determined

https://doi.org/10.1017/S0033583598003412 Published online by Cambridge University Press

concentration of labelled metabolite (e.g. Yamaguchi *et al.* 1986; Portais *et al.* 1993; Rollin *et al.* 1995). (ii) The labelled metabolite is transformed into a chemical derivative using a non-enriched agent. The covalently linked moiety gives rise to a reference signal in ^{1}D ^{13}C-NMR representing a known enrichment (1·1 %), which allows to determine the IEs of the other carbon atoms. A spectrum recorded for the same derivative comprising non-enriched metabolite is used to account for relaxation effects, and also to compensate for small variations in instrumental setup (e.g. Bacher *et al.* 1983). (iii) In rare instances it may result from the topology of the metabolic network that a certain carbon in a metabolite is not enriched. The signal of this carbon can then be used as a reference to determine the IEs of the other carbon atoms (e.g. Cline & Shulman, 1991). (iv) Enrichments can also be calculated from the ratio of the centre and ^{13}C-satellite peak intensities of a ^{1}H–^{13}C moiety manifested in 1D ^{1}H-NMR spectroscopy, and improved accuracy can be achieved by recording a ^{13}C-decoupled 1D ^{1}H-NMR spectrum that is subtracted from a 1D ^{1}H-NMR spectrum acquired without ^{13}C-decoupling (e.g. Sonntag *et al.* 1993). (v) To avoid the determination of the concentration of labelled metabolite, approach (i) may be combined with (iv) (e.g. Eisenreich *et al.* 1993). (vi) Besides ^{1}H, ^{31}P is a spin-$\frac{1}{2}$ nucleus with nearly 100 % natural abundance occurring in many biological samples, e.g. in phosphorylated sugars participating in central carbon metabolism. For such compounds, the enrichment of ^{13}C spins that are scalarly coupled to ^{31}P can be inferred from the intensity of the resulting doublet in 1D ^{31}P-NMR spectroscopy (Lutz *et al.* 1996). Note, that an analogues approach has been chosen by Nieto *et al.* (1992) for the determination of ^{15}N enrichments via ^{15}N–^{13}C scalar couplings in 1D ^{13}C-NMR spectra recorded for ^{13}C-enriched metabolites, and by Lapidot & Gopher (1997) for probes studied at natural ^{13}C abundance. (vii) Based on probabilistic equations, the ^{13}C enrichment can be determined from the relative intensities of ^{13}C–^{13}C spin–spin scalar coupling multiplets arising from different isotopomers (e.g. Künnecke & Seelig, 1991; see also chapter 3.4).

2.1.3 ^{13}C-*isotopomer abundances from NMR data*

NMR spectroscopy is unique in providing also direct access to the relative abundances of ^{13}C isotopomers (e.g. London *et al.* 1975; Jeffrey *et al.* 1991; Wüthrich *et al.* 1992; Szyperski, 1995). Since the number of isotopomers, 2^n for a molecule with n carbons, generally exceeds the number of positional enrichments, n, an extended body of experimental data is required to calculate isotopomer abundances. The additional information can be derived from ^{13}C–^{13}C spin–spin scalar coupling interactions, which are manifested as resonance line splittings in solution ^{13}C-NMR spectra (Ernst *et al.* 1987). Since these interactions allow identification of pairs of ^{13}C-nuclei within the carbon skeleton, the determination of a complete set of relative isotopomers becomes, at least in principle, feasible. However, two major limitations exist for this theoretically appealing approach. Firstly, only the one-bond scalar couplings, $^{1}J_{CC}$, are usually large enough ($\sim$ 30–60 Hz; Horak *et al.* 1985; Krivdin & Kalabin, 1989) to be well resolved in ^{13}C-NMR spectroscopy, while long-range couplings are often too

https://doi.org/10.1017/S0033583598003412 Published online by Cambridge University Press

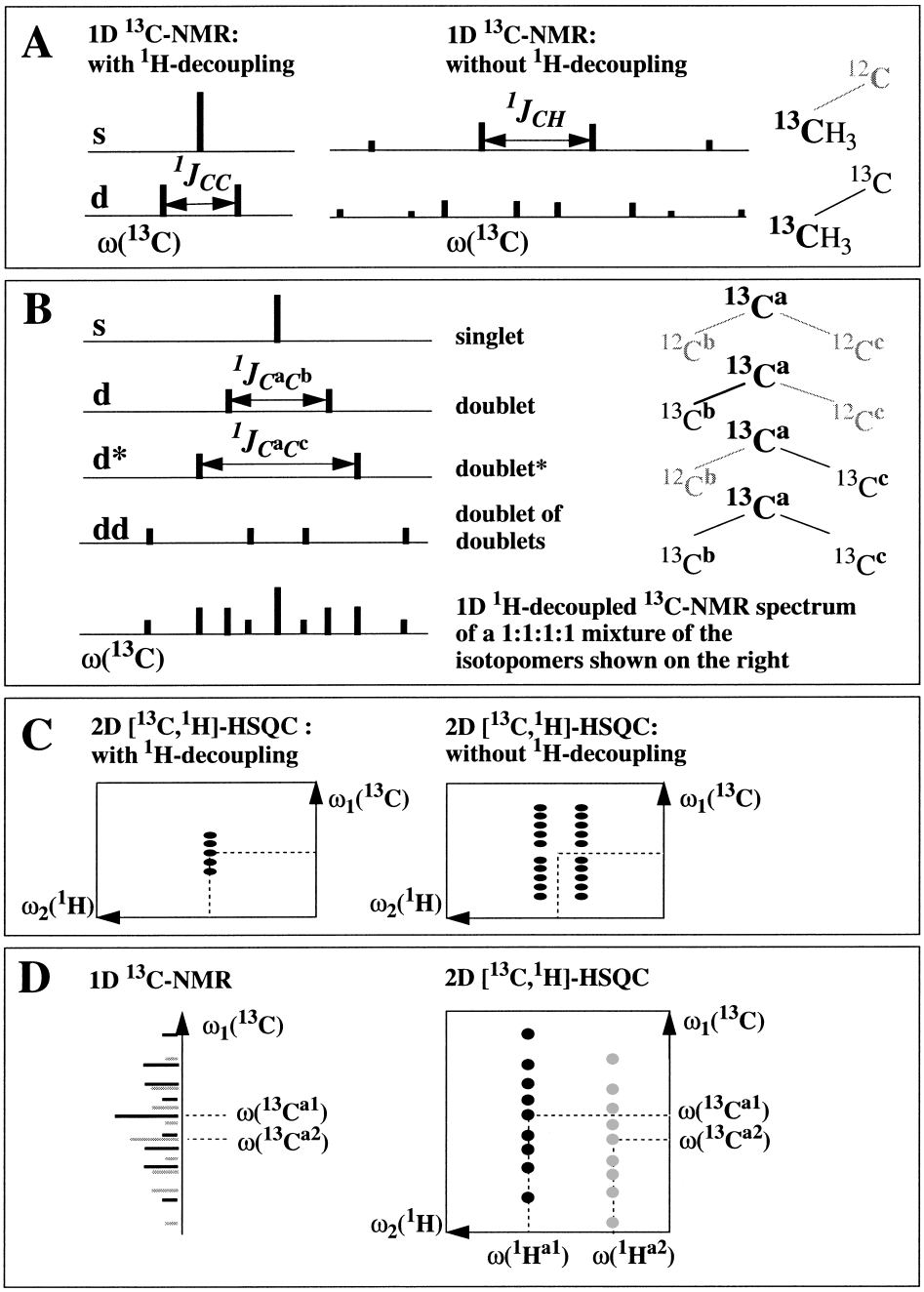

Fig. 3. Fine structures arising from ^{13}C–^{13}C scalar coupling interactions which are observed in ^{13}C-NMR spectra. (A) Signals for a terminal methyl group observed in 1D ^{13}C-NMR with (on the left) and without (on the right) ^{1}H-decoupling. The right-most column presents the isotopomeric ^{13}C-labelling pattern yielding a singlet ('s') or a doublet ('d'), respectively, when ^{1}H-decoupling is applied. The observed ^{13}C nuclei are depicted in bold and the ^{12}C nuclei are in grey. (B) Signals for a carbon that is centrally embedded in a C_3-fragment. On the right, the isotopomeric ^{13}C-labelling pattern leading to a singlet ('s'), a doublet split by a smaller scalar coupling ('d'), a doublet split by a larger scalar coupling ('d*') or a doublet of doublets ('dd') are shown. At the bottom of section (B), the fine

https://doi.org/10.1017/S0033583598003412 Published online by Cambridge University Press

small (< 5 Hz; Krivdin & Della, 1991). Hence, pairs of neighbouring spins can be routinely detected, while $^{2}\mathcal{J}_{CC}$ and $^{3}\mathcal{J}_{CC}$ scalar couplings are only in favourable cases sufficiently resolved to derive isotopomer abundances (e.g. London & Walker, 1985; Sauer *et al.* 1997; Werner *et al.* 1997). Secondly, the dispersion of the $^{1}\mathcal{J}_{CC}$ values (Krivdin & Kalabin, 1989) is often insufficient to distinguish the signals from two different spin pairs $^{13}C^{a}$–^{13}C and $^{13}C^{b}$–^{13}C, where the second spin is detected, simply because $^{1}\mathcal{J}_{C^{a}C} = {}^{1}\mathcal{J}_{C^{b}C}$ within the resolution of the spectrum. Hence, even for systems with excellent ^{13}C chemical shift dispersion, isotopomers analysis may be hampered by scalar coupling degeneracy. Due to these drawbacks, complete isotopomers analyses are often not possible for molecules with more than three carbon atoms, and ^{13}C-NMR spectral analysis is limited to revealing the abundance of groups of isotopomers. Nonetheless, the ability to monitor the formation or cleavage of the covalent bonds connecting neighbouring ^{13}C–^{13}C spin pairs makes isotopomer analysis by NMR spectroscopy the most powerful tool to unravel the organic chemistry of metabolic networks, and to quantify fluxes through these networks.

A qualitative or semi-quantitative assessment of the relative abundance of isotopomer groups can be inferred from several carbon–carbon correlation experiments (chapter 1.1.1.2), e.g. 2D ^{13}C–^{13}C TOCSY (Eisenreich *et al.* 1993; Koch *et al.* 1993) or ^{1}H-detected 2D DQ/TQ [^{13}C–^{13}C]-COSY (Beale & Foster, 1996). Moreover, due to a magnetization transfer proceeding via several one-bond couplings, 2D ^{13}C–^{13}C TOCSY allows identification of larger contiguously ^{13}C-labelled fragments (e.g. Eisenreich *et al.* 1997). However, the complex dependence of the transfer amplitudes of these experiments on the magnitude of the carbon–carbon scalar couplings, the spin relaxation times and radio-frequency pulse imperfections usually prevent calculation of accurate abundances. In fact, 2D DQ-filtered [^{13}C,^{13}C]-COSY is the only carbon–carbon correlation experiment that has been shown to allow for an accurate identification of $^{13}C_{2}$ and $^{13}C_{3}$ fragments in biosynthetically labelled metabolites (Jones & Sanders, 1989; Berthon *et al.* 1993). This is because the desired information is extracted from the in-phase splittings arising from passive scalar couplings, i.e. the carbon–carbon magnetization transfer merely serves to gain spectral resolution and the determination of isotopomer abundances itself does not rely on the carbon–carbon magnetization transfer.

Accurate isotopomer abundances can usually be obtained from the spin–spin scalar coupling fine structure detected either in ^{1}H-decoupled 1D ^{13}C-NMR (e.g. Seto *et al.* 1973; McInnes *et al.* 1974; London *et al.* 1975) or 2D [^{13}C,^{1}H]-

---

structure that is detected for a 1 : 1 : 1 : 1 mixture of isotopomers exhibiting all four pattern is shown. A maximal number of nine resonance lines is then observed, and the integration of the multiplet components yields the relative abundance of groups of isotopomers. (C) Fine structure of a cross peak in 2D [^{13}C,^{1}H]-HSQC arising from a CH-group in a $^{13}C_{3}$-fragment, which was recorded with (on the left) and without (on the right) 1H-decoupling. (D) Illustration of the impact of increased spectral resolution in 2D spectroscopy. The signals of two carbons overlapping in the 1D ^{13}C NMR spectrum (on the left) are resolved according to the chemical shift of their attached protons in the 2D [^{13}C,^{1}H]-HSQC spectrum (on the right). See also Fig. 4.

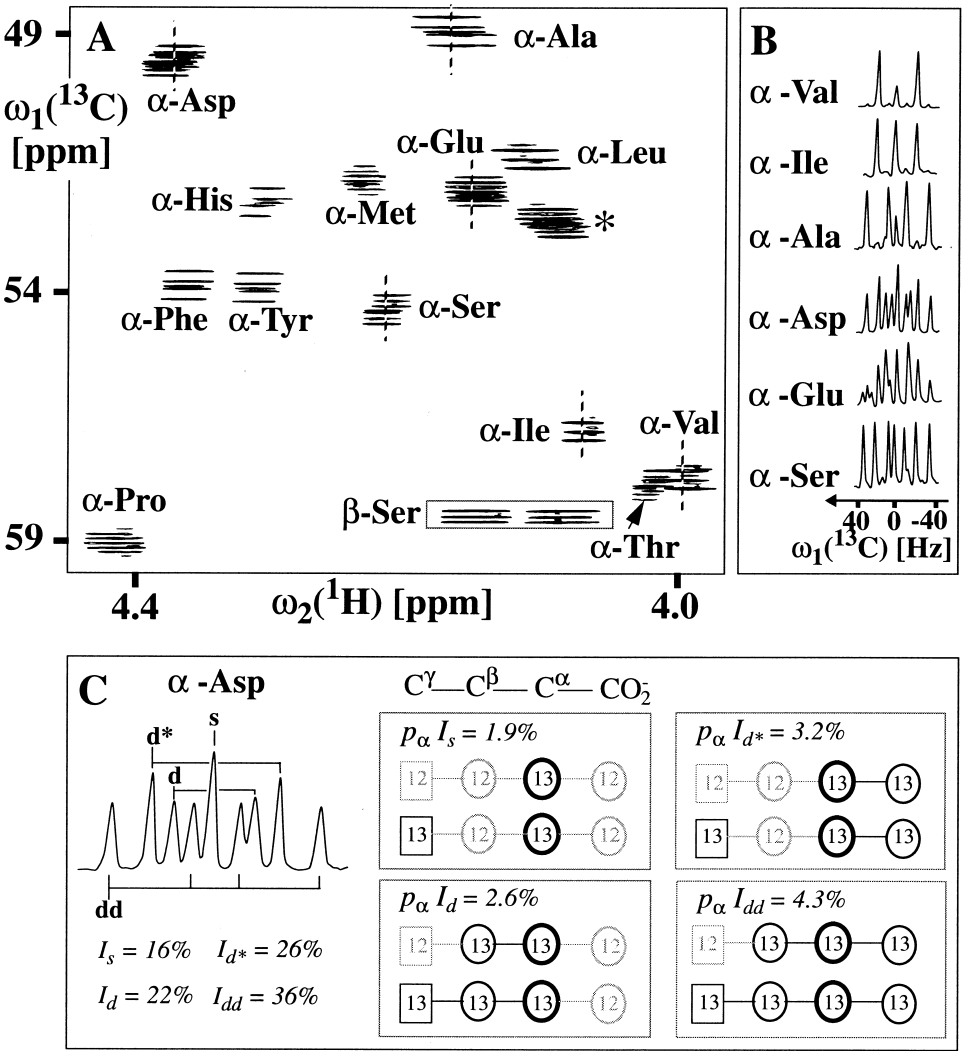

Fig. 4. Determination of relative ^{13}C isotopomer abundances from NMR data. (A) Region of a 2D [^{13}C, ^{1}H]-HSQC spectrum (Bodenhausen & Ruben, 1980) containing the $^{13}C^{\alpha}$–$^{1}H^{\alpha}$ cross peaks of all amino acids except glycine in a hydrolysate of cellular protein, and the $^{13}C^{\beta}$–$^{1}H^{\beta}$ cross peaks of serine ($T = 21$ °C; pH = 1; ^{1}H resonance frequency: 600 MHz; $t_{1max} = 273$ ms, $t_{2max} = 111$ ms; solvent: D_2O). The spectrum was recorded with the mixture of biosynthetic fractionally ^{13}C-labelled amino acids obtained from hydrolysis of P22c2 repressor overexpressed in *E. coli* cells under aerobic growth conditions (Wüthrich *et al.* 1992; Szyperski, 1995). The resonance assignments are given using the three-letter code of the amino acids and Greek letters for the carbon positions (note that tryptophan and cysteine were lost during hydrolysis due to oxidation, and that asparagine and glutamine were deamidated, so that the resonances of these four amino acids are not observed). The asterisk indicates the overlapping cross peaks belonging to α-Lys and α-Arg. (B) Cross sections taken along $\omega_1(^{13}C)$ at the broken vertical lines in (A), showing the ^{13}C–^{13}C scalar coupling fine structures of selected peaks. (C) Determination of the relative abundance of groups of isotopomers exemplified with the ^{13}C–^{13}C scalar coupling fine structure observed for the α-carbon of aspartate. I_s, I_d, I_{d^*} and I_{dd} indicate the relative intensities of the singlet, the doublet, the doublet* and the doublet of doublets (see Fig. 3). Provided that spin relaxation and strong spin–spin scalar coupling effects can be neglected (see text), these

https://doi.org/10.1017/S0033583598003412 Published online by Cambridge University Press

HSQC spectra (Szyperski *et al.* 1992, 1996*a*; Szyperski, 1995; Sauer *et al.* 1997) recorded, for example, with the pulse scheme devised by Bodenhausen & Ruben (1980) (chapter 2.1.1.1). Observation of the fine structure crucially depends on the efficient removal of the large $^1\mathcal{J}_{CH}$ scalar coupling interactions (Fig. 3A, C). This can be accomplished with a composite pulse decoupling scheme, e.g. WALTZ-16 (Shaka *et al.* 1983), during ^{1}H-detection, and with a 180° pulse applied on ^{1}H during ^{13}C chemical shift evolution. For a peripheral carbon, e.g. a methyl group, two multiplets are then observable: a doublet ('d') split by $^1\mathcal{J}_{CC}$ and a singlet ('s') (Fig. 3A). Four different multiplets can be detected for carbon that is centrally embedded in a C_3-fragment, provided that the two scalar couplings with the central carbon are not equal (Fig. 3B): a singlet ('s'), a doublet split by a small coupling ('d'), a doublet split by a larger coupling ('d*'), and a doublet of doublets ('dd'). For example, this situation is encountered for the α-carbons of the proteinogenic amino acids, since $^1\mathcal{J}_{C\alpha_{C=O}}$ coupling constants ($\sim$ 60 Hz; Krivdin & Kalabin, 1989) are significantly larger than $^1\mathcal{J}_{CC}$ coupling constants between aliphatic carbons ($\sim$ 35 Hz; Krivdin & Kalabin, 1989). Clearly, a further increased number of muliplet pattern can be anticipated for carbons centrally located in C_4-fragments. The key advantages of recording 2D [^{13}C,^{1}H]-HSQC spectra (Fig. 4) are, firstly, the higher sensitivity when compared with 1D ^{13}C-NMR (chapter 2.1.1.1), and, secondly, the increased spectral dispersion in two dimensions (Fig. 3D) that allows analysis of several metabolites without prior separation (Szyperski *et al.* 1992; Wüthrich *et al.* 1992; Szyperski, 1995). The major advantage of 1D ^{13}C-NMR spectroscopy is due to the fact that ^{13}C–^{13}C connectivities involving two quaternary carbons can be detected, which is not possible in ^{1}H-detected 2D [^{13}C,^{1}H]-HSQC.

For the precise determination of isotopomer abundances from ^{13}C fine structures (Fig. 4), (i) nuclear spin relaxation, (ii) strong spin–spin scalar coupling effects and (iii) ^{13}C isotope effects on carbon chemical shifts have to be considered. (i) Spin relaxation may distort the resonance intensities originating from differently labelled molecules. The incorporation of ^{13}C introduces additional relaxation pathways for ^{13}C and ^{1}H *via* ^{13}C–^{13}C and ^{13}C–^{1}H dipolar interactions, so that different isotopomers may exhibit different carbon steady-state magnetization present during the NMR experiment. Since ^{13}C–^{13}C dipolar interactions are very small compared to the one-bond ^{13}C–^{1}H dipolar interaction (Moreland & Carroll, 1974), significant effects will usually be registered in 1D ^{13}C-NMR spectroscopy only for non-protonated carbons. Hence, isotopomer

---

intensities yield the abundances shown on the right, i.e. the eight isotopomers carrying a ^{13}C nucleus in the α-position are subdivided in four groups. p_α denotes the positional enrichment of the α-carbon of aspartate (12% in this particular case; Wüthrich *et al.* 1992; Szyperski, 1995). The eight isotopomers with ^{12}C in the α-position (total abundance: $1-p_\alpha = 88\%$) are not detectable in ^{13}C-NMR spectroscopy and are not shown. For the presentation of the isotopomers, the observed α-carbon is indicated by a thick circle, and the β- and carboxyl-carbons are represented by thin circles. The γ-carboxyl carbon, whose labelling cannot be inferred from the α-carbon fine structure because two-bond scalar couplings are not resolved, is indicated by a box. '13' and '12' denote ^{13}C and ^{12}C isotopes and are depicted in black and grey, respectively.

https://doi.org/10.1017/S0033583598003412 Published online by Cambridge University Press

analyis via observation of quaternary carbons requires long relaxation delays between pulses (often well above 10 seconds; e.g. Schrader *et al.* 1993; Senn *et al.* 1991), or the addition of relaxation agents which dominate over the relatively small ^{13}C–^{13}C dipolar interactions. In 2D [^{13}C,^{1}H]-HSQC, where magnetization is initially excited on ^{1}H, signals arising from ^{13}C steady-state magnetization are eliminated by appropriate phase cycling (see Fig. 1 in Szyperski *et al.* 1992) and/or by the application of PFGs (Keeler *et al.* 1994). Hence, the intensities depend on the longitudinal relaxation of the observed protons, which is governed by ^{1}H–^{1}H dipolar interactions and the one-bond ^{13}C–^{1}H dipolar interaction (London *et al.* 1977), while long-range ^{13}C–^{1}H dipolar interactions are weak and can quite generally be neglected. Consequently, the longitudinal relaxation time of a proton bound to the observed ^{13}C nucleus does not depend on the number of attached ^{13}C atoms, and the relative intensities can be accurately linked to isotopomers abundances (Fig. 4), even if the relaxation delay between scans is set too short to ensure equilibrium longitudinal proton magnetization before the first ^{1}H-90 ° pulse (Szyperski, 1995). Furthermore, transverse ^{13}C relaxation during the indirect evolution time, t_1, likewise does not depend on the number of attached ^{13}C nuclei, because the ^{13}C–^{13}C dipolar interactions are very small relative to the one-bond ^{13}C–^{1}H dipolar interaction. (ii) Strong spin–spin coupling effects are anticipated whenever the scalar coupling constant $\mathcal{J}_{CC}$ involving two carbons is comparable to or larger than the corresponding chemical shift difference (Ernst *et al.* 1987). Then, significant distortions of the line intensities of a given multiplet occur, and a computer simulation of the spectrum has to be performed for a quantitative analysis (London, 1988). Such strong coupling effects were assumed to be absent for the construction of the pattern shown in Fig. 3. (iii) The chemical shift of a given carbon depends slightly on the number of attached ^{13}C nuclei (Hansen, 1988). Due to these ^{13}C isotope effects multiplet components arising from isotopomers with ^{13}C–^{13}C spin pairs, e.g. doublets and doublets of doublets, are shifted by $\sim$ 1–4 Hz to higher field relative to the singlet line. Consequently, the superposition of the multiplets arising from different isotopomers is not symmetric with respect to the singlet line (Fig. 4). This has to be considered when integrating partly overlapping multiplet components.

2.2 *Mass spectrometry*

The isotopes ^{12}C and ^{13}C differ not only in nuclear spin, which is of fundamental importance for the application of NMR spectroscopy (chapter 2.1), but also by one atomic mass unit. For smaller molecules ($<$ 2000 Da), this difference can readily be resolved using modern MS. Compared to NMR spectroscopy, MS is a highly sensitive tool (McLafferty & Turecek, 1993). This fostered the development of integrated systems combining MS with gas chromatography (GC). Most metabolic studies employing MS are performed with such GC-MS devices (Rosenblatt *et al.* 1992), since they warrant the separation of complex mixtures prior to mass spectral analysis. A metabolite comprising n carbon atoms may be labelled with up to n ^{13}C nuclei, i.e. the molecular mass detected in MS may range from M (only ^{12}C atoms) to $M+n$ (only ^{13}C atoms). Thus, MS

https://doi.org/10.1017/S0033583598003412 Published online by Cambridge University Press

measures the total mass of a given isotopomer but is not sensitive to the position of the label within the carbon skeleton. For special applications, multiple site-specific labelling introducing an additional stable isotope, e.g. ^{2}H in D-[1,6-$^{13}C_2$, 6,6-$^{2}H_2$] glucose (Ross *et al.* 1994), is attractive, since a mass spectral analysis of the labelled metabolite(s) then allows the unambiguous identification of the positional origin of the ^{13}C nuclei.

The relative intensities of the peaks at $M+i$ (with $i = 1..j..n$) yield a mass isotopomer distribution (MID) and the intensity of a given peak at $M+j$ reflects the abundance of all $\binom{n}{j}$ ^{13}C-isotopomers with j ^{13}C atoms. Like NMR spectroscopy, MS thus provides abundances of groups of isotopomers (e.g. Lanks, 1987; Lee, 1993). However, the observation of ^{13}C–^{13}C scalar couplings in NMR spectra permits the grouping of isotopomers according to their local ^{13}C labelling pattern (chapter 2.1.2): $m-1$ experimental constraints, i.e. relative abundances of isotopomers groups, can in principle be obtained for each carbon with m neighbours (Fig. 4) yielding $n(m-1)$ partly linear dependent constraints for n carbons. The MS data differ twofold from the NMR data. Firstly, only $n-1$ constraints can be extracted from the frequencies of a MID. Secondly, the constraints subdivide the isotopomers according to their global labelling pattern: a peak at $M+j$ represents all isotopomers with j ^{13}C nuclei, irrespective of their location in the carbon skeleton. Consequently, positional ^{13}C isotope enrichments (IEs) can be calculated only if the MIDs of both, the molecular ion and fragments thereof are accessible (Beylot *et al.* 1993; DiDonato *et al.* 1993; Katz *et al.* 1993; Portais *et al.* 1993; Brunengraber *et al.* 1997). This can be accomplished only by analysis of two or more chemical derivatives of the metabolite which give rise to distinct fragmentation patterns (Fig. 5). Furthermore, MS is not readily applicable to determine the relative abundance of ^{13}C–^{13}C fragments in larger carbon skeletons, which would be important for monitoring covalent bonds in a bioreaction network (chapter 2.1.3). Only if uniformly ^{13}C-labelled, i.e. statistically ^{13}C-enriched, source molecules are fed into a network in which cleavage products are diluted from non-labelled metabolite pools, the mass spectral detection of the source molecules allows to directly infer a uniform, and thus also position-specific conservation of covalent bonds (e.g. Kalderon *et al.* 1988, 1989; Katz *et al.* 1991). Clearly, GC-MS and ^{13}C-NMR spectroscopy may fruitfully complement each other, and their joint employment offers a widened experimental description of the system under consideration (e.g. Kalderon *et al.* 1987; Portais *et al.* 1993).

Although the accuracy of routine MS can be improved by so called selected ion monitoring (SIM) which focuses the analyser on a few specific masses, its precision for the measurement of IEs is limited to about 0·1 atom per cent. This restricts routine MS to experiments yielding significantly enriched metabolites, while studies performed close to the natural ^{13}C abundance level are hardly feasible. About 10^2–10^3 higher accuracy can be achieved with gas isotope ratio mass spectrometry (IRMS) (Brenna, 1994). Such spectrometry is designed to accomplish optimal performance with a few selected gases which have to be generated when using IRMS, e.g. CO_2 for the carbon isotopes. When employed

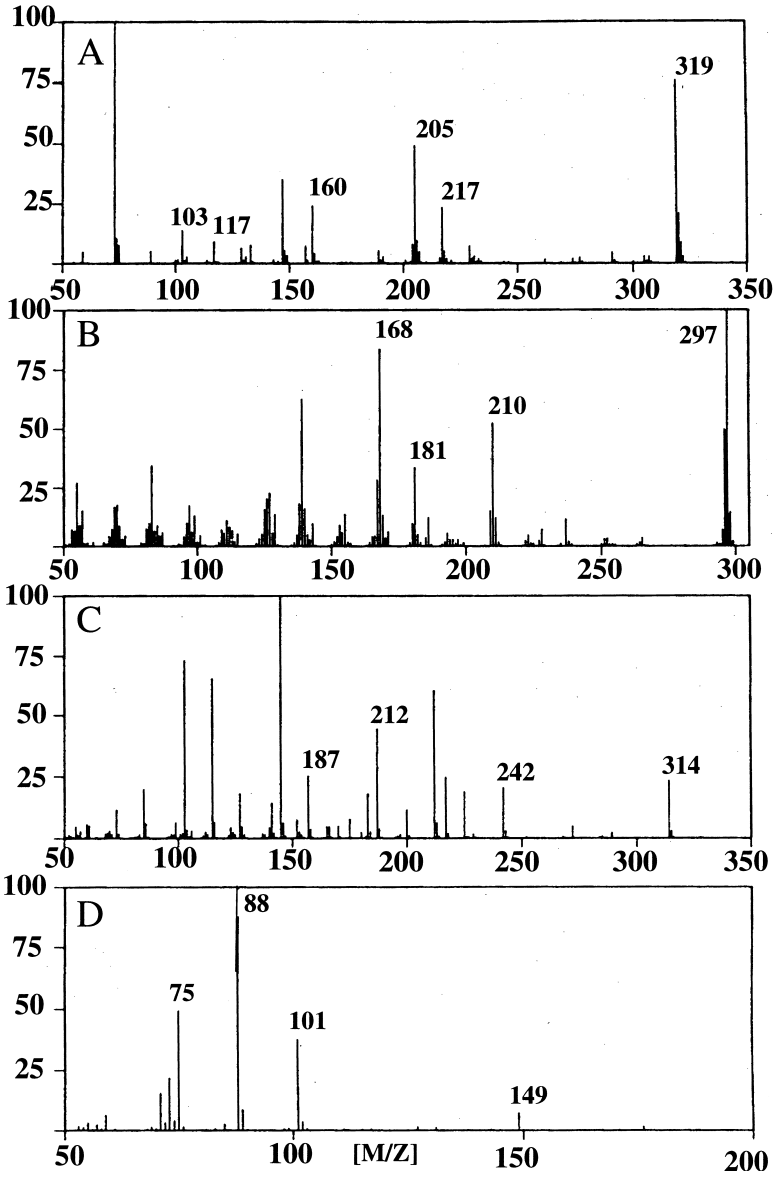

Fig. 5. Mass spectra of different glucose derivatives that were recorded to determine positional ^{13}C-isotope enrichments. (A) methyloxime pentamethylsilyl, (B) bisbutylboronate acetate, (C) aldonitril pentaacetate, (D) permethylglucose. In each spectrum, those peaks which served to compute the enrichments are indicated by numbers. Reproduced with permission from Beylot *et al.* (1993).

in conjunction with GC, the separated metabolite is oxidized to CO_2 and its average enrichment can be precisely determined (e.g. Cunnane *et al.* 1994; Parker *et al.* 1997). In contrast, a complete determination of positional enrichments requires, in principle, a chemical decomposition yielding a position specific isolation of each carbon and its subsequent combustion to CO_2. Very recently, an

approach to circumvent this tedious procedure has been established for methyl palmitate, in which pyrolytic fragmentation is used for obtaining the desired position-specific data (Corso & Brenna, 1997). Such developments promise to pave the way for a wider use of IRMS for future labelling studies pursued at low levels of ^{13}C-enrichment.

3. ^{13}C-LABELLING STRATEGIES

3.1 *Assessing ^{13}C-labelling patterns in metabolites*

After the administration of ^{13}C-labelled compounds to a living system, the redistribution of the label arising from the action of metabolism must be assessed. This requires a suitable preparation of the biological system in order to perform the NMR spectroscopic or mass spectral analysis. A variety of approaches have been worked out using *in vivo* NMR spectroscopy with whole animals (e.g. Künnecke, 1995), intact organs (e.g. beating hearts; Malloy *et al.* 1988) and parts thereof (e.g. rabbit kidney tubules; Chauvin *et al.* 1994), whole cells (e.g. *Escherichia coli*, Ogino *et al.* 1982; *Microbacterium ammoniaphilum*, Walker *et al.* 1982; *Halobacterium salinarium*, Bhaumik & Sonawat, 1994; *Hyphomicrobium*, Higgins *et al.* 1996; *Pyrococcus furiosus*, Kengen *et al.* 1994; *Saccharomyces cerevisiae*, den Hollander *et al.* 1986; Tran-Dinh *et al.* 1991) or intact organelles (e.g. mitochondria, Perrin *et al.* 1994). Since the majority of industrial processes rely on unicellular organisms, *in vivo* NMR experiments designed to cope with intact single cells are of primary interest for biotechnological research (Gadian, 1995; Weuster-Botz & de Graaf, 1996). *In vivo* NMR spectroscopy is attractive because it allows (i) the generation of time-resolved data when cells are not in a metabolic steady-state (e.g. Ugurbil *et al.* 1978; Walker *et al.* 1982; Jeffrey *et al.* 1991; Robitaille *et al.* 1993), and (ii) the determination of intracellular metabolite concentrations (Gadian, 1995). Moreover, artifacts that may arise from the extraction and possible isolation of metabolites can be excluded. However, high cell densities are usually required to achieve a workable signal-to-noise ratio, which requires sophisticated experimental approaches to mimic the process parameters characterizing the biotechnological process under consideration (Weuster-Botz & de Graaf, 1996), and metabolic intermediates with low concentrations may well escape detection (Künnecke, 1995). A comparably direct access to the *in vivo* state of the cells is warranted only by employment of solid-state ^{13}C-NMR spectroscopy, i.e. DCP/CP-MAS ^{13}C spectroscopy performed with frozen biopsies (Quistorff *et al.* 1993), or DCP/CP-MAS (e.g. Jacob *et al.* 1987) and REDOR ^{13}C-NMR spectroscopy (McDowell *et al.* 1993) performed with lyophilized cells.

For the isolation of metabolites from the living system, sonication (e.g. Bhaumik & Sonawat, 1994) and extraction with formic acid (e.g. Walsh & Koshland, 1984), hydrochloric acid (e.g. Evans *et al.* 1986; Kostanos *et al.* 1997) or perchloric acid (e.g. Jans *et al.* 1989; Malloy *et al.* 1988; Portais *et al.* 1993; Rollin *et al.* 1995) are commonly used. In favourable cases, overproduced metabolites are secreted into the growth medium. For example, sufficient amounts

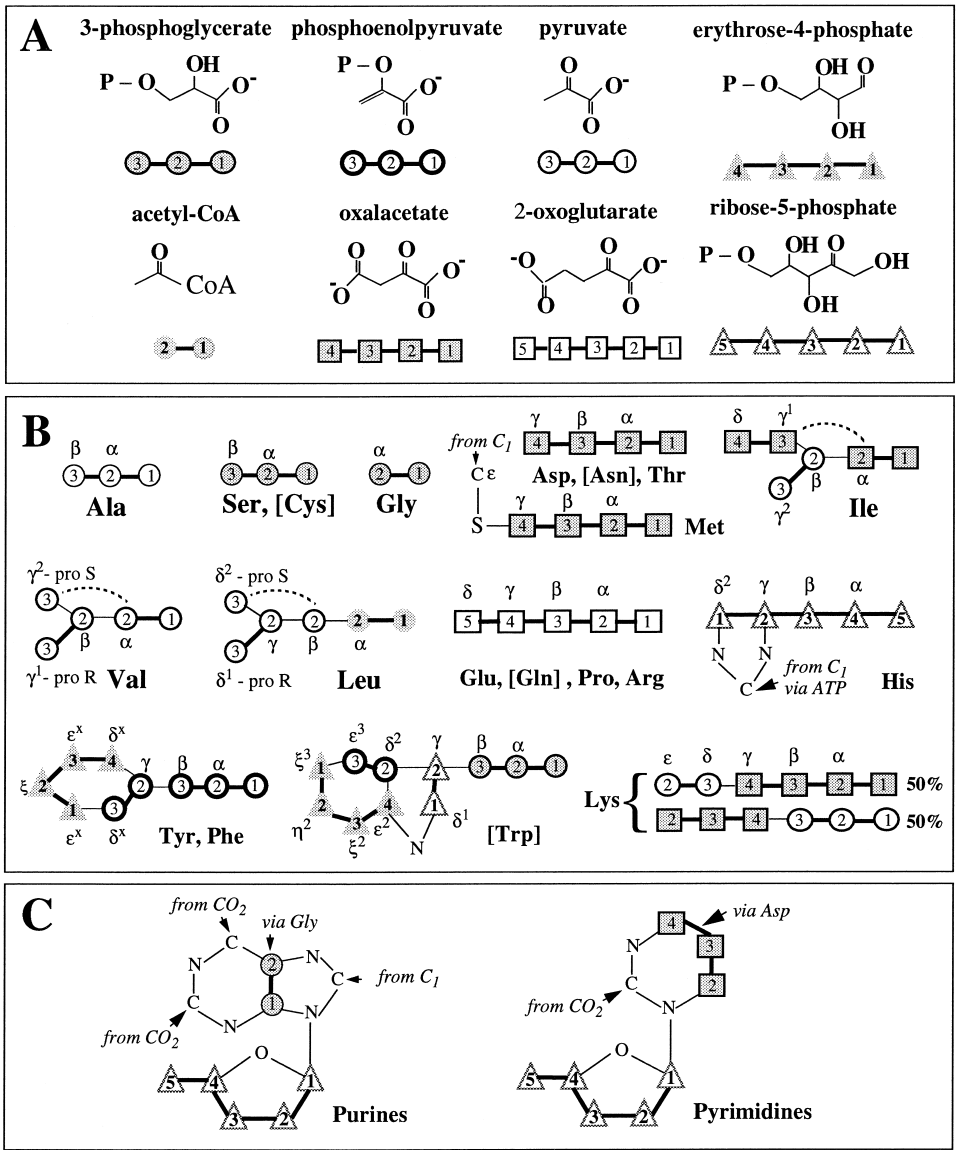

Fig. 6. Carbon fragments originating from a single intermediate molecule present in proteinogenic amino acids and nucleosides, provided that only anabolic pathways are active in *E. coli* cells (Neidhardt *et al.* 1996). (A) Representation of the carbon skeleton of the intermediates of glycolysis, tricarboxylic acid cycle and pentose phosphate pathway with circles, squares and triangles, respectively. Acetyl-Coenzyme A (CoA) is also represented with circles, and phosphoryl groups are denoted by 'P'. (B) Representation of the carbon skeletons of amino acids and (C) nucleosides, as well as the origin of their carbon atoms with respect to the metabolic intermediates displayed in (A). Thin lines denote carbon bonds that are formed between fragments arising from different intermediate molecules, while thick lines indicate carbon–carbon connectivities in intact fragments arising from a single intermediate molecule. Dashed lines connect fragments arising from the same intermediate molecule that are not directly attached in the amino acid carbon skeleton. Unlabelled carbon atoms in the amino acids are C′ carbons, and atoms originating from C_1-metabolism and CO_2 are indicated with '*from* C_1' and 'from CO_2', respectively. In *E. coli*,

https://doi.org/10.1017/S0033583598003412 Published online by Cambridge University Press

of trehalose (London & Walker, 1985), L-lysine (Yamaguchi *et al.* 1986; Park *et al.* 1997*a*), L-histidine (Ishino *et al.* 1986), succinate (Christie *et al.* 1987), L-malate (Perrin *et al.* 1994), and acetate and/or lactate (Ross *et al.* 1994; Neese *et al.* 1995) could be obtained from the media to derive the desired information about metabolism. Two central pathways, namely glycolysis and pentose phosphate pathway (PPP), involve mainly sugars as intermediates, some of which are interconverted to polysaccharides in many organisms. Provided that the cells under investigation synthesize sufficient amounts of polysaccharide, their analysis provides direct access to the intermediates of glycolysis and PPP (Gagnaire & Taravel, 1980; Jones & Sanders, 1989; Neese *et al.* 1995; Beale & Foster, 1996). When studying whole animals or organs, e.g. the liver, a special approach which has been coined 'chemical biopsy' (Magnusson *et al.* 1991) might be of interest. The idea is to administer a compound (e.g. phenylacetate) that induces secretion of a certain metabolite (e.g. glutamine) in the form of a covalent adduct (e.g. phenylacetylglutamine) followed by analysis of the adduct.

For eucaryotes, cell compartmentation must be taken into account since it results in the formation of two or more spatially separated pools of the same metabolite (e.g. Lapidot & Gopher, 1994; Pasternack *et al.* 1994; 1996; Dieuaide-Noubhani *et al.* 1995; Künnecke, 1995). Hence, the physical separation of the cell's compartments, e.g. the organelles, is most often required specifically to assess the different pools. Notably, Gout *et al.* (1993) have established an approach using paramagnetic Mn^{2+} ions to dissect metabolite pools in plant vacuols and cytoplasm: the paramagnetic ions penetrate into the vacuole and broaden the NMR signals beyond detection, while those arising from the cytoplasm remain unaffected.

An indirect approach to unravel the labelling pattern of intermediary metabolites exploits the fact that their isotopomeric composition determines the labelling of the anabolic products generated by primary metabolism (Stryer, 1994), i.e. amino acids (Ekiel *et al.* 1983, 1985; Walsh & Koshland, 1985; Schäfer *et al.* 1989; Wüthrich *et al.* 1992; Eisenreich *et al.* 1993; Pickett *et al.* 1994; Szyperski, 1995; Marx *et al.* 1996), nucleosides (Ekiel *et al.* 1983; Eisenreich *et al.* 1993; Pasternack *et al.* 1994, 1996; Kostanos *et al.* 1997) or secondary metabolites (e.g. Senn *et al.* 1991; Inbar & Lapidot, 1991). Analysis of these products, in conjunction with the mapping of their carbon skeletons to those of the intermediates (Fig. 6), thus enables the determination of ^{13}C-labelling pattern of

---

Lys is synthesized *via* the symmetric intermediate L,L-diaminopimelate so that it is represented by two equally abundant species. It is also indicated that the intact carbon fragments of the nucleosides are incorporated via Gly and Asp, and that the ϵ-carbon of His arises from C_1-metabolism via ATP. Only heterocyclic heavy atoms and the sulphur atom of Met are shown. In (B), those amino acids that are lost due to oxidation (Cys, Trp) or that are deamidated (Asn, Gln) during routine hydrolysis of cellular protein are indicated in brackets. Please note, that Ser and Gly are affected by C_1-metabolism so that their ^{13}C fine structures generally do not represent the isotopomeric composition of 3-phosphoglycerate. The superscript 'x' indicates that the two carbons δ^1 and-δ^2, and ϵ^1 and ϵ^2, respectively, of Tyr and Phe give rise to only one ^{13}C fine structure each (Szyperski, 1995). The nomenclature of the carbon atoms follows IUPAC-IUB recommendations (1970).

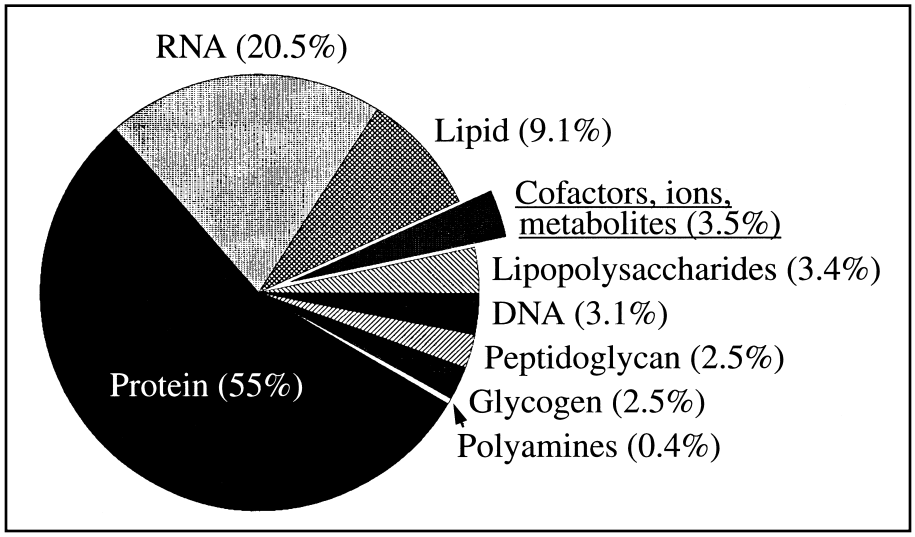

Fig. 7. Composition of an average *E. coli* B/r cell from a population in balanced growth at 37 °C in an aerobic glucose minimal medium (mass doubling time: 40 min; see Neidhardt, 1987: table 1).

the intermediates. This allows the determination of ratios of metabolic fluxes (chapter 3.3), or the reliable exploration of unknown biosynthetic pathways since the interpretation of the labelling pattern is not based on assumptions about the regulatory state of central metabolism. The largest amount of information can be deduced from the proteinogenic amino acids, which are linked to eight intermediates favourably spread over the network of central carbon metabolism (Stryer, 1994; Fig. 6). Consequently, several major biosynthetic pathways can be analysed in a single experiment. A major advantage of this indirect, biomass-oriented approach emerges when amino acids or ribonucleosides are derived from cellular protein or RNA, which are the two most abundant components of biomass (Fig. 7). For example, cellular protein represents about 55 % of the biomass of an average *E. coli* cell, and the protein thus acts as a large storage device in which the labelling patterns of the intermediates accumulate during cellular growth. This indirect avenue to the investigation of glycolysis, pyruvate metabolism, tricarboxylic acid (TCA) cycle and PPP, which is complemented by the analysis of C_1-metabolism *via* serine and glycine (Szyperski, 1995), is particularly attractive in view of the small steady-state concentrations of the metabolic intermediates (Fig. 7). It results in a sensitivity enhancement, i.e. higher yields of molecules carrying the desired ^{13}C-labelling pattern, of three orders of magnitude or more. To ensure a responsive metabolism (Jeong *et al.* 1990), concentrations of intracellular metabolites range from about 20 to 100 % of the corresponding saturation constants which are usually less than 1 mM and virtually never exceed about 10 mM (Fraenkel, 1992; Stryer, 1994). For NMR spectroscopic analyses (chapter 2.1) it is also of utmost practical importance that the proteinogenic amino

acids exhibit excellent ^{13}C chemical shift dispersion (Wüthrich, 1976). Thus, strong ^{13}C–^{13}C spin–spin scalar coupling effects are largely absent when using modern high-field NMR spectrometer (Szyperski, 1995), and isotopomer analyses (chapter 2.1.3) can be performed in a straightforward fashion considering only first order scalar coupling fine structures (Fig. 3; Szyperski, 1995). Clearly, a biomass-oriented approach is not feasible for biological systems that are characterized by an insufficient de novo synthesis of biomass, e.g. resting cells performing biotransformations.

3.2 *Selectively versus uniformly ^{13}C-labelled precursor*

The large number of published labelling studies can be subdivided in two classes, based either on selectively or uniformly ^{13}C-labelled ([U-^{13}C]) metabolic precursors. Studies with specifically labelled precursors have the longer tradition and aim at the introduction of isolated ^{13}C nuclei into the bioreaction network. The resulting positional ^{13}C IEs, which can be determined either by NMR spectroscopy or by MS (chapter 2), are the key observables. A complementary analysis of isotopomer distributions may be performed based on the detection of the ^{13}C–^{13}C spin–spin scalar coupling fine structures in NMR spectra (Fig. 3), which provides the fraction and positions of carbon–carbon bonds formed during biosynthesis (e.g. Walker *et al*. 1982; Malloy *et al*. 1990). In view of recent articles that present a comprehensive overview about labelling experiments performed with selectively labelled precursors (London, 1988; Cerdan & Seelig, 1990; Lundberg *et al*. 1990; Künnecke, 1995; Sherry & Malloy, 1996) and multiple selectively ^{13}C-labelled precursors aiming at the sensitivity enhancement for NMR studies (e.g. Pahl-Wostl & Seelig, 1986), a survey focusing on experiments with [U-^{13}C] metabolites shall be given in this chapter.

[U-^{13}C] metabolites arising exclusively from [U-^{13}C] source molecules exhibit neither position-dependent enrichments nor variations in isotopomer abundances, and thus do not carry biosynthetic information. For example, the analysis of metabolites taken from *E. coli* cells grown on a minimal medium containing only [U-^{13}C]glucose as a carbon source would reveal uniform IEs for all carbon positions as well as the sole presence of [U-^{13}C] isotopomers. Hence, in order to gain insight into the action of metabolism, [U-^{13}C] molecules and/or fragments thereof must be diluted with non-enriched endogenous pools, i.e. intracellular metabolites, or non-enriched exogeneous pools, i.e. carbon source molecules provided in the growth medium. Although a non-uniform endogenous dilution of different metabolites may yield biosynthetic information, the use of [U-^{13}C] molecules primarily aims at the tracing of ^{13}C–^{13}C connectivities in a bioreaction network, and thus corresponds to a carbon–carbon bond-labelling approach. When ^{13}C-NMR spectroscopy is used to analyse the labelling pattern, the ^{13}C-scalar coupling fine structure, which is linked to the extent to which a certain carbon is attached to carbons stemming from the same source molecule (Fig. 3), becomes the key observable. Mass spectral analysis often aims at the determination of the relative abundance of the [U-^{13}C] isotopomer, which originates mainly from

the [U-^{13}C] precursors without intermediate bond breakages (chapter 2.2). Moreover, mathematical models and corresponding non-linear fitting procedures have been implemented to assess quantitatively endogenous dilution occurring during biopolymer synthesis and turnover from MIDs (Hellerstein & Neese, 1992; Kelleher, & Masterson, 1992).

The ability to monitor the cleavage of carbon bonds makes labelling experiments with [U-^{13}C] precursors a powerful technique that was established in the 1970s to unravel the covalent structure of secondary metabolites (Seto *et al.* 1973; McInnes *et al.* 1974; London *et al.* 1975). A large number of such investigations have subsequently been pursued (Horak *et al.* 1985) using, for example, [U-^{13}C]acetate (e.g. Seto *et al.* 1973; McInnes *et al.* 1974; Ekiel *et al.* 1985), [U-^{13}C]D-glucose (e.g. London *et al.* 1975; Gould & Cane, 1982; Bacher *et al.* 1985; Takahashi *et al.* 1995; Werner *et al.* 1997), [U-^{13}C]D-ribulose (Volk & Bacher, 1991), [U-^{13}C] polyunsaturated fatty acids (Cunnane *et al.* 1994) or crude [U-^{13}C] lipid mixtures (Eisenreich *et al.* 1997). If the endogenous dilution becomes too large, the identification of ^{13}C-NMR fine structures is hampered by the background signals arising from natural 13C abundance. In this case, the use of ^{13}C-depleted precursors, e.g. [U-^{12}C]D-glucose, represents a viable, though expensive, methodological improvement (Rinehardt *et al.* 1982).

Since the late 1970s, [U-^{13}C] precursors have also been employed for the elucidation of intermediary metabolism (Gagnaire & Taravel, 1979, 1980). Examples include the use of (i) [U-^{13}C]acetate to explore the carbon supply of the TCA cycle in mammalian liver (e.g. Jones *et al.* 1993) and brain (Künnecke, 1995), (ii) [U-^{13}C]glucose to assess glucose metabolism in the bacterium *Acetobacter xylinium* (Gagnaire & Taravel, 1980), in mammalian glioma cells (Lanks, 1987), in the bacterium *Klebsiella rhinoscleramatis* (Jones & Sanders, 1989), in the trematode *Schistosoma japonicum* (Kawanaka *et al.* 1989), in the bacterium *Azotobacter vinelandii* (Beale & Foster, 1996) and in the yeast species *Schizosaccharomyces pombe* (Tsai *et al.* 1995), or to assess central carbon metabolism in *E. coli* (Szyperski, 1995), (iii) [U-^{13}C]lactate (Katz *et al.* 1993), or [U-^{13}C]lacate and [U-^{13}C]pyruvate (Des Rosiers *et al.* 1995), to study gluconeogenesis and regulation of the TCA cycle in the liver, (iv) [U-^{13}C] propionate to assess liver metabolism (Jones *et al.* 1993; Sherry *et al.* 1994), (v) [U-^{13}C]fructose to investigate fructose-intolerance in humans (Gopher *et al.* 1990), (vi) [U-^{13}C]glutamate to elucidate the regulation of the TCA cycle in mammalian astrocytes (Sonnewald *et al.* 1993), (vii) [U-^{13}C]D-gluconate, [U-^{13}C]D-glucose and [U-^{13}C]L-lysine to investigate anaplerotic pathways in *Corynebacterium glutamicum* (Park *et al.* 1997*a*), or (viii) [U-^{13}C]fructose, [U-^{13}C] glutamate and [U-^{13}C]aspartate to study carbon metabolism of the fungus *Streptomyces parvulus* (Inbar & Lapidot, 1991). The principles outlined for the use of [U-^{13}C] precursors are also valid for experiments performed with metabolites comprising contiguously ^{13}C-labelled fragments (Brainard *et al.* 1989), e.g. [1,2-$^{13}C_2$]glucose (Künnecke & Seelig, 1991), where the non-enriched segment of the molecule contributes to the dilution of the $^{13}C_2$-fragments. This approach could be designated as 'specific bond labelling', and its major advantage

compared with protocols based on selectively labelled compounds arises for studies pursued at low ^{13}C enrichments ($\sim 2\,\%$). Because of the $^{1}\mathcal{J}_{CC}$ scalar coupling, the labelled bond is manifested as a doublet in a ^{13}C-NMR spectrum (Fig. 3), while the natural ^{13}C abundance gives rise to a singlet (note that at low enrichment the signal arising from a selectively labelled precursor would simply add to the singlet line). Specific bond labelling thus makes use of the fact that the natural background of ^{13}C–^{13}C spin pairs (abundance $\sim 10^{-4}$) is negligibly small and allows the reliable detection of the labelled species at concentration levels of about $1\,\%$ or less of the endogenous pools.

Experimental protocols ensuring the exclusive exogeneous dilution of [U-^{13}C] precursor with its non-enriched form are of special interest. Provided that the living system is in both a metabolic and an isotopic steady-state, i.e. that intermediates and isotopomers in the network are produced and consumed at equal rates, the composition of the growth medium determines the dilution of the precursor. This allows accurate tracing of the fate of carbon fragments in a bioreaction network in a single experimental setup (chapter 3.4). Then, the IEs are uniform for all carbon positions and, using NMR spectroscopy, the ^{13}C scalar coupling fine structure remains as the sole observable providing biosynthetic information. For the proteinogenic amino acids, this approach has been introduced as 'biosynthetically directed fractional ^{13}C-labelling' in biomolecular NMR spectroscopy to obtain ^{1}H and ^{13}C resonance assignments of proteins (Neri *et al.* 1989; Senn *et al.* 1989; Szyperski *et al.* 1992). Subsequently it became clear that, owing to the regiospecificity of the anabolic pathways, such labelling can likewise be used as an efficient and easily applicable method to monitor fluxes in central carbon metabolism (Szyperski, 1995; chapter 3.4).

3.3 *Metabolic flux ratios from ^{13}C-labelling experiments*

Ratios of metabolic fluxes determined by ^{13}C-labelling experiments are of great interest for metabolic studies in biotechnological research. Firstly, they directly reflect the cells' metabolic state. Secondly, they provide an experimental test for theoretical predictions deduced, for example, in the framework of MCA (Fell, 1997), and thirdly, they may well complement metabolic flux balancing to obtain more reliable estimates of absolute *in vivo* fluxes (chapters 5, 6).

Processing of a ^{13}C-labelled precursor in a metabolic network through two or several alternative pathways to the same metabolite often requires different sequences of cleavage and formation of carbon–carbon bonds, and depending on the actual labelling protocol, also different endogenous dilution. Hence, the resulting labelling pattern of the metabolite reflects the relative importance of the alternative pathways. This makes ^{13}C-labelling experiments an ideally suited technique to determine flux ratios. The determination of absolute fluxes also requires concentration measurements of metabolites that are connected to the (sub)network assessed by the labelling experiment. An extension of this concept provides, in some cases, information on the relative forward and backward rates of a metabolic step, as the unidirectional forward reaction may yield a labelling

pattern different from a possible forward–backward–forward reaction (e.g. Szyperski 1995, 1996*a*).

The derivation of flux ratios is based on three key prerequisites. Firstly, the metabolic network must be known at least on the level of its topological structure, i.e. the location of the pathway branching points must be known. It is thus desirable to design ^{13}C-labelling experiments for the determination of flux ratios in a fashion that concomitantly allows defininition of the network topology. For several biotechnologically important microorganisms with a largely explored carbon metabolism, e.g. *E. coli* (Neidhardt *et al.* 1996) or *Bacillus subtilis* (Sonenshein *et al.* 1993), this task reduces to the identification of pathways that are activated when the cells are in a physiologically defined metabolic state (e.g. Szyperski, 1995; Sauer *et al.* 1997). Secondly, interpretation of ^{13}C-labelling data relies on the assumption that kinetic and thermodynamic ^{13}C isotope effects on the metabolic reaction rates and equilibria can be neglected. Since the mass ratio $m(^{13}C)/m(^{12}C)$ is close to one, this is quite generally warranted, and the relative changes of isotopomer abundances due to isotope shifts are smaller than about 1 % (e.g. Galimov, 1985; Gleixner & Schmidt, 1997). Hence, the influence of these effects on the flux determination is at least one order of magnitude smaller than the experimental uncertainty that is currently achievable for the measurement of flux ratios. Thirdly, it must be assured that the determination of IEs and isotopomer abundances is not deteriorated by technical limitations, e.g. the influence arising from ^{13}C spin relaxation in NMR spectroscopic studies (chapters 2.1.2, 2.1.3; London, 1988), or ^{13}C isotope effects influencing the ionization and fragmentation reactions in IRMS (Corso & Brenna, 1997).

When interpreting ^{13}C-labelling experiments in terms of flux ratios, the influence potentially arising from additional phenomena should be considered. There is now ample evidence that interactions between sequential metabolic enzymes can lead to the formation of supramolecular complexes *in vivo* (e.g. Hrazdina & Jensen, 1992; Sherry & Malloy, 1996). These complexes, sometimes called metabolons (Ovádi & Srere, 1992), are believed to provide a structural basis (Vélot *et al.* 1997) for metabolite channelling, i.e. processes in which pathway intermediates are transferred from one enzyme to another without complete equilibration with the molecules in the bulk medium. Channelling potentially accelerates metabolic flow through a pathway and may also provide a mechanism to reduce the pool sizes of pathway intermediates (Kholodenko *et al.* 1996). Recently studied systems include TCA enzymes located at the inner membrane of the mitochondrial matrix (Sherry *et al.* 1994) and the enzymes of the oxidative PPP (Debnam *et al.* 1997) in yeast cells. The most apparent manifestation of channelling in ^{13}C-labelling experiments stems from incomplete randomization of symmetric intermediates, e.g. fumarate and succinate in the TCA cycle (Sherry *et al.* 1994), so that neglecting the channelling phenomena may yield erroneous estimates of the flux ratios. In fact, this view has been supported by the determination of *in vivo* fluxes of glioma cells performed by Portais *et al.* (1993). Similarly, futile cycling (Stryer, 1994), i.e. the cyclic interconversion of metabolites with zero net flux under ATP consumption (e.g. Patnaik *et al.* 1992;

Chao & Liao, 1994; Chauvin *et al*. 1994), may hamper straightforward data analysis, if not recognized and appropriately considered for data interpretation. Finally, for the investigation of eucaryotic cells their compartmentation has to be considered (e.g. Sharfstein *et al*. 1994; Lapidot & Gopher, 1994; Pasternack *et al*. 1994, 1996; Dieuaide-Noubhani *et al*. 1995; Künnecke, 1995).

Many unicellular systems grow on a minimal medium containing the ^{13}C-labelled substrate as the sole carbon source. This allows the derivation of ratios of fluxes distributed over the entire network of central carbon metabolism, including the relative supply of glycolysis and oxidative PPP, the relative importance of the oxidative *versus* the non-oxidative branch of PPP, flux ratios through reactions at the interface of glycolysis and TCA cycle, and flux ratios of pathways through TCA cycle and glyoxalate shunt. Such studies were performed by Walsh & Koshland (1984; 1985) for a Met^- strain of *E. coli*, by Szyperski (1995) for *E. coli* strain W3110, by Ishino *et al*. (1986) for *C. glutamicum*, by Senn *et al*. (1991) for *Tolypocladium inflatum*, by Rollin *et al*. (1995) for *C. melassecola*, by Marx *et al*. (1996) for a Leu^- strain of *C. glutamicum*, by Park *et al*. (1997*a*) for *C. glutamicum*, and by Sauer *et al*. (1997) for *B. subtilis*. Based on fermentation protocols using rich media, Walker *et al*. (1982) and Mancuso *et al*. (1994) studied the central metabolism of *Microbacterium ammoniaphilum* and hydridoma cells, respectively, Kengen *et al*. (1994) and Beale & Foster (1996) could assess the relative importance of glycolysis *versus* Entner–Doudoroff pathway in *Pyrococcus furiosus* and *Azotobacter vinelandii*, respectively, Jones & Sanders (1989) quantitatively evaluated the interplay of glucose catabolism and polysaccharide synthesis in *Klebsiella rhinoscleramatis*, and, introducing ^{13}C,^{15}N-labelled serine, McDowell *et al*. (1993) determined flux ratios characterizing the C_1-metabolism of *Klebsiella pneumonia*. Perrin *et al*. (1994) investigated the central metabolism in adrenocortical mitochondria supplied with L-malate and determined the relative flux through the reactions catalysed by malic enzyme and isocitrate dehydrogenase. Pasternack *et al*. (1994) analysed the intercompartmental flow of one-carbon units into choline and purines in *Saccharomyces cerevisiae*. Owing to complex endogenous dilution effects and the fact that few ^{13}C-labelled metabolites are sufficiently abundant, a single ^{13}C labelling experiment usually provides only selected flux ratios in more complex systems. Since the TCA cycle represents a major amphibolic pathway whose regulation is of central importance for the balance of catabolic and anabolic processes, several studies focused on the network comprising the TCA cycle, its interface to glycolysis and the glyoxalate shunt. Malloy *et al*. (1988) evaluated the relative supply of the TCA cycle through the oxidative versus the anaplerotic pathway when supplying pyruvate (Pyr) to rat heart cells by analysis of glutamate representing 2-oxoglutarate (2Og). Most remarkably, their approach to obtain the flux ratio does not depend on a steady-state assumption, so that time-resolved data could be collected (Walker *et al*. 1982; Jeffrey *et al*. 1991). Comparable analyses were subsequently performed, e.g. for rabbit renal proximal tubular cells fed with citrate (Jans *et al*. 1989), for glial tumour cells fed with Pyr (Brand *et al*. 1992) and for rabbit brain cells fed with glucose (Lapidot & Gopher, 1994). Administering glycerol to rabbit renal

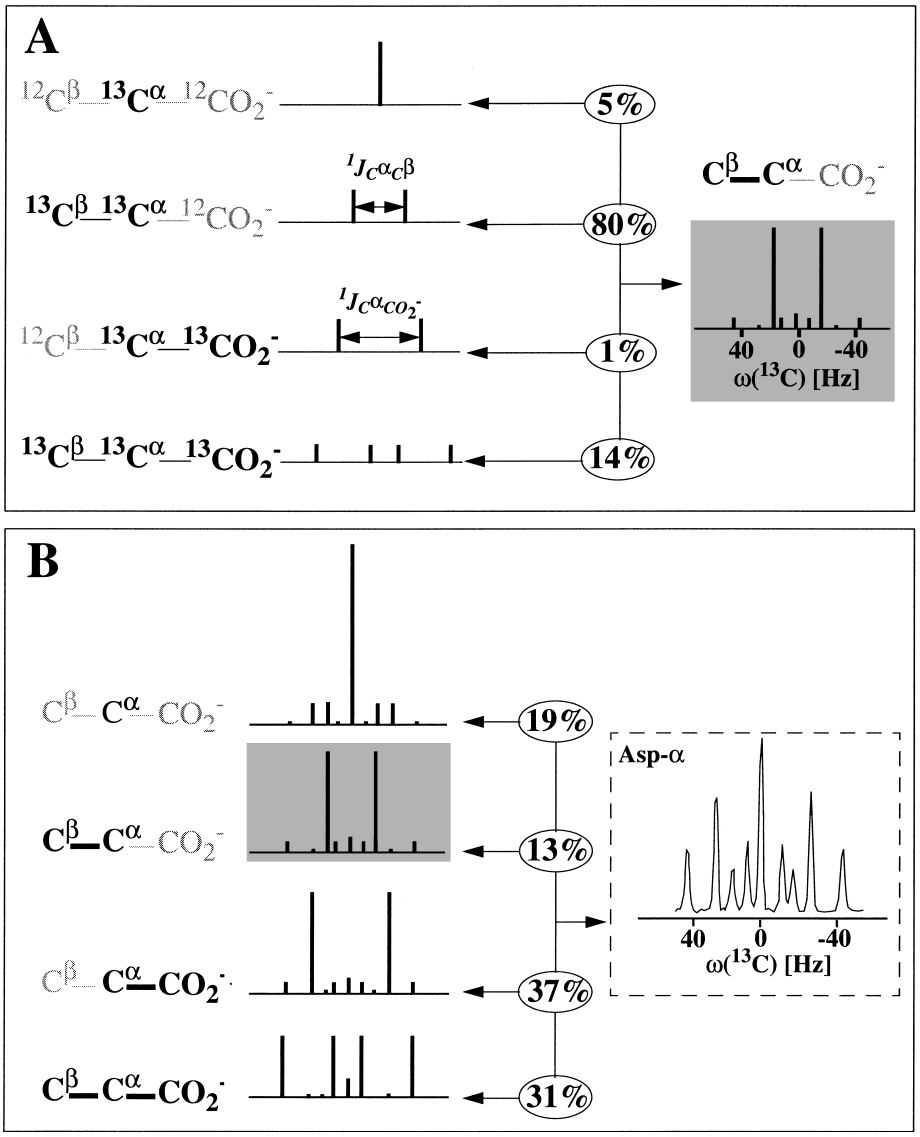

Fig. 8. Abundances of intact carbon fragments arising from a single source molecule as determined with a biosynthetically-directed fractional ^{13}C labelling experiment performed with a minimal medium containing 15% fully ^{13}C-labelled glucose and 85% non-enriched glucose as the sole carbon source. (A) The ^{13}C $^1\mathcal{J}_{CC}$ scalar coupling fine structure (grey background) expected for the α-carbon of aspartate in an intact C^{α}–C^{β} fragment, i.e. the α- and β- carbons stem from one glucose molecule while the carboxyl-carbon (shown in grey) arises from a different one, as calculated with probabilistic equations (Szyperski, 1995). The isotopomers and the corresponding multiplets are shown on the left (see Fig. 3). ^{12}C nuclei are displayed in grey. The relative intensities of the multiplets in the calculated fine structure shown on the right are given in the corresponding ellipses. (B) Decomposition of the ^{13}C $^1\mathcal{J}_{CC}$ scalar coupling fine structure observed at the α-carbon of aspartate (shown in the box) according to the fine structures calculated for the different intact fragments shown in the left-most column. Carbon atoms originating from the same source molecule as the detected-α-carbon are indicated with black letters, while carbons arising from a different one

https://doi.org/10.1017/S0033583598003412 Published online by Cambridge University Press

proximal tubular cells allowed Jans & Willem (1988) to assess the TCA cycle supply as well as to determine the relative flux into the gluconeogenetic pathway. Since gluconeogenesis plays a central role for glucose homeostasis of mammals, the gluconeogenetic flux in liver cells was determined by several research groups (e.g. DiDonato *et al*. 1993; Katz *et al*. 1993; Neese *et al*. 1995; see also Künnecke, 1995). In an elegant experiment, Ross *et al*. (1994) determined glycolysis *versus* PPP activity in glioma cells by incubation with doubly labelled D-[1,6-$^{13}C_2$, 6,6-$^{2}H_2$]glucose, which avoids the necessity to make corrections accounting for endogenous dilution (Kingsley-Hickman *et al*. 1990).

3.4 *Tracing carbon fragments in a bioreaction network*

Biosynthetically-directed fractional (BDF) ^{13}C-labelling (Neri *et al*. 1989; Senn *et al*. 1989; Szyperski *et al*. 1992; Szyperski, 1995) employed with a minimal medium containing a mixture of roughly 10% [U-^{13}C] precursor and 90% non-enriched precursor as the sole carbon source, ensures that metabolic dilution (chapter 3.2) of the [U-^{13}C] fragments is entirely determined by the composition of the minimal medium. Hence, the isotopomer abundances generated during the BDF labelling experiment are solely dependent on (i) the natural ^{13}C isotope abundance, (ii) the fraction of [U-^{13}C] precursor in the medium and its degree of ^{13}C-labelling, and (iii) the structure of the metabolic network and the corresponding fluxes. To date, many [U-^{13}C] compounds are commercially available with a labelling degree that is 99% or larger. Then, the precursor can be assumed to be fully labelled, and effects stemming from incomplete ^{13}C-labelling of the [U-^{13}C] precursor can be neglected (Szyperski, 1995). The ultimate goal of the BDF ^{13}C-labelling experiment performed for metabolic studies is to trace contiguous carbon fragments arising from a single source molecule in a bioreaction network (Szyperski, 1995). Its principles and merits shall be illustrated with data that were obtained for riboflavin-producing *B. subtilis* cells grown on a minimal medium containing 15% [U-^{13}C]glucose and 85% non-enriched glucose as the sole carbon source (Sauer *et al*. 1997). As described in the first application of this approach for *E. coli* cells (Szyperski, 1995), the proteinogenic amino acids were analysed for sensitivity enhancement (chapter 3.2), thereby making use of the fact that contiguous carbon fragments originating from a single source molecule of glucose are incorporated into the proteinogenic amino acids during biosynthesis (Fig. 6). The relative abundances, as well as the location of such fragments within the carbon skeleton of the metabolic intermediates may thus be deduced from the amino acids. Note that the analysis of ribonucleosides extracted from cellular RNA (Fig. 7) would not contribute additional information, since contiguous carbon fragments present in the ribonucleosides can be equally well assessed in the proteinogenic amino acids histidine, glycine and aspartate (Fig. 6), while the carbons not bound to another carbon do not provide biosynthetic information in

are in grey. The relative abundances of the fragments derived from the decomposition are given in the corresponding ellipses, and the fine structure of the intact C^{α}–C^{β} fragment, whose calculation is illustrated in (A), is shown with a grey background.

https://doi.org/10.1017/S0033583598003412 Published online by Cambridge University Press

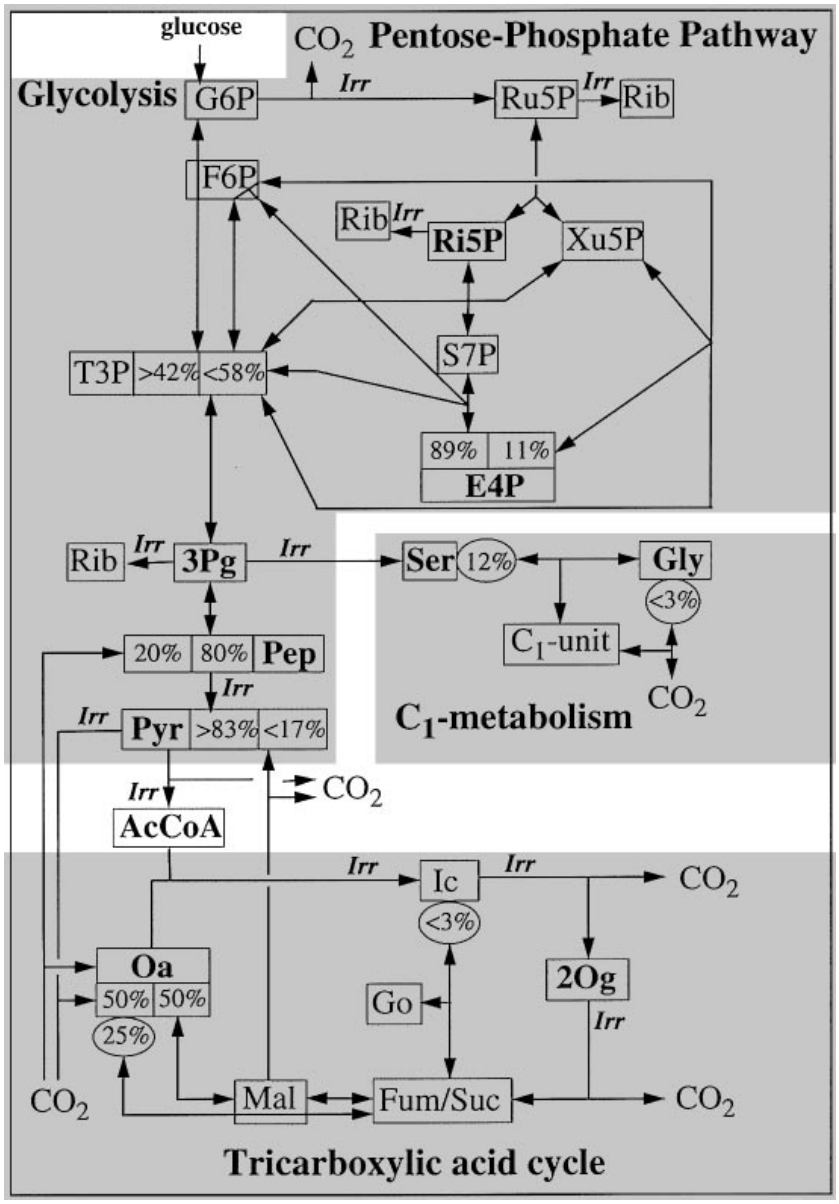

Fig. 9. Presentation of metabolic flux ratios determined by analysis of biosynthetically-directed fractional ^{13}C-labelling of proteinogenic amino acids (Szyperski, 1995; Szyperski *et al.* 1996) when a mixture of 15 % [U-^{13}C]glucose and 85 % non-enriched glucose is used as the sole carbon source for riboflavin-producing *B. subtilis*. The cells were grown in a glucose-limited chemostat at a dilution rate of 0·11 h^{-1} (data taken from Sauer *et al.* 1997; see Fig. 12). Irreversible reactions are indicated by single-headed arrows and are denoted with '*Irr*', while mutual interconversions are represented by double-headed arrows. The fractions of molecules given in square boxes are synthesized *via* the fluxes pointing into them. The fractions displayed in ellipses indicate the extent of reversible interconversion of the molecule in question. Metabolic intermediates used for synthesis of the proteinogenic amino acids are shown in bold. Abbreviations: AcCoA, acetyl-CoA; E4P, erythrose 4-phosphate; F6P, fructose 6-phosphate; Fum, fumarate; G6P, glucose 6-phosphate; Gly, glycine; Go, glyoxalate, Ic, isocitrate; Mal, malate; Oa; oxalacetate; 2Og, 2-oxoglutarate;

https://doi.org/10.1017/S0033583598003412 Published online by Cambridge University Press

BDF ^{13}C-labelling experiments (Szyperski, 1995). To elucidate the carbon flux from glucose to the metabolic precursors, the quantitative analysis of the ^{13}C fine structures must eventually unravel to which extent a certain carbon atom possesses neighbouring carbons originating from the same source molecule of glucose. For example, for the aspartyl α-carbon, which is centrally embedded in a C_3-fragment and exhibits different scalar coupling constants to the attached C^{β} and C′ carbons (Fig. 4), four cases are possible. First, all three carbons, i.e. C^{α}, C^{β} and C′, may originate from the same source molecule of glucose. Alternatively, C^{α}-and-C^{β}, or C^{α}-and C′ may arise from the same source molecule, while the remaining third carbon does not. Finally, the three carbons may originate from three different source molecules (Fig. 8). Hence, the relative intensities of the multiplet components derived from the ^{13}C spin–spin scalar coupling fine structure (Figs 3, 4), which reflect the relative abundance of groups of isotopomers, have to be related to the relative abundance of such intact fragments arising from a single source molecule of glucose.

This can be accomplished using probabilistic equations (Szyperski, 1995) that allow calculation of the expected ^{13}C scalar coupling fine structure for a given intact fragment (Fig. 8A). For fully ^{13}C-labelled glucose, the calculated multiplet patterns reflect the background from the natural ^{13}C isotope abundance in the 85 % non-enriched glucose molecules, and the statistical recombination of [U-^{13}C] fragments due to finite dilution. Subsequently, the observed ^{13}C scalar coupling fine structure is decomposed according to the fine structures calculated for the possible intact fragments, thus yielding their relative abundance (Fig. 8B). In accordance with the dissection of the pool of isotopomers into groups (Fig. 4), the intact fragments inferred from the $^{1}\mathcal{J}_{CC}$ scalar coupling fine structure likewise represent groups of intact fragments when considering the whole molecule. For example, the abundance of intact C^{β}-C^{α}-C′ fragments obtained from the α-carbon resonance of aspartate (Fig. 8) comprises both intact C^{β}-C^{α}-C′ and C^{γ}-C^{β}-C^{α}-C′ fragments (although the latter is not generated by known metabolic networks when feeding solely glucose).

Once the observed fine structures have been translated into fragment abundances, the breakdown of the six-carbon skeleton of glucose can be interpreted. This allows (i) definition of the metabolic pathways that are activated under the physiological conditions of the experiment, (ii) identification of irreversible reaction steps in the thus defined bioreaction network (chapter 5.2) and, assuming that the cells are in a metabolic steady-state, (iii) investigation of exchange reactions (chapter 5.2), and (iv) derivation of ratios of metabolic fluxes in the network (Szyperski, 1995; Szyperski *et al.* 1996*a*). The information that was obtained from the BDF ^{13}C-labelling experiment performed with riboflavin-producing B. subtilis (Sauer *et al.* 1997) is summarized in the flux chart of Fig. 9 (see also chapter 5.2). A crucial result of this analysis is the evidence provided for

---

3Pg, 3-phosphoglycerate; Pep, phosphoenolpyruvate; Pyr, pyruvate; Rib, riboflavin; Ri5P, ribose 5-phosphate; Ru5P, ribulose 5-phosphate; S7P, seduheptulose 7-phosphate; Ser, serine; Suc, succinate; T3P, triose 3-phosphate, i.e. glyceraldehyde 3-phosphate and dihydroxyacetone-phosphate; Xu5P, xylulose 5-phosphate.

https://doi.org/10.1017/S0033583598003412 Published online by Cambridge University Press

the activity of malic enzyme and phosphoenolpyruvat (Pep) carboxykinase, both of which were previously assumed to be inactive (Diesterhaft & Freese, 1973; Sauer *et al*. 1996). The labelling experiment thus turned out to be a powerful tool to unravel the complex interplay between glycolysis and TCA cycle. Moreover, the data showed that the glyoxalate shunt is inactive as was expected (Sauer *et al*. 1996), and yielded flux ratios that could be incorporated into a metabolic flux balancing calculation (Sauer *et al*. 1997; see chapter 6).

^{13}C-labelling of proteinogenic amino acids combined with 2D [^{13}C,^{1}H]-HSQC obviously provides a wealth of information on major biosynthetic pathways in a single experiment (Fig. 9), and the set of ^{13}C fine structures observed in the hydrolysate of cellular proteins (Fig. 4; for a complete survey see Fig. 3 in Szyperski, 1995) actually constitutes one kind of a 'fingerprint' of intermediary metabolism. The information from this approach could not readily be obtained in a single experiment using conventional 1D ^{13}C-NMR with selective ^{13}C-labelling (chapter 3.2), but BDF and selective ^{13}C-labelling protocols may fruitfully complement each other, since selective labelling experiments can be tailored to analyse specific metabolic subsystems. Although [U-^{13}C]glucose is rather expensive, the fact that only about 10% of the glucose are labelled in the growth medium makes this approach also economically interesting: the costs for [U-^{13}C] glucose required for the currently discussed BDF ^{13}C-labelling experiment performed for *B. subtilis* (Fig. 9; see also Fig. 12 and Sauer *et al*. (1997) for experimental details) amount to about 100 US$. BDF ^{13}C-labelling of proteinogenic amino acids in the biomass offers the additional great advantage that preparation of the NMR sample is simple because only the ensemble of all cellular proteins must be isolated and hydrolysed. Moreover, the demands for NMR instrument time are low due to the high inherent sensitivity of 2D [^{13}C,^{1}H]-HSQC (chapter 2.1.1.1), and the employment of such 2D spectroscopy also allows analysis of the amino acids without prior separation (Fig. 4). Finally, the data analysis is quite straightforward (Szyperski, 1995) and offers itself for implementation of automatic data interpretation in terms of (i) checks for the assumed network topology, (ii) the identification of irreversible reaction steps and (iii) determination of metabolic flux ratios. Hence, the approach promises to be useful as a standard analytical tool which can be applied in grid-search based protocols for the rapid investigation of the response of the cellular metabolism to perturbations.

4. METABOLIC FLUX BALANCING

The stoichiometry of the biochemical reactions constituting a metabolic network represents a firm body of knowledge, that is independent of reaction kinetics or thermodynamics. In conjunction with the likewise hardly challengeable law of mass conservation, the stoichiometry allows the formulation of a balancing equation for each metabolite (Fig. 10) stating that its net rate of synthesis is equal to the sum of fluxes generating the metabolite minus the sum of fluxes consuming the metabolite. For a network comprising n metabolites and m fluxes, this yields

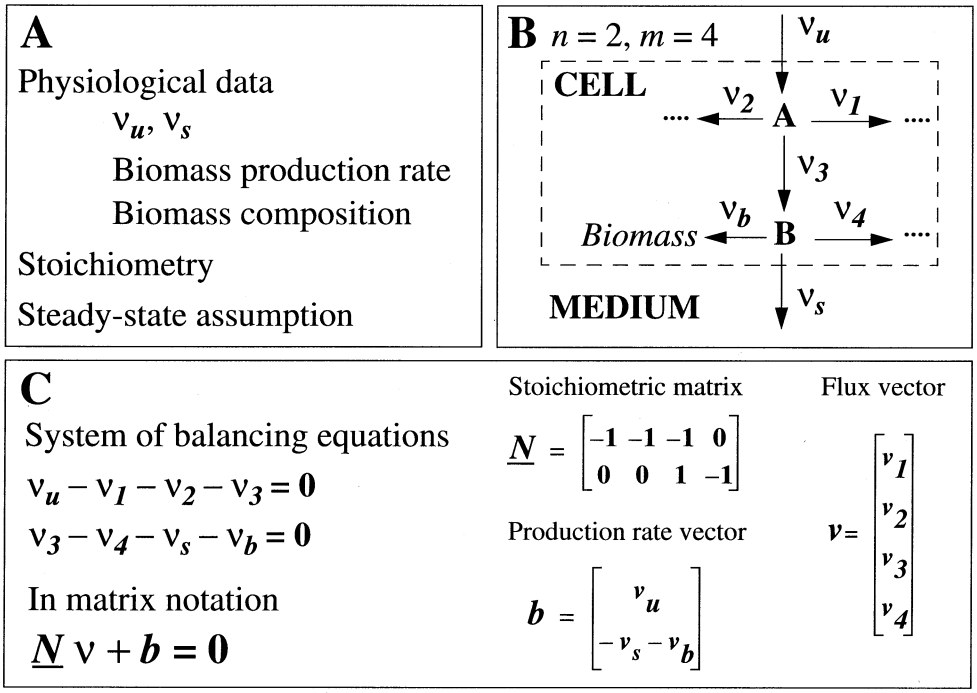

Fig. 10. Principles of metabolic flux balancing (MFB). (A) MFB relies on (i) physiological data as nutrient uptake rates, v_u, the secretion rates of metabolites, v_s, and the biomass production rate, (ii) the stoichiometry of the biochemical reactions, and (iii) a steady-state assumption for the operation of the bioreaction network. The drain of metabolites for biomass synthesis, v_b, can be inferred from the biomass production rate and the biomass composition. (B) Model for a bioreaction sub-network comprising two metabolites ($n = 2$) and four fluxes ($m = 4$). The resulting system of balancing equations (C) is underdetermined (see text).

a system of n differential equations with m unknown time-dependent fluxes. Provided that the network operates in a steady-state, the net rates of synthesis vanish for those intracellular metabolites which are not required for the generation of biomass, while those of extracellular metabolites and intracellular metabolites serving to create biomass are constant. Considering the biomass composition, which itself defines the demands for central metabolic precursors during cell growth, the non-zero net rates of intracellular metabolites can be determined from the measurement of the biomass production rate. The impact of a growth-rate dependent biomass composition has very recently been discussed by Pramanik & Keasling (1997), and it may well be that future MFB investigations will be performed with a biomass composition adapted to a given growth-rate. The net rates of the extracellular metabolites, i.e. the nutrient uptake, the oxygen consumption rate, and the excretion rate of metabolic by-products (e.g. acetate or lactate) can likewise be experimentally determined (e.g. Schügerl, 1991). Overall, combination of steady-state assumption, stoichiometry and measurement of consumption/production rates of extracellular metabolites and biomass yields a system of n linear equations connecting the m unknown time-independent fluxes

https://doi.org/10.1017/S0033583598003412 Published online by Cambridge University Press

of the bioreaction network. In a matrix notation, the production rate vector $\boldsymbol{b}$ is equal to the product of the stoichiometric matrix $\underline{\mathbf{N}}$ and the flux vector $\boldsymbol{v}$ (Fig. 10). This approach, consisting of the derivation of balancing equations and their subsequent interpretation to obtain *in vivo* fluxes (Verhoff & Spradlin, 1976; Papoutsakis, 1984; Fell & Small, 1986), has been coined 'metabolic flux balancing' (MFB) (Varma & Palsson, 1994). An important limitation of MFB is that it yields solely *net* fluxes and thus does not provide insight into exchange reaction rates, which are, however, of crucial importance for metabolic regulation.

A key drawback of MFB arises from the fact that the number of metabolites, n, involved in a realistic bioreaction network model is usually smaller than the number of fluxes, m, i.e. the resulting system of linear equations (Fig. 10) is underdetermined. Consequently, no unique solution exists, that is a multidimensional solution space satisfies the constraints. Its dimensionality may be further increased if some of the balances are linearly dependent, which results in $\underline{\mathbf{N}}$ having a rank smaller than n. To approach a low-dimensional solution space (e.g. Bonarius *et al.* 1997), the number of fluxes can be reduced, firstly, by lumping together those reactions that yield the linearly dependent balances for intracellular metabolites (Vallino & Stephanopoulos, 1990). This leads to a branch-point associated network characterized by a non-singular matrix $\underline{\mathbf{N}}$, but concomitantly it also leads to a less well resolved description of the *in vivo* flux distribution. Secondly, biochemical experiments, for example, enzyme assays (e.g. Walsh & Koshland, 1984, Vallino & Stephanopoulos, 1993; Park *et al.* 1997*b*), can be performed to identify those pathways which are actually active under the given experimental conditions. For future metabolic studies the application of DNA microarray technology (Hoheisel, 1997) may provide a comprehensive description of gene expression for the entire metabolic network (De Risi *et al.* 1997). Thirdly, the identification of irreversible reaction steps can be used to introduce lower boundaries for the corresponding fluxes, which further restricts the solution space. Here, the estimation of *in vivo* free enthalpies of biochemical reactions (Jones, 1979; Mavrovouniotis, 1990; Pissarra & Nielsen, 1997; Sauer *et al.* 1997) plays a key role, since large free enthalpies are indicative for irreversibility. Furthermore, additional balances involving co-metabolites such as ATP and nicotinamide adenine dinucleotide (phosphate) (NADPH or NADH) can be derived. However, this may easily lead to an unacceptable distortion of the flux distribution: the ATP balance can hardly be accurately interpreted since the ATP yield of the respiratory system and the ATP requirements for maintenance processes can only be estimated (e.g. Nicholls & Ferguson, 1992; Varma *et al.* 1993*a*; van Gulik & Heijnen, 1995), and separate balances for NADPH and NADH are inappropriate whenever the organism under consideration may posses a transhydrogenase interconverting these two co-metabolites (Sauer *et al.* 1996). Moreover, the calculated *in vivo* flux distribution is very sensitive to small changes in a NAD(P)H balance (Sauer *et al.* 1996), which is itself critically dependent on the measurement of the oxygen consumption rate. As a result, MFB calculations performed for virtually the same system have yielded significantly different flux distributions (Goel *et al.* 1993; Sauer *et al.* 1996), suggesting that such balances

have to be applied with care. In principle, a minimum number of measurements exists that provides a non-singular square matrix **N**, i.e. a determined system of equations. However, it is desirable to include more than this minimal number of measurements to reduce the experimental error of the flux determination and possibly to check the consistency of the experimental values and validity of the assumed bioreaction network (Vallino & Stephanopoulos, 1990). In particular, the measurement of the CO2 production rate allows determination of the overall carbon balance of the system under investigation.

A second critical issue for the application of MFB is the inherent sensitivity of the calculated flux distribution to the experimental error of measured extracellular rates and/or modifications of the bioreaction network model. The calculation of a scalar quantity, termed 'condition number' of the stoichiometric matrix **N**, provides a first indication if the system is well-posed, and the determination of a 'sensitivity matrix' reveals which fluxes react strongly on modifications of the network (Vallino & Stephanopoulos, 1990). When combining MFB calculations with measurements of intracellular fluxes, e.g. using data obtained from ^{13}C-labelling experiments (chapter 5), a sensitivity analysis may guide the selection of those intracellular fluxes which are most suitably measured to complement MFB (Savinell & Palsson, 1992).

Careful design of the network model according to the principles outlined above, in conjunction with the determination of additional extracellular metabolites, has yielded either determined systems of balancing equations which can be solved by inversion of the stoichiometric matrix (e.g. Jin *et al.* 1997), or overdetermined systems for which a least-squares algorithm is used to find a unique flux distribution (e.g. Goel *et al.* 1993; Vallino & Stephanopoulos, 1993; Sauer *et al.* 1996). However, for many MFB studies published so far, the system of equations turned out to be underdetermined. The resulting solution space for the *in vivo* fluxes has been dubbed the 'stoichiometrically-defined domain' (Varma *et al.* 1993*a*). To obtain a single flux distribution, it is necessary to define an objective function depending on the fluxes that implements a defined criterion, for example, maximal (or minimal) production of a co-factor (e.g. Fell & Small, 1986), maximal cellular growth (e.g. Varma *et al.* 1993*a*) or maximal production of a certain metabolite (Holms, 1996; Sauer *et al.* 1998). The search for an extremum of this function by an appropriate optimization algorithm (Gill *et al.* 1981) then yields an unique solution. Obviously, the true *in vivo* flux distribution does not necessarily have to be close to the one with an extremum objective function, but for wild-type strains one may argue that maximizing cellular growth coincides with a major selection criterion in natural evolution (Varma & Palsson, 1994). Nonetheless, this strategy has allowed the exploration of the extremes of stoichiometrically-defined domains in various biotechnologically important cells, i.e. to assess metabolic production capacities (e.g. Papoutsakis, 1984; Varma & Palsson, 1993; Jørgensen *et al.* 1995; Holms, 1996; Sauer *et al.* 1998), to study recombinant mutants (e.g. Tsai *et al.* 1996; Jin *et al.* 1997; Park *et al.* 1997*b*), or to find a rationale for by-product secretion at high growth rates (Majewski & Domach, 1990) or under oxygen limitation (Varma *et al.* 1993*b*). Principle advantages of such MFB studies

are, firstly, their applicability to cell culture processes of any scale and, secondly, their sole dependence on extracellular measurements. This makes MFB also most attractive for a variety of biotechnological applications such as on-line process control or growth medium optimization (Bonarius *et al.* 1997).

5. SYNERGY OF ^{13}C-LABELLING EXPERIMENTS AND FLUX BALANCING

5.1 *Methodology*

To assure that the fluxes derived from combined use of ^{13}C-labelling data and MFB equations properly reflect the actual metabolic steady-state, the system also needs to be in an isotopic steady-state. For biomass-oriented ^{13}C-labelling experiments (chapter 3.1) performed in a nutrient-limited chemostat, it suffices to ensure an isotopic steady-state for the metabolites constituting the central bioreaction network. This is because the fraction of harvested non-enriched biomass can be assessed according to a first-order wash-out kinetic, characterizing the dilution behaviour of an ideal continuously operated vessel (Sauer *et al.* 1997). The isotopic steady-state of bacterial central metabolism is established in a time-span much shorter than the doubling time of the culture. Walsh & Koshland (1984) could demonstrate than the isotopic steady-state in central metabolism *of E. coli* is reached within 1 min after incubation with medium containing the labelled precursor. A significantly longer time-span has to elapse if the establishment of an isotopic steady-state is retarded by dynamic equilibria connecting central metabolite pools to large pools of other non-enriched metabolites (e.g. Marx *et al.* 1996).

The integration of data from ^{13}C-labelling protocols and MFB can be accomplished at different levels of sophistication. (i) The results of the labelling experiment can be used as a mere control for *in vivo* fluxes obtained from MFB (Zupke & Stephanopoulos, 1995) in order to support the development of MFB protocols suitable for large-scale applications (chapter 4) where ^{13}C-labelling experiments are prohibitive expensive. (ii) Flux ratios are calculated from balance equations formulated either for IEs (e.g. Walsh & Koshland, 1984; Schuster *et al.* 1992; Sharfstein *et al.* 1994) or intact carbon fragments arising from a single precursor molecule (Szyperski, 1995; chapter 3.4). Then, the flux ratios are expressed according to the flux definitions of the bioreaction network model, and are merged with the underdetermined system of MFB equations (Szyperski *et al.* 1996*a*; Sauer *et al.* 1997) and possibly complemented by an objective function (e.g. for minimal NADH production; Sharfstein *et al.* 1994). This yields an (over)determined system that can be solved by minimizing a non-linear, but convex target function representing the sum of the squares of the deviations from the linear constraints calculated for a flux distribution (Sauer *et al.* 1996; 1997). Most important, the convexity of the target function ensures the existence of an unique solution (Gill *et al.* 1981). Subsequently, the combination of the net fluxes with information about exchange processes inferred from the labelling experiment allows a rough estimation of exchange fluxes (Sauer *et al.* 1997; T. Szyperski, M. Hochuli & K. Wüthrich, unpublished results). (iii) The MFB equations are

directly extended by balance equations for IEs (Portais *et al*. 1993; Marx *et al*. 1996) and/or isotopomers (Wiechert & de Graaf, 1996), and the resulting system of equations is solved by a least-squares calculation. This approach promises to make use of the entire information provided by the labelling experiment and allows incorporation of bidirectional fluxes into the formalism (Marx *et al*. 1996; Wiechert & de Graaf, 1997; Wiechert *et al*. 1997). However, the resulting target function contains terms that are bilinear in flux and IE/isotopomer distributions. This gives rise to multiple minima on the target function surface, and thus a solution can only be assumed to be unique, i.e. to represent the global minimum, if a large number of initial flux distributions converge to the same final distribution. Furthermore, very rapid equilibration between different metabolite pools leads to additional numerical uncertainties (Wiechert & de Graaf, 1997).

For the setup of the IE/isotopomer balancing equations it is of practical and computational interest that formalisms using atom mapping matrices (Goebel *et al*. 1982; Zupke & Stephanopoulos, 1994) and isotopomer mapping matrices (Schmidt *et al*. 1997) have been established, which allow dissection of IE/isotopomer balances and metabolic flux balances. In particular, the 2^n isotopomer balances derived for each metabolite with n carbons can be condensed to a single matrix equation (Schmidt *et al*. 1997).

When comparing approaches (ii) and (iii) it appears that the major advantage of (ii) is due to the fact that no extension of the linear MFB formalism (Fig. 10; chapter 4) is required, while (iii) promises to fully exploit the ^{13}C-labelling data thereby yielding also more accurate estimates than (ii) for the exchange fluxes. These are themselves of utmost importance for metabolic regulation (Fell, 1997).

5.2 *Applications in support of biotechnological research*

Sharfstein *et al*. (1994) have studied hybridoma cells which play an important role for the large-scale production of antibodies for biomedical and analytical purposes. Understanding the metabolism of such cells is of interest to develop a rational approach increasing antibody productivity by application of recombinant DNA technology (e.g. Park *et al*. 1996) and/or growth medium optimization (e.g. Stoll *et al*. 1996). Remarkably, hybridoma cells derive a significant fraction of their metabolic energy from glutamine catabolism, i.e. glutamine is deamidated to glutamate and subsequently to 2Og, a key intermediate of the TCA cycle. The ammonia generated during glutaminolysis is transferred to Pyr resulting in the secretion of alanine. Carbon entering at 2Og leaves the TCA cycle primarily (i) via the action of the malic enzyme, (ii) via the action of Pep carboxykinase, or (iii) as citrate recruited for lipid synthesis. Moreover, hybridoma cells exhibit high rates of aerobic lactate formation. Sharfstein *et al*. (1994) have studied the response of hybridoma central metabolism to a variation of the glutamine concentration in a rich medium that was complemented with glucose as a major carbon source (see also Mancuso *et al*. 1994). Their investigation showed: (i) that a decreased glutamine feed concentration diminished glutamine uptake in the cells but had little effect on glucose catabolism, (ii) that the antibody production increased in

concert with a decreasing glutamine level, (iii) that about 92 % of the glucose is catabolised *via* glycolysis while only about 8 % are introduced into the PPP, (iv) that lipid biosynthesis from citrate dominates over the action of malic enzyme and Pep carboxykinase, and (v) that protein turnover leads to an exchange between the TCA intermediate and amino acid pools. A major conclusion from these findings is that antibody production in hybridoma cells is apparently not energy-limited. This finding supports the view that the high metabolic rates in tumorigenic cells are primarily afforded to create the ability for an immediate increase of the proliferation rate when required (Newsholme, 1985).

Marx *et al*. (1996) have determined metabolic fluxes in central metabolism of the bacterium *C. glutamicum* which is of industrial interest for the large-scale production of amino acids (e.g. Eggeling *et al*. 1996). *C. glutamicum* possesses a control architecture of central metabolism that is simpler than those of *E. coli* or *B. subtilis*. This is of importance in view of its metabolic engineering (Eggeling *et al*. 1997). Moreover, fewer isoenzymes are expressed, degrading enzymes are absent for many amino acids and acetate by-product secretion is significantly reduced when compared with enterobacteria such as *E. coli*. Fig. 11 displays a chart comprising the fluxes through central metabolic pathways of a lysine producing Leu$^-$ *C. glutamicum* strain grown in a nutrient-limited chemostat with a minimal medium that contained D-glucose and L-leucine as the sole carbon sources. The fluxes were calculated by Wiechert *et al*. (1997) based on the data published by Marx *et al*. (1996). These data showed (i) that as much as 66 % of the glucose enters the oxidative branch of PPP rather than glycolysis, (ii) that the oxidative pathway exceeds the anaplerotic supply of the TCA cycle by a factor of about 1·5, (iii) that the glyoxalate shunt is virtually switched off, an observation that cannot be derived from a MFB calculation alone (Walsh & Koshland, 1984), and (iv) that fast exchange rates were found in the sub-network comprising glycolysis and PPP, and, remarkably also between the C4 pool of the TCA cycle and the pool containing Pyr and Pep, which implies futile cycling at the glycolysis/TCA interface. Similiarly rapid exchange in the non-oxidative branch of the PPP had previously been reported *in vivo* for human erythrocytes (Berthon *et al*. 1993) as well as *in vitro* (Flanigan *et al*. 1993). These studies suggest that ^{13}C-labelling data can be interpreted accurately only if such exchange reactions are properly considered (e.g. Flanigan *et al*. 1993; Rognstad, 1995; Wiechert *et al*. 1997). Since the fluxes of Fig. 11 were determined without balances for NAD(P)H, the production of NADPH *via* the oxidative branch of the PPP and the isocitrate dehydrogenase reaction in the TCA cycle can be compared with the demands for biosynthesis calculated from lysine and biomass production rates. Marx *et al*. (1996) found an excess production of about 10 % relative to the NADPH demands. The fact that *C. glutamicum* possesses no transhydrogenase led the authors to postulate a NADPH oxidase ensuring NADPH regeneration.

Sauer *et al*. (1997) investigated a metabolically-engineered riboflavin-producing *B. subtilis* strain. These studies are important in view of the fact that, firstly, *B. subtilis* serves for the industrial production of riboflavin (vitamin B_2) (Perkins *et al*. 1991), that, secondly, various *Bacillus* species are nowadays used as hosts in

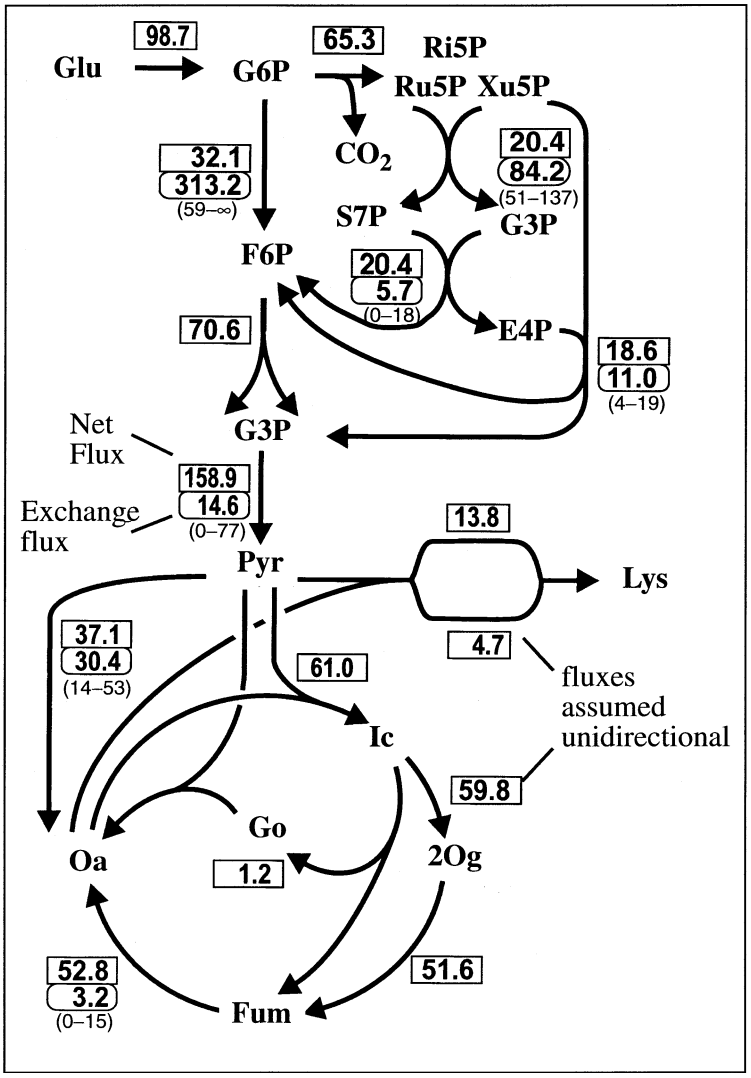

Fig. 11. *In vivo* flux distribution in central carbon metabolism of *C. glutamicum* cells that were grown in a continuous culture under lysine-producing conditions (for details see Marx *et al.* 1996; Wiechert *et al.* 1997). All fluxes are normalized relative to the glucose uptake rate which was set to 100. Net fluxes are indicated in boxes. Exchange fluxes are given in boxes with rounded corners, and their 90% confidence error intervals are indicated in parentheses below these boxes (Wiechert *et al.* 1997). For simplicity, biomass and CO_2 effluxes are not shown. Abbreviations: Lys, lysine; Glu, glucose. For the other abbreviations see the legend of Fig. 9. Adapted with permission from Wiechert *et al.* (1997).

fermentation industry (Harwood, 1992) since they are able to secrete large quantities of protein directly into the medium, and that, thirdly, *B. subtilis* has become a model organism representing the gram-positive bacteria (Sonenshein *et al.* 1993). In particular, future research targeting *B. subtilis* is likely to profit from its recently published complete genome sequence (Kunst *et al.* 1997). Sauer *et al.* (1997) have grown *B. subtilis* cells in a glucose-limited chemostat at three different

https://doi.org/10.1017/S0033583598003412 Published online by Cambridge University Press

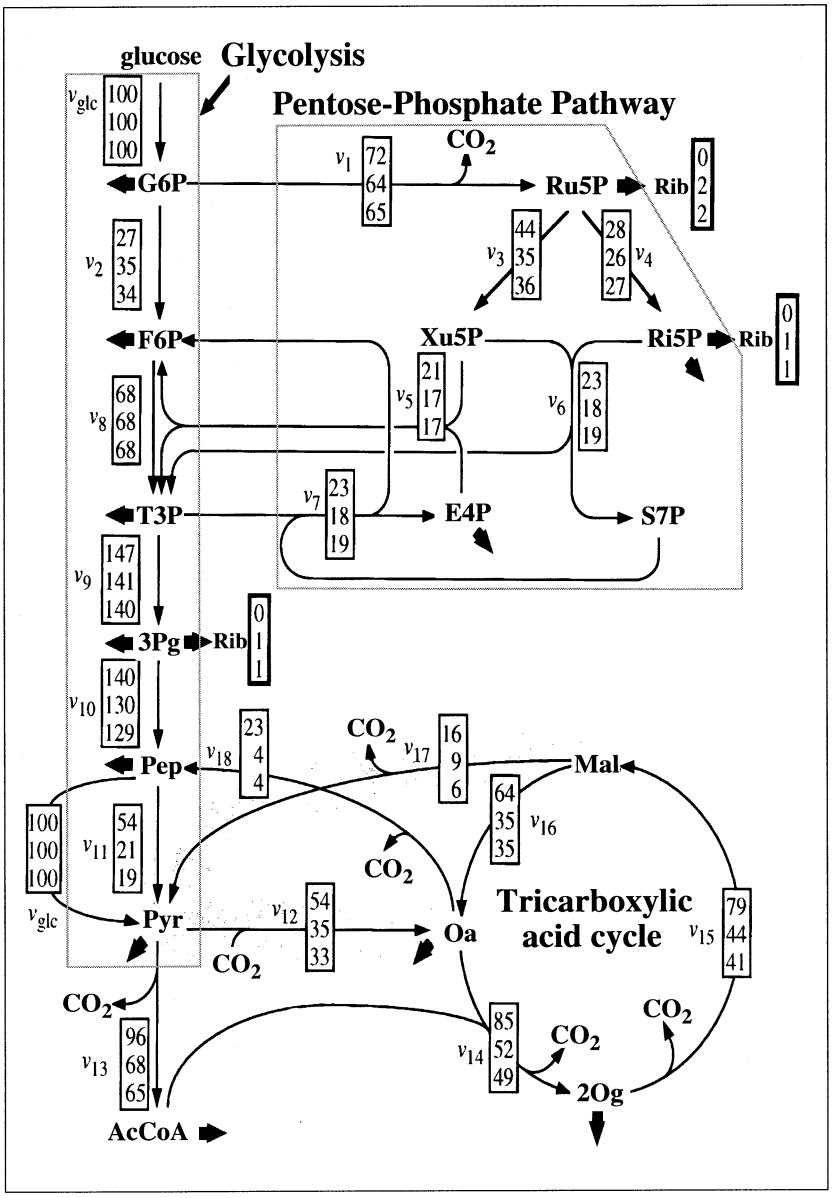

Fig. 12. *In vivo* flux distribution in central carbon metabolism of the riboflavin-producing *B. subtilis* strain PRF grown in a glucose-limited chemostat as obtained from the combined application of metabolic flux balancing and the following NMR-derived equality constraints derived from a biosynthetically-directed fractional ^{13}C labelling experiment (see Fig. 9): (i) fraction of Pyr originating from Mal ($= \nu_{17}/\nu_{17}+\nu_{11}+\nu_{glc}$), (ii) the fraction of Oa originating from Pyr ($= \nu_{12}/\nu_{12}+\nu_{16}$), (iii) the fraction of Pep originating from Oa ($= \nu_{18}/\nu_{18}+\nu_{10}$) and (iv) an upper limit for the fraction of T3P generated through PPP ($= \nu_9+\nu_{bs}^{F6P}+\nu_{bs}^{F3P}-2\nu_2/\nu_9+\nu_{bs}^{F6P}+\nu_{bs}^{F3P}$), where ν_{bs} represent fluxes accounting for biosynthetic requirements (Sauer *et al.* 1997). Only the branch point-associated metabolites indicated in the figure were considered in the biochemical reaction network. Withdrawal of precursor metabolites for biomass and riboflavin biosynthesis is indicated by arrows. Numbers in white rectangles represent the estimated molar net fluxes, normalized to the glucose uptake rates set to 100,

https://doi.org/10.1017/S0033583598003412 Published online by Cambridge University Press

dilution rates, *D*, in order to assess the adaptation of central metabolism to changing nutrient supply. The results of this investigation are summarized in the flux chart of Fig. 12 (see also Fig. 9) and provided the following insights. (i) Between 65 and 72% (with increasing *D*) of the glucose enters the oxidative branch of the PPP, showing that the PPP must be considered a major pathway of glucose catabolism (a similar value was obtained for *C. glutamicum*; Fig. 11). (ii) The interplay of fluxes at the interface of glycolysis and the TCA cycle could be evaluated at unprecedented resolution: the reactions catalysed by the malic enzyme and the Pep carboxykinase, which were previously considered to be inactive (Diesterhaft & Freese, 1973; Sauer *et al.* 1996), consumed up to 23% of the metabolized glucose at the lowest dilution rate thus indicating significant futile cycling. In addition, the oxidative pathway for introducing Acetyl-CoA into the TCA cycle exceeds the anaplerotic supply via pyruvate carboxylase by a factor of about 1·5 nearly independent of *D*. (iii) Exchange processes could be studied in the PPP and the TCA cycle: the degree of reversibility of the first transketolase reaction in the PPP interconverting two pentose phosphate molecules into seduheptulose 7-phosphate and glyceraldehyde 3-phosphate decreases with increasing *D*. Less than 15% of the erythrose 4-phosphate originates from fructose 6-phosphate indicating that the employment of the non-oxidative branch for pentose synthesis is small. Multiple cycling through the PPP was found to be $< 10\%$ at all dilution rates, and a high exchangeability was observed in the dicarboxylic acid segment of the TCA cycle. (iv) The glyoxalate shunt was found to be switched off, (v) C_1-metabolism assessed *via* Ser and Gly appeared not to be affected by a variation of *D*, and (vi) the first step of riboflavin biosynthesis was found to be irreversible. The *in vivo* fluxes of Fig. 12 subsequently provided valuable information about cellular energetics and the turnover of reducing equivalents. Comparison of NADPH production and consumption (Fig. 13) revealed a high capacity for reoxidation of NAPDH by a transhydrogenase, which provides a rationale for understanding the unique ability of transketolase-deficient mutants of *Bacillus* species to accumulate D-ribose (Sasajima & Yoneda, 1984) and the fact that these species are generally good producers of purines and riboflavin. Likewise, ATP production by glucose catabolism can be estimated when a certain energy stoichiometry is assumed, e.g. that 2 ATP molecules are generated per oxygen atom (see Fig. 3 in Sauer *et al.* 1997). In particular at lower *D*, a major fraction of ATP was found to be generated in excess of biosynthetic requirements, partly to satisfy cellular maintenance processes and, to about 10% of the total ATP production at lowest D, to drive futile cycling in the Pep-Pyr-Oa triangle. It thus turned out that riboflavin production was limited neither by supply of metabolic precursors nor by the supply of the co-factors NADPH and ATP. This indicated that the bottleneck for riboflavin production very likely occurs in its biosynthetic pathway and thus suggested a focus for future metabolic engineering.

---

at, from the top to the bottom, dilution rates, *D* (defined as the ratio of the medium feed rate [L h^{-1}] and the culture volume [L]) of 0·11, 0·41 and 0·62 h^{-1}. For the abbreviations see Fig. 9. Adapted with permission from Sauer *et al.* (1997).

https://doi.org/10.1017/S0033583598003412 Published online by Cambridge University Press

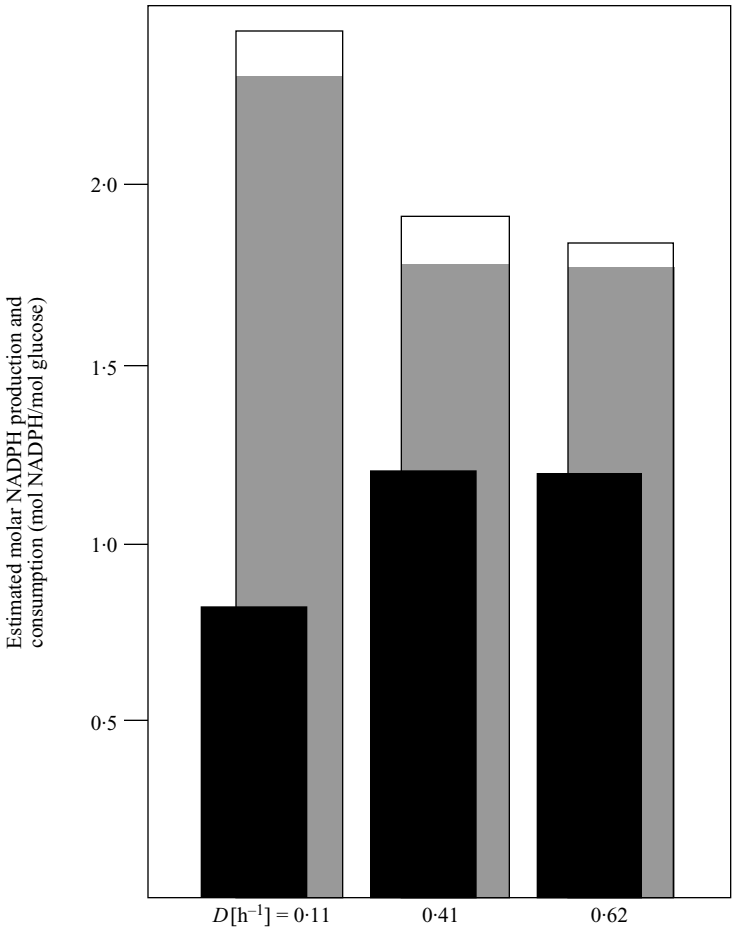

Fig. 13. Estimated molar production and consumption of NADPH per mol of glucose, calculated on the basis of the *in vivo* net fluxes (Fig. 12) that were obtained for riboflavin-producing *Bacillus subtilis* strain PRF grown in a glucose-limited chemostat at three dilution rates, D. The black bars represent the total theoretical NADPH requirements for synthesis of biomass (16·06 mol NADPH/g of cells) and riboflavin formation (3·5 mol NADPH/mol riboflavin). The dark grey bars indicate the estimated NADPH formation *via* the oxidative PPP (v_1 in Fig. 12) and the isocitrate dehydrogenase (v_{14} in Fig. 12). Additional NADPH generation by a potentially NADPH-dependent malic enzyme (v_{18} in Fig. 12) in indicated by the white bars. Reproduced with permission from Sauer *et al.* (1997).

6. PERSPECTIVES

Future metabolic studies using ^{13}C isotope labelling will greatly benefit from recent methodological advances such as (i) new NMR experiments designed for solution and also solid state measurements (chapter 2.1), (ii) increased sensitivity of commercially available NMR spectrometer accomplished, for example, through the development of cryogenic probeheads (e.g. Kim *et al.* 1995), (iii) integrated liquid chromatography NMR/MS (LC-NMR/MS) systems (e.g. Spraul *et al.*

1993; Stevenson & Dorn, 1994), or (iv) high precision gas IRMS (chapter 2.2). Furthermore, integrated approaches to comprehensively assess a cell's metabolic state will exploit the synergy arising from the combined use of ^{13}C-labelling experiments with, firstly, techniques such as DNA microarray chips (e.g. Lockhardt *et al*. 1996; Hoheisel, 1997) or fibre-optic biosensors (Ferguson *et al*. 1996), which offer a high degree of parallelism (Pennisi, 1996) and thus allow for a genomewide exploration of gene expression (De Risi *et al*. 1997), and, secondly, the 'proteome approach' (e.g. Wilkens *et al*. 1995) which aims at the construction of complete protein maps (James, 1997) in order to assess protein expression quantitatively.

These developments promise to yield extremely powerful analytical tools to support metabolic engineering and process design in biotechnology, and they will be complemented (i) by advances in bioinformatics (e.g. Palsson, 1997) and the formulation of a more uniform and predictive theory of metabolism incorporating, for example, MCA and biochemical systems theory (chapter 1), (ii) by advances in recombinant DNA technology including, for example, the establishment of multicistronic expression vectors (e.g. Fussenegger *et al*. 1997) or mammalian artificial chromosomes (e.g. Vos, 1997) which pave the way to realize theoretically derived claims for metabolic engineering such as the coordinated and adjusted overexpression of several genes constituting a metabolic sub-network, and (iii) by an ever-increasing amount of data from structural biology which will give insight into the functioning of molecular processes at atomic resolution (e.g. Hendrickson & Wüthrich, 1991–7; Han *et al*. 1995). With respect to harvesting the fruits of metabolic engineering also in medicine (Yarmush & Berthiaume, 1997), the extension of ^{13}C-NMR approaches for metabolic studies in humans (Beckmann, 1995) will be of high interest, in particular because stable isotope tracers offer a degree of medical safety that cannot be achieved with radioactive tracers.

The impact of ^{13}C-labelling experiments, potentially employed in conjunction with MFB (chapter 5), for redesign of a metabolic network remains to be shown: none of the recently published successful examples for metabolic engineering (e.g. Alvarez *et al*. 1996; Flores *et al*. 1996; Morbach *et al*. 1996; Volschenk *et al*. 1997; Jacobsen *et al*. 1997) was based on knowledge derived from such experiments. This led Bailey *et al*. (1996) to introduce a phenotype-oriented approach dubbed 'inverse metabolic engineering'. However, the extremely rapid development of all fields connected to metabolic engineering, including ^{13}C-labelling protocols, will foreseeably engender many more successful cases of metabolic engineering in the future. The impact of ^{13}C-labelling experiments for our understanding of the crucial concepts of metabolism is obvious, and I may conclude this article with a quotation from Shulman & Rothman (1996) stating that 'the control of metabolism is entering a flourishing period of understanding and quantitation'.

7. ACKNOWLEDGEMENTS

The author is indebted to Professor K. Wüthrich for continuous support for nearly a decade, to Professor J. E. Bailey and Dr U. Sauer for constructive

criticism, to Dr F. Damberger, Dr G. Wider and M. Hochuli for the careful reading of the manuscript, and again to M. Hochuli for preparing Figure 9.

8. REFERENCES

ALVAREZ, M. A., FU, H., KHOSLA, C., HOPWOOD, D. A. & BAILEY, J. E. (1996). Engineered biosynthesis of novel polyketides: properties of the *whiE* aromatase/cyclase. *Nature Biotechnol.* **14**, 335–338.

BACHER. A., VAN, Q. L. & FLOSS, H. G. (1983). Biosynthesis of riboflavin. *J. biol. Chem.* **258**, 13431–13437.

BACHER. A., VAN, Q. L., KELLER, P. J. & FLOSS, H. G. (1985). Biosynthesis of riboflavin. Incorporation of multiply ^{13}C-labelled precursors into the xylene ring. *J. Am. chem. Soc.* **107**, 6380–6385.

BAILEY, J. E. (1991). Toward a science of metabolic engineering. *Science* **252**, 1668–1675.

BAILEY, J. E. & OLLIS, D. F. (1986). *Biochemical Engineering Fundamentals*. New York: McGraw-Hill.

BAILEY, J. E., SBURLATI, A., HATZIMANIKATIS, V., LEE, K., RENNER, W. A. & TSAI, P. S. (1996). Inverse metabolic engineering: a strategy for directed engineering of useful phenotypes. *Biotechnol. Bioeng.* **52**, 109–121.

BALDUS, M. & MEIER, B. H. (1996). Total correlation in the solid state. The use of scalar couplings to determine the through-bond connectivity. *J. magn. Reson. A* **121**, 65–69.

BARJAT, H., MORRIS, G. A., SMART, S., SWANSSON, A. G. & WILLIAMS, S. C. (1995). High-resolution diffusion-ordered 2D spectroscopy (HR-DOSY) – a new tool for the analysis of complex mixtures. *J. magn. Reson. B* **108**, 170–172.

BAX, A., CLORE, G. M. & GRONENBORN, A. M. (1990). ^{1}H-^{1}H correlation via isotropic mixing of ^{13}C magnetization, a new three-dimensional approach for assigning ^{1}H and ^{13}C spectra of ^{13}C-enriched proteins. *J. magn. Reson.* 88, 425–431.

BAX, A., FARLEY, K. A. & WALKER, G. S. (1996). Increased sensitivity for correlating poorly resolved proton multiplets to carbon-13 using selective or semi-selective pulses. *J. magn. Reson. A* **119**, 134–138.

BAX, A., FREEMAN, R. & KEMPSELL, S. P. (1980). Natural abundance ^{13}C–^{13}C coupling observed *via* double-quantum coherence. *J. Am. chem. Soc.* **102**, 4849–4852.

BAX, A. & POCHAPSKY, S. (1992). Optimized recording of heteronuclear multidimensional NMR spectra using pulsed field gradients. *J. magn. Reson.* **99**, 638–643.

BAX, A. & SUMMERS, M. F. (1986). ^{1}H and ^{13}C assignments from sensitivity-enhanced detection of heteronuclear multiple-bond connectivity by multiple-quantum NMR. *J. Am. chem. Soc.* **108**, 2093–2094.

BEALE, J. M., COTTRELL, C. E., KELLER, P. J. & FLOSS, H. G. (1987). Development of triple-quantum 'INADEQUATE' for biosynthetic studies. *J. magn. Reson.* **72**, 574–578.

BEALE, J. M. & FOSTER, J. L. (1996). Carbohydrate fluxes into alginate biosynthesis in *Azotobacter vinelandii* NCIB 8789: NMR investigation of the triose pools. *Biochemistry* **35**, 4492–4501.

BECKMANN, N. (1995). ^{13}C magnetic resonance spectroscopy as a noninvasive tool for metabolic studies on humans (ed. N. Beckmann), pp. 269–334. San Diego: Academic Press.

BENNETT, W. S. & HUBER, R. (1983). Structural and functional aspects of domain motions in proteins. *CRC crit. Rev. Biochem.* **15**, 291–384.

Berthon, H. A., Bubb, W. A. & Kuchel, P. W. (1993). ^{13}C n.m.r. isotopomer and computer-simulation studies of the non-oxidative pentose phosphate pathway of human erythrocytes. *Biochem. J.* **296**, 379–387.

Beylot, M., Previs, S. F., David, F. & Brunengraber, H. (1993). Determination of the ^{13}C-labelling pattern of glucose by gas chromatography-mass spectrometry. *Anal. Biochem.* **212**, 526–531.

Bhaumik, S. R. & Sonawat, H. M. (1994). Pyruvate metabolism *in Halobacterium salinarium*. *J. Bacteriol.* **176**, 2172–2176.

Bodenhausen, G. & Ruben, D. J. (1980). Natural abundance nitrogen-15 NMR by enhanced heteronuclear spectroscopy. *Chem. Phys. Lett.* **69**, 185–188.

Bonarius, H. P. J., Schmid, G. & Tramper, J. (1997). Flux analysis of underdetermined metabolic networks: the quest for the missing constraints. *Trends Biotechnol.* **15**, 308–314.

Brainard, J. R., Downey, R. S., Bier, D. M. & London, R. E. (1989). Use of multiple ^{13}C-labelling strategies and ^{13}C NMR to detect low levels of exogeneous metabolites in the presence of large endogenous pools: measurement of glucose turnover in a human subject. *Anal. Biochem.* **176**, 307–312.

Brand, A., Engelmann, J. & Leibfritz, D. (1992). A ^{13}C NMR study on fluxes into the TCA cycle of neuronal and glial tumor cell lines and primary cells. *Biochimie* **74**, 941–948.

Brenna, J. T. (1994). High-precision gas isotope ratio mass spectrometry: recent advances in instrumentation and biomedical application. *Acc. chem. Res.* **27**, 340–346.

Brunengraber, H., Kellher, J. K., & Des Rosiers, C. (1997). Applications of mass isotopomer analysis to nutrition research. *Ann. Rev. Nutr.* **17**, 559–596.

Cameron, D. C. & Tong, I.-T. (1993). Cellular and metabolic engineering. *Appl. biochem. Biotechnol.* **38**, 105–140.

Cavanagh, J., Fairbrother, J., Palmer, A. G., Skelton, N. J. (1996). *Protein NMR Spectroscopy*. London: Academic Press.

Cerdan, S. & Seelig, J. (1990). NMR studies of metabolism. *Annu. Rev. Biophys. biophys. Chem.* **19**, 43–67.

Chao, Y. & Liao, J. C. (1994). Metabolic responses to substrate futile cycling in *Escherichia coli*. *J. biol. Chem.* **269**, 5122–5126.

Chauvin, M. -F., Mégnin-Chanet, F., Martin, G., Lhoste, J.-M. & Bavarel, G. (1994). The rabbit kidney tubule utilizes glucose for glutamine synthesis. *J. biol. Chem.* **269**, 26025–26033.

Chen, A., Wu, D. & Johnson, C. S. (1995). Determination of molecular weight distributions for polymers by diffusion-ordered NMR. *J. Am. chem. Soc.* **117**, 7965–7970.

Christie, D. A., Powell, J. W., Stables, J. N. & Watt, R. A. (1987). A nuclear magnetic resonance study of the role of phosphoenolpyruvate carboxykinase (PEPCK) in the glucose metabolism of *Dipetalonema vitae*. *Mol. Biochem. Parasitol.* **24**, 125–130.

Chung, J., Tolman, J. R., Howard, K. P. & Prestegard, J. H. (1993). Three-dimensional ^{1}H-detected ^{13}C–^{13}C correlation experiments on oligosaccharides. *J. magn. Reson. B* **101**, 137–147.

Clayden, N. J. & Hesler, B. D. (1992). Multiexponential analysis of relaxation delays. *J. magn. Reson.* **98**, 271–282.

Cline, G. W. & Shulman, G. I. (1991). Quantitative analysis of the pathways of

glycogen repletion in periportal and perivenous hepatocytes *in vivo*. *J. biol. Chem.* **266**, 4094–4096.

Corso, T. N. & Brenna, J. T. (1997). High-precision position-specific isotope analysis. *Proc. natn. Acad. Sci. USA* **94**, 1049–1053.

Cunnane, S. C., Williams, S. C. R., Bell, J. D., Brookes, S., Craig, K., Iles, R. A. & Crawford, M. A. (1994). Utilization of uniformly labelled ^{13}C-polyunsaturated fatty acids in the synthesis of long-chain fatty acids and cholesterol accumulating in the neonatal rat brain. *J. Neurochem.* **62**, 2429–2436.

Debnam, P. M., Shearer, G., Blackwood, L. & Kohl, D. H. (1997). Evidence for channeling of intermediates in the oxidative pentose phosphate pathway by soybean and pea nodule extracts, yeast extracts, and purified yeast enzymes. *Eur. J. Biochem.* **246**, 283–290.

Den Hollander, J. A., Ugurbil, K., Brown, T. R., Bednar, M., Redfield, C. & Shulman, R. G. (1986). Studies of anaerobic and aerobic glycolysis *in Saccharomyces cerevisiae*. *Biochemistry* **25**, 203–211.

De Risi, J. L., Iyer, V. R. & Brown, P. O. (1997). Exploring the metabolite and genetic control of gene expression on a genomic scale. *Science* **278**, 680–686.

Des Rosiers, C., Di Donato, L., Comte, B., LaPlante, A., Marcoux, C., David, F., Fernandez, C. A. & Brunengraber, H. (1995). Isotopomer analysis of citric acid cycle and gluconeogenesis in rat liver. *J. biol. Chem.* **270**, 10027–10036.

Didonato, L., Des Rosiers, C., Montgomery, J. A., David, F., Garneau, M. & Brunengraber, H. (1993). Rates of gluconeogenesis and citric acid cycle in perfused livers, assessed from the mass spectrometric assay of the ^{13}C labelling pattern in glutamate. *J. biol. Chem.* **268**, 4170–4180.

Diesterhaft, M. D. & Freese, E. (1973). Role of pyruvate carboxylase, phospho*enol*pyruvate carboxykinase, and malic enzyme during growth and sporulation of *Bacillus subtilis*. *J. biol. Chem.* **248**, 6062–6070.

Dieualde-Noubhani, M., Raffard, G., Canioni, P., Pradet, A. & Raymond, P. (1995). Quantification of compartmented metabolic fluxes in maize root tips using isotope distribution from ^{13}C- or ^{14}C-labelled glucose. *J. biol. Chem.* **270**, 13147–13159.

Distefano, J. J. (1980). Design and optimization of tracer experiments in physiology and medicine. *Federation Proc.* **39**, 84–90.

Eberstadt, M., Gemmecker, G., Mierke, D. F. & Kessler, H. (1995). Scalar coupling constants – their analysis and their application for the elucidation of structures. *Angew. Chem. Int. Ed. Engl.* **34**, 1671–1695.

Edison, A. S., Abildgaard, F., Westler, W. M., Mooberry, E. S. & Markley, J. (1994). Practical introduction to theory and implementation of multinuclear, multidimensional nuclear magnetic resonance experiments. *Meth. Enzymol.* **239**, 3–78.

Eggeling, L., Sahm, H. & De Graaf, A. A. (1996). Quantifying and directing metabolic flux: application to amino acid overproduction. In *Advances in Biochemical Engineering Biotechnology* **54** (ed. T. Scheper), pp. 1–30. New York: Springer.

Eggeling, L., Morbach, S. & Sahm, H. (1997). The fruits of molecular physiology: engineering the L-isoleucine biosynthesis in *Corynebacterium glutamicum*. *J. Biotechnol.* **56**, 167–182.

Eisenreich, W., Strauss, G., Werz, U., Fuchs, G. & Bacher, A. (1993). Retrobiosynthetic analysis of carbon fixation in the phototrophic eubacterium *Chloroflexus aurantiacus*. *Eur. J. Biochem.* **215**, 619–632.

Eisenreich, W., Kupfer, E., Weber, W. & Bacher, A. (1997). Tracer studies with crude U-^{13}C-lipid mixtures. *J. biol. Chem.* **272**, 867–874.

Ekiel, I., Smith, I. C. P. & Sprott, G. D. (1983). Biosynthetic pathways in Methanospirillum hungatei as determined by ^{13}C nuclear magnetic resonance. *J. Bacteriol.* **156**, 316–326.

Ekiel, I., Jarrell, K. F. & Sprott, G. D. (1985). Amino acid biosynthesis and sodium-dependent transport in *Methanococcus voltae*, as revealed by ^{13}C NMR. *Eur. J. Biochem.* **149**, 437–444.

Ernst, R. R., Bodenhausen, G. & Wokaun, A. (1987). *Principles of Nuclear Magnetic Resonance in One and Two Dimensions*. Oxford: Clarendon Press.

Evans, J. N. S., Raleigh, D. P., Tolman, C. J. & Roberts, M. F. (1986). ^{13}C NMR spectroscopy of *Methanobacterium thermoautotrophicum*. Carbon fluxes and primary metabolic pathways. *J. biol. Chem.* **261**, 16323–16331.

Fell, D. A. (1992). Metabolic control analysis: a survey of its theoretical and experimental development. *Biochem. J.* **286**, 313–330.

Fell, D. A. (1997). *Understanding the Control of Metabolism*. London: Portland Press.

Fell, D. A. & Small, J. R. (1986). Fat synthesis in adipose tissue. An examination of stoichiometric constraints. *Biochem. J.* **238**, 781–786.

Fell, D. A. & Thomas, S. (1995). Physiological control of metabolic flux: the requirement for multisite regulation. *Biochem. J.* **311**, 35–39.

Ferguson, J. A., Boles, T. C., Adams, C. P. & Walt, D. R. (1996). A fiber-optic DNA biosensor microarray for the analysis of gene expression. *Nature Biotechnol.* **14**, 1681–1684.

Fersht, A. (1985). *Enzyme Structure and Mechanism*. New York: Freeman.

Flanigan, I., Collins, J. G., Arora, K. K., Macleod, J. K. & Williams, J. F. (1993). Exchange reactions catalysed by group-transferring enzymes oppose the quantitation and unravelling of the identity of the pentose pathway. *Eur. J. Biochem.* **213**, 477–485.

Flores, N., Xiao, J., Berry, A., Bolivar, F. & Valle, F. (1996). Pathway engineering for the production of aromatic compounds in *Escherichia coli*. *Nature Biotechnol.* **14**, 620–623.

Fodor, S. P. A. (1997). Massively parallel genomics. *Science* **277**, 393–395.

Fraenkel, D. G. (1992). Genetics and intermediary metabolism. *Ann. Rev. Genet.* **26**, 159–177.

Fujiwara, T., Sugase, K., Kainosho, M., Ono, A., Ono, A. M. & Akutsu, H. (1995). ^{13}C–^{13}C and ^{13}C–^{15}N dipolar correlation of uniformly labelled organic solids for the complete assignment of their ^{13}C and ^{15}N signals: an application to adenosine. *J. Am. chem. Soc.* **117**, 11351–11352.

Fussenegger, M., Moser, S., Mazur, X. & Bailey, J. E. (1997). Autoregulated multicistronic expression vectors provide one-step cloning of regulated gene expression in mammalian cells. *Biotechnol. Prog.* **13**, 733–740.

Gadian, D. G. (1995). *NMR and its Applications to Living Systems*. Oxford: Oxford University Press.

Gagnaire, D. Y. & Taravel, F. R. (1979). New nuclear magnetic resonance methodology in biosynthetic studies of mixtures of statistically enriched ^{13}C and unlabelled precursors. *J. Am. chem. Soc.* **101**, 1625–1626.

Gagnaire, D. Y. & Taravel, F. R. (1980). Biosynthèse de cellulose bactérienne à partir de D-glucose uniformément enrichi en ^{13}C. *Eur. J. Biochem.* **103**, 133–143.

Galimov, E. M. (1985). *The Biological Fractionation of Isotopes*. New York: Academic Press.

Garbow, J. R., Weitekamp, D. P. & Pines, A. (1982). Bilinear rotation decoupling of homonuclear scalar interactions. *Chem. Phys. Lett.* **93**, 504–509.

Gavin, J. A., Pons, J. L. & Delsuc, M. A. (1996). Relative sensitivity of different acquisition schemes for ^{13}C natural-abundance HSQC experiments. *J. magn. Reson. A* **122**, 64–66.

Gemmecker, G. & Kessler, H. (1995). Methodology and applications of heteronuclear and multidimensional ^{13}C NMR to the elucidation of molecular structure and dynamics in the liquid state. In *Carbon-13 NMR Spectroscopy of Biological Systems* (ed. N. Beckmann), pp. 7–64. San Diego: Academic Press.

Gibbs, S. J. & Johnson, C. S. (1991). A PFG NMR experiment for accurate diffusion and flow studies in the presence of eddy currents. *J. magn. Reson.* **93**, 395–402.

Gill, P. E., Murray, W. & Wright, M. H. (1981). *Practical Optimization*. London: Academic Press.

Gleixner, G. & Schmidt, H. (1997). Carbon isotope effects on the fructose-1,6-bisphosphate aldolase reaction, origin for non-statistical ^{13}C distributions in carbohydrates. *J. biol. Chem.* **272**, 5382–5387.

Goebel, R., Berman, M. & Foster, D. (1982). Mathematical model for the distribution of isotopic carbon atoms through the tricarboxylic acid cycle. *Federation Proc.* **41**, 96–103.

Goel, A., Ferrance, J., Jeong, J. & Ataai, M. M. (1993). Analysis of metabolic fluxes in batch and continuous cultures of *Bacillus subtilis*. *Biotechnol. Bioeng.* **42**, 686–696.

Gopher, A., Vaisman, N., Mandel, H. & LaPidot, A. (1990). Determination of fructose metabolic pathways in normal and fructose-intolerant children: a ^{13}C NMR study using [U-^{13}C] fructose. *Proc. natn. Acad. Sci. U.S.A.* **87**, 5449–5453.

Gosser, Y. Q., Howard, K. P. & Prestegard, J. H. (1993). Three-dimensional ^{1}H-detected^{13}C–^{13}C correlation experiments for carbon backbone assignments of enriched natural products. *J. magn. Reson.* **B 101**, 126–133.

Gottschalk, G. (1986). *Bacterial Metabolism*. New York: Springer-Verlag.

Gould, S. J. & Cane, D. E. (1982). Biosynthesis of streptonigrin from [U-$^{13}C_6$]-D-glucose. Origin of the quinoline quinone. *J. Am. chem. Soc.* 104, 343–346.

Gout, E., Bligny, R., Pascal, N. & Douce, R. (1993). ^{13}C Nuclear magnetic resonance studies of malate and citrate synthesis and compartmentation in higher plant cells. *J. biol. Chem.* **268**, 3986–3992.

Gozansky, E. K. & Gorenstein, D. G. (1996). DOSY-NOESY: diffusion ordered NOESY. *J. magn. Reson. B* **111**, 94–96.

Grzesiek, S., Kuboniwa, H., Hinck, A. P. & Bax, A. (1995). Multiple-quantum line narrowing for measurement of H^{α}–H^{β} J couplings in isotopically enriched proteins. *J. Am. chem. Soc.* **117**, 5312–5315.

Gullion, T. & Schaefer, J. (1989a). Rotational-echo double-resonance NMR. *J. magn. Reson.* **81**, 196–200.

Gullion, T. & Schaefer, J. (1989b). Detection of weak heteronuclear dipolar coupling by rotational-echo double-resonance nuclear magnetic resonance. *Adv. magn. Reson.* **13**, 57–83.

Hamer, G. (1985). Chemical engineering and biotechnology. In *Biotechnology* (eds. I. J. Higgins, D. J. Best & J. Jones), pp. 346–414. Oxford: Blackwell Science Publications.

Han, S., Eltis, L. D., Timmis, K. N., Muchmore, S. W. & Bolin, J. T. (1995). Crystal structure of the biphenyl-cleaving extradiol dioxygenase from PCB-degrading pseudomonad. *Science* **270**, 976–980.

Hansen, P. E. (1981). Carbon-hydrogen spin-spin coupling constants. *Prog. nucl. magn. Reson.* **14**, 175–296.

Hansen, P. E. (1988). Isotope effects in nuclear shielding. *Prog. NMR Spectrosc.* **20**, 207–255.

Hardy, G. & Oliver, K. G. (1985). Genetics and biotechnology. In *Biotechnology* (eds. I. J. Higgins, D. J. Best & J. Jones), pp. 257–282. Oxford: Blackwell Science Publications.

Harwood, C. R. (1992). *Bacillus subtilis* and its relatives: molecular biological workhorses. *Trends Biotechnol.* **10**, 247–256.

Hatzimanikatis, V. & Bailey, J. E. (1996). MCA has more to say. *J. theor. Biol.* **182**, 233–242.

Hatzimanikatis, V. & Bailey, J. E. (1997). Effects of spatiotemporal variations on metabolic control: approximate analysis using (log)linear kinetic models. *Biotechnol. Bioeng.* **54**, 91–104.

Hatzimanikatis, V., Emmerling, M., Sauer, U. & Bailey, J. E. (1998). Application of mathematical tools for metabolic design of microbial ethanol production. *Biotechnol. Bioeng.*, in press.

Heinrich, R. & Rapoport, T. A. (1974). A linear steady-state treatment of enzymatic chains. *Eur. J. Biochem.* **42**, 89–95.

Hellerstein, M. K. & Neese, R. A. (1992). Mass isotopomer distribution analysis: a technique for measuring biosynthesis and turnover of polymers. *Am. J. Physiol.* **263**, E988–E1001.

Hendrickson, W. A. & Wüthrich, K. (eds.) (1991–1997). *Macromolecular Structures*. London: Current Biology.

Hess, B. (1997). Periodic patterns in biochemical reactions. *Quart. Rev. Biophys.* **30**, 121–176.

Hesse, M., Meier, H. & Zeeh, B. (1995). *Spektroskopische Methoden der Chemie*. Stuttgart: Thieme Verlag.

Higgins, T. P., Hewlins, M. J. E. & White, G. F. (1996). A ^{13}C NMR study of the mechanism of bacterial metabolism of monomethyl sulfate. *Eur. J. Biochem.* **236**, 620–625.

Horoaki, H., Klaus, W. & Senn, H. (1996). Determination of the solution structure of the SH3 domain of human p56 Lck tyrosine kinase. *J. biomol. NMR* **8**, 105–122.

Hoffman, R. E., Weitz, A. & Rabinovitz, M. (1993). Improved pulse program for long-range heteronuclear correlation. *J. magn. Reson. A* **102**, 1–7.

Hoheisel, J. D. (1997). Oligomer-chip technology. *Trends Biotechnol.* **15**, 465–469.

Holms, W. H. (1986). The central metabolic pathways of *Escherichia coli*: relationship between flux and control at a branch point, efficiency of conversion to biomass, and excretion of acetate. In *Curr. top. cell. Reg.* **28**, pp. 69–105. New York: Academic Press.

Holms, W. H. (1996). Flux analysis and control of the central metabolic pathways in Escherichia coli. *FEMS Microbiol. Rev.* **19**, 85–116.

Homans, S. W. (1989). *A Dictionary of Concepts in NMR*. Oxford: Clarendon Press.

Horak, R. M., Steyn, P. S. & Vleggar, R. (1985). Carbon-carbon coupling constants derived from biosynthetic studies. *Magn. Reson. Chem.* **23**, 995–1039.

Hrazdina, G. & Jensen, R. A. (1992). Spatial organization of enzymes in plant metabolic pathways. *Annu. Rev. Plant Physiol. Plant mol. Biol.* **43**, 241–267.

Hull, W. E. (1987). *Two-dimensional NMR spectroscopy. Applications for Chemists and Biochemists*. (ed. W. R. Croasmun & R. M. K. Carlson) New York: VCH.

Hurd, R. E. & John, B. K. (1991). Three-dimensional gradient enhanced relay-edited proton spectroscopy. GREP-HMQC-COSY. *J. magn. Reson.* **92**, 658–668.

Inbar, L. & LaPidot, A. (1991). ^{13}C nuclear magnetic resonance and gas chromatography-mass spectrometry studies of carbon metabolism in the actinomycin D producer *Streptomyces parvulus* by use of ^{13}C-labelled precursors. *J. Bacteriol.* **173**, 7790–7801.

Ishino, S., Kuga, T., Yamaguchi, K. Shirahata, K. & Araki, T. (1986). ^{13}C NMR studies of histidine fermentation with a *Corynebacterium glutamicum* mutant. *Agric. biol. Chem.* **50**, 307–310.

Iupac-Iub Commission on Biochemical Nomenclature (1970). Abbreviations and symbols for the description of the conformation of polypeptide chains. *Biochemistry* **9**, 3471–3479.

Jacob, G. S., Garbow, J. R. & Schaefer, J. (1986). Direct measurement of poly(β-hydroxybutyrate) in a pseudomonad by solid-state ^{13}C NMR. *J. biol. Chem.* **261**, 16785–16787.

Jacob, G. S., Schaefer, J., Garbow, J. R. & Stejskal, E. O. (1987). Solid-state studies of *Klebsiella pneumoniae* grown under nitrogen-fixing conditions. *J. biol. Chem.* **262**, 254–259.

Jacobsen, J. R., Hutchinson, C. R., Cane, D. E. & Koshla, C. (1997). Precursor-directed biosynthesis of erythromycin analogs by an engineered polyketide synthase. *Science* **277**, 367–369.

James, P. (1997). Protein identification in the post-genome era: the rapid rise of proteomics. *Quart. Rev. Biophys.*, **30**, 279–331.

Jans, A. W. & Willem, R. (1988). ^{13}C-NMR study of glycerol metabolism in rabbit renal cells of proximal convoluted tubules. *Eur. J. Biochem.* **174**, 67–73.

Jans, A. W. H., Winkel, C., Buitenhuis, L. & Lugtenburg, J. (1989). ^{13}C-nmr study of citrate metabolism in rabbit renal proximal-tubule cells. *Biochem J.* **257**, 425–429.

Jeffrey, F. M. H., Rajagopal, A., Malloy, C. R. & Sherry, A. D. (1991). ^{13}C-NMR: a simple yet comprehensive method for analysis of intermediary metabolism. *Trends biochem. Sci.* **16**, 5–10.

Jeong, J. W., Snay, J. & Ataai, M. M. (1990). A mathematical model for examining growth and sporulation processes of *Bacillus subtilis*. *Biotechnol. Bioeng.* **35**, 160–184.

Jerschow, A. & Müller, N. (1996). 3D Diffusion-ordered TOCSY for slowly diffusing molecules. *J. magn. Reson. A* **123**, 222–225.

Jerschow, A. & Müller, N. (1997). Suppression of convection artifacts in stimulated-echo diffusion experiments. Double-stimulated-echo experiments. *J. magn. Reson.* **125**, 372–375.

Jin, S., Ye, K. & Shimizu, K. (1997). Metabolic flux distribution in recombinant *Saccharomyces cerevisiae* during foreign protein production. *J. Biotechnol.* **54**, 161–174.

Jones, D. N. M. & Sanders, J. K. M. (1989). Biosynthetic studies using ^{13}C-COSY: the *Klebsiella K3* serotype polysaccharide. *J. Am. chem. Soc.* **111**, 5132–5137.

Jones, J. G., Sherry, A. D., Jeffrey, F. M. H., Storey, C. J. & Malloy, C. R. (1993). Sources of acetyl-CoA entering the tricarboxylic acid cycle as determined by analysis of succinate ^{13}C isotopomers. *Biochemistry* **32**, 12240–12244.

Jones, M. N. (ed.) (1979). *Biochemical Thermodynamics*. Amsterdam: Elsevier.

Jørgensen, H., Nielsen, J., Villadsen, J. & Møllgaard, H. (1995). Metabolic flux distributions in *Penicillium chrysogenum* during fed-batch cultivations. *Biotechnol. Bioeng.* **46**, 117–131.

Kacser, H. & Burns, J. A. (1973). The control of flux. *Symp. Soc. exp. Biol.* **27**, 65–104.
Kacser, H. & Burns, J. A. (1979). Molecular democracy: who shares the control? *Biochem. Soc. Trans.* **7**, 1149–1160.
Kalderon, B., Gopher, A. & LaPidot, A. (1987). A quantitative analysis of the metabolic pathways of hepatic glucose synthesis *in vivo* with ^{13}C-labelled substrates. *FEBS Lett.* **213**, 209–214.
Kalderon, B., Korman, S. H., Gutman, A. & LaPidot, A. (1989). Estimation of glucose carbon recycling in children with glycogen storage disease: a ^{13}C NMR study using [U-^{13}C]glucose. *Proc. natn. Acad. Sci. U.S.A.* **86**, 4690–4694.
Kalderon, R., LaPidot, A., Korman, S. H. & Gutman, A. (1988). Glucose recycling and production in children with glycogen storage disease type I, studied by gas chromatography/mass spectrometry and (U-^{13}C)-glucose. *Biomed. environ. Mass Spectrom.* **16**, 305–308.
Katz, J., Wals, P. A. & Lee, W. N. P. (1991). Determination of pathways of glycogen synthesis and the dilution of the three-carbon pool with [U-^{13}C] glucose. *Proc. natn. Acad. Sci. U.S.A.* 88, 2103–2107.
Katz, J., Wals, P., Lee, W. N. P. (1993). Isotopomer studies of gluconeogenesis and the Krebs cycle with ^{13}C-labelled lactate. *J. biol. Chem.* **34**, 25509–25521.
Kawanaka, M., Matsushita, K., Kato, K. & Ohsaka, A. (1989). Glucose metabolism of adult Schistosoma japonicum as revealed by nuclear magnetic resonance spectroscopy with D-[$^{13}C_6$]-glucose. *Physiol. Chem. Phys. Med. NMR* **21**, 5–12.
Kay, L. E. (1995). Field gradient techniques in NMR spectroscopy. *Curr. Opin. struc. Biol.* **5**, 674–681.
Kay, L. E., Ikura, M. & Bax, A. (1990). Proton–proton correlation *via* carbon–carbon couplings: a three-dimensional NMR approach for the assignment of aliphatic resonances in proteins labelled with carbon-13. *J. Am. chem. Soc.* **112**, 888–889.
Kay, L. E., Keifer, P. & Saarinen, T. (1992). Pure absorption gradient enhanced heteronuclear single quantum correlation spectroscopy with improved sensitivity. *J. Am. chem. Soc.* **114**, 10663–10665.
Keeler, J., Clowes, R. T., Davis, A. L. & Laue, E. D. (1994). Pulsed-field gradients: theory and practice. *Meth. Enzymol.* **239**, 145–207.
Kellher, J. K. & Masterson, T. M. (1992). Model equations for condensation biosynthesis using stable isotopes and radioisotopes. *Am. J. Physiol.* **262**, E118–E125.
Kengen, S. W. M., De Bok, F. A. M., Van Loo, N., Dijkema, C., Stams, A. J. M. & De Vos, W. M. (1994). Evidence for the operation of a novel Emden–Meyerhof pathway that involves ADP-dependent kinases during sugar fermentation by *Pyrococcus furiosus*. *J. biol. Chem.* **269**, 17537–17541.
Kessler, H., Gehrke, M. & Griesinger, C. (1988). Two-dimensional NMR spectroscopy: background and overview of the experiments. *Angew. Chem. Int. Ed. Engl.* **27**, 490–536.
Kholodenko, B. N., Westerhoff, H. V. & Cascante, M. (1996). Effect of channeling on the concentration of bulk-phase intermediates as cytosolic proteins become more concentrated. *Biochem. J.* **313**, 921–926.
Kim, Y. W., Earl, W. L. & Norberg, R. E. (1995). Cryogenic probe with low-loss transmission line for nuclear magnetic resonance. *J. magn. Reson.* A **116**, 139–144.
Kingsley-Hickman, P. B., Ross, B. D. & Krick, T. (1990). Hexose monophosphate shunt measurement in cultured cells with [1−^{13}C] glucose: correction for endogenous carbon sources using [6−^{13}C] glucose. *Anal. Biochem.* **185**, 235–237.

Koch, J., Eisenreich, W., Bacher, A. & Fuchs, G. (1993). Products of enzymatic reduction of benzoyl-CoA, a key reaction in aromatic metabolism. *Eur. J. Biochem.* **211**, 649–661.

Kogler, H., Sørensen, O. W., Bodenhausen, G. & Ernst, R. R. (1983). Low-pass J filters. Suppression of neighbour peaks in heteronuclear relayed correlation spectroscopy. *J. magn. Reson.* **55**, 157–163.

Kostanos, E. K., Woldman, Y. Y. & Appling, D. R. (1997). Role of mitochondrial and cytoplasmic serine hydroxymethyltransferase isozymes in *de novo* purine synthesis in *Saccharomyces cerevisiae*. *Biochemistry* **36**, 14956–14964.

Kozinski, W. & Nanz, D. (1996). Sensitive measurement and unambiguous assignment of long-range $^{13}C,^{13}C$ coupling constants at natural isotope abundance. *J. magn. Reson. A* **122**, 245–247.

Krämer, R. (1996). Analyis and modeling of substrate uptake and product release by procaryotic and eucaryotic cells. In *Adv. Biochem. Eng. Biotechnol.* **54** (ed. T. Scheper), pp. 31–74. Springer: New York.

Krivdin, L. B. & Kalabin, G. A. (1989). Structural applications of one-bond carbon–carbon coupling constants. *Prog. NMR Spectrosc.* **21**, 293–443.

Krivdin, L. B. & Della, E. W. (1991). Spin-spin coupling constants between carbons separated by more than one bond. *Prog. NMR Spectrosc.* **23**, 301–610.

Künnecke, B. (1995). Application of ^{13}C NMR spectroscopy to metabolic studies on animals. In *Carbon-13 NMR Spectroscopy of Biological Systems* (ed. N. Beckmann), pp. 159–267. San Diego: Academic Press.

Künnecke, B. & Seelig, J. (1991). Glycogen metabolism as detected by *in vivo* and *in vitro* ^{13}C-NMR spectroscopy using [1,2-$^{13}C_2$]glucose as substrate. *Biochim. Biophys. Acta* **1095**, 103–113.

Kunst, F. et al. & Danchin, A. (1997). The complete genome sequence of the gram-negative bacterium *Bacillus subtilis*. *Nature* **390**, 249–256.

Lambert, J. & Buddrus, J. (1993). Sensitivity enhancement of two-dimensional $^{13}C,^{13}C$-INADEQUATE spectroscopy by considering symmetry and isotopic shifts. *J. magn. Reson. A* **120**, 307–312.

Lanks, K. W. (1987). End products of glucose and glutamine metabolism by L929 cells. *J. biol. Chem.* **262**, 10093–10097.

Lapidot, A. & Gopher, A. (1994). Cerebral metabolic compartmentation. *J. biol. Chem.* **269**, 27196–27208.

Lapidot, A. & Gopher, A. (1997). Quantitation of metabolic compartmentation in hyperammonemic brain by natural abundance ^{13}C-NMR detection of ^{13}C–^{15}N coupling patterns and isotopic shifts. *Eur. J. Biochem.* **243**, 597–604.

Lee, W-N. P. (1993). Analysis of tricarboxylic acid cycle using mass spectrometry. *J. biol. Chem.* **268**, 25522–25526.

Lerner, L. & Bax, A. (1986). Sensitivity-enhanced two-dimensional heteronuclear relayed coherence transfer NMR spectroscopy. *J. magn. Reson.* **69**, 375–380.

Lesage, A., Auger, C., Caldarelli, S. & Emsley, L. (1997). Determination of through-bond carbon–carbon connectivities in solid-state NMR using the INADEQUATE experiment. *J. Am. chem. Soc.* **119**, 7867–7868.

Lessard, P. (1996). Metabolic engineering: the concept coalesces. *Nature Biotechnol.* **14**, 1654–1655.

Liao, J. C. & Lightfoot, E. N. (1988). Characteristic reaction paths of biochemical reaction systems with time scale preparation. *Biotechnol. Bioeng.* **31**, 847–854.

Liu, M., Farrant, R. D., Nicholson, J. K. & Lindon, J. C. (1995). Selective detection

of ^{1}H NMR resonances of $^{13}CH_n$ groups using two-dimensional maximum-quantum correlation spectroscopy. *J. magn. Reson. A* **112**, 208–219.

Liu, M., Mao, X., Ye, C., Nicholson, J. K. & Lindon, J. C. (1997). Three-dimensional maximum-quantum correlation HMQC NMR spectroscopy (3D MAXY-HMQC). *J. magn. Reson.* **129**, 67–73.

Lockhart, D. J., Dong, H., Byrne, M. C., Follettie, M. T., Gallo, M. V., Chee, M. S., Mittmann, M., Wang, C., Kobayashi, M., Horton, H. & Brown, E. L. (1996). Expression monitoring by hydridization to high-density oligonucleotide arrays. *Nature Biotechnol.* **14**, 1675–1680.

London, R. E. (1988). ^{13}C labelling in studies of metabolic regulation. *Prog. NMR Spectrosc.* **20**, 337–383.

London, R. E., Kollman, V. H. & Matwiyoff, N. A. (1975). The quantitative analysis of carbon–carbon coupling in the ^{13}C nuclear magnetic resonance spectra of molecules biosynthesized from ^{13}C enriched precursors. *J. Am. chem. Soc.* **97**, 3565–3573.

London, R. E. & Walker, T. E. (1985). Biosynthesis of trehalose by *Brevibacterium flavum*: use of long range ^{13}C–^{13}C coupling data to characterize triose phosphate isomerase activity. Biosci. Rep. **5**, 509–515.

London, R. E., Walker, T. E., Kollman, V. H. & Matwiyoff, N. A. (1977). Proton relaxation in ^{13}C-enriched molecules; ^{13}C T1 and NOE data from proton magnetic resonance measurements. *J. magn. Reson.* **26**, 213–218.

Lundberg, P., Harmsen, E., Ho, C. & Vogel, H. J. (1990). Nuclear magnetic resonance studies of cellular metabolism. *Anal. Biochem.* **191**, 193–222.

Lutz, N. W., Yahi, N., Fantini, J. & Cozzone, P. J. (1996). A new method for the determination of specific ^{13}C enrichments in phosphorylated [1-^{13}C] glucose metabolites. ^{13}C-coupled, ^{1}H-decoupled ^{31}P-NMR spectroscopy of tissue perchloric extracts. *Eur. J. Biochem.* **238**, 470–475.

Mackin, G. & Shaka, A. J. (1996). Phase-sensitive two-dimensional HMQC and HMQC-TOCSY spectra obtained using double pulsed-field-gradient spin echoes. *J. magn. Reson. A* **118**, 247–255.

Magnusson, I., Schumann, W. C., Bartsch, G. E., Chandramouli, V., Kumaran, K., Wahren, J. & Landau, B. R. (1991). Noninvasive tracing of Krebs cycle metabolism in liver. *J. biol. Chem.* **266**, 6975–6984.

Majewski, R. A. & Domach, M. M. (1990). Simple constrained-optimization view of acetate overflow in *E. coli*. *Biotechnol. Bioeng.* **35**, 732–738,

Malloy, C. R., Sherry, A. D. & Jeffrey, F. M. H. (1988). Evaluation of carbon flux and substrate selection through alternate pathways involving the citric acid cycle of the heart by ^{13}C NMR spectroscopy. *J. biol. Chem.* **263**, 6964–6971.

Malloy, C. R., Sherry, A. D. & Jeffrey, F. M. H. (1990) Analysis of tricarboxylic acid cycle of the heart using ^{13}C isotope isomers. *Am. J. Physiol.* **259**, H987–H995.

Mancuso, A., Sharfstein, S. T., Tucker, S. N., Clark, D. S. & Blanch, H. W. (1994). Examination of primary metabolic pathways in a murine hydridoma with carbon-13 nuclear magnetic resonance spectroscopy. *Biotechnol. Bioeng.* **44**, 563–585.

Marx, A., De Graaf, A. A., Wiechert, W., Eggeling, L. & Sahm, H. (1996). Determination of fluxes in central metabolism of *Corynebacterium glutamicum* by NMR spectroscopy combined with metabolic balancing. *Biotechnol. Bioeng.* **49**, 111–129.

Mattila, S., Koskinen, A. M. P. & Otting, G. (1995). Long-range HSQC with spin-lock purge pulses for the observation of heteronuclear correlations with ^{1}H detection and low t_1 noise. *J. magn. Reson. B* **109**, 326–328.

Mavrovouniotis, M. L. (1990). Group contributions for estimating standard Gibbs energies of formation of biochemical compounds in aqueous solution. *Biotechnol. Bioeng.* **36**, 1070–1082.

McInnes, A. G., Smith, D. G., Walter, J. A., Vining, L. C. & Wright, J. L. C. (1974). New techniques in biosynthetic studies using ^{13}C nuclear magnetic resonance spectroscopy. The biosynthesis of tenellin enriched from singly and doubly labelled precursors. *J. chem. Soc. chem. Commun.*, 282–284.

McDowell, L. M., Cohen, E. R. & Schaefer, J. (1993). Two-dimensional, rotational-echo double-resonance NMR of cell culture metabolism. *J. biol. Chem.* **268**, 20768–20771.

McDowell, L. M. & Schaefer, J. (1996). High-resolution NMR of biological solids. *Curr. Opin. struc. Biol.* **6**, 624–629.

McLafferty, F. W. & Turecek, F. (1993). *Interpretation of Mass Spectra*. Mill Valley: University Science Books.

Meissner, A., Duus, J. Ø. & Sørensen, O. W. (1997a). Spin-state selective excitation. Application for E. COSY-type measurement of J_{HH}coupling constants. *J. magn. Reson.* **124**, 245–249.

Meissner, A., Moskau, D., Nielsen, N. C. & Sørensen, O. W. (1997b). Proton-detected ^{13}C–^{13}C double-quantum coherence. *J. magn. Reson.* **124**, 245–249.

Mendz, G. L., Ball, G. E. & Meek, D. J. (1997). Pyruvate metabolism in *Campylobacter* spp. *Biochim. Biophys. Acta* **1334**, 291–302.

Mitschang, L., Ponstingl, H., Grindrod, D. & Oschkinat, H. (1995). Geometrical representation of coherence transfer selection by pulsed field gradients in high-resolution nuclear magnetic resonance. *J. Chem. Phys.* **102**, 3089–3098.

Morbach, S., Kelle, R., Winkels, S., Sahm, H. & Eggeling, L. (1996). Engineering the homoserine dehydrogenase and threonine dehydratase control points to analyse flux towards L-isoleucine in *Corynebacterium glutamicum*. *Appl. Microbiol. Biotechnol.* **45**, 612–620.

Moreland, C. G. & Carroll, F. I. (1974). ^{13}C–^{13}C dipolar relaxation as a relaxation mechanism. *J. magn. Reson.* 15, 596–599.

Morris, K. F. & Johnson, C. S. (1992). Diffusion-ordered two-dimensional nuclear magnetic resonance spectroscopy. *J. Am. chem. Soc.* **114**, 3139–3141.

Morris, K. F., Stilbs, P. & Johnson, C. S. (1994). Analysis of mixtures based on molecular size and hydrophobicity by means of diffusion-ordered 2D NMR. *Anal. Chem.* **66**, 211–215.

Müller, L. (1979). Sensitivity enhanced detection of weak nuclei using heteronuclear multiple quantum coherence. *J. Am. chem. Soc.* **101**, 4481–4484.

Nakazawa, T., Sengstschmid, H. & Freeman, R. (1996). Enhancement of INADEQUATE spectra according to symmetry criteria. *J. magn. Reson. A* **120**, 269–273.

Neese, R. A., Schwarz, J. -M., Faix, D., Turner, S., Letscher, A. Vu, D. & Hellerstein, M. K. (1995). Gluconeogenesis and intrahepatic triose phosphate flux in response to fasting or substrate loads. *J. biol. Chem.* **270**, 14452–14463.

Neidhardt, F. C. (1987). Chemical composition of *Escherichia coli*. In *Escherichia coli* and *Salmonella typhimurium*, vol. 1. (ed. F. C. Neidhardt), pp. 3–6. Washington: American Society for Microbiology.

Neidhardt, F. C., Curtiss, R., Ingraham, J. L., Liu, E. C. C., Low, K. B., Magasamik, B., Reznikoff, W. G., Riley, M., Schaechter, M. & Umbarger, H. E.

(eds.) (1996). *Escherichia coli* and *Salmonella typhimurium*. 2nd edition. Washington: American Society for Microbiology.

Neri, D., Szyperski, T., Otting, G., Senn, H. & Wüthrich, K. (1989). Stereospecific nuclear magnetic resonance assignments of the methyl groups of valine and leucine in the DNA-binding domain of the 434 repressor by biosynthetically directed fractional ^{13}C labelling. *Biochemistry* **28**. 7510–7616.

Newholme, E. A., Crabtree, B. & Ardawi, M. S. M. (1985). The role of high rates of glycolysis and glutamine utilization in rapidly dividing cells. *Biosci. Rep.* **5**, 393–400.

Nicholls, D. G. & S. J. Ferguson (1992). *Bioenergetics 2*. New York: Academic Press.

Nielsen, N. C., Thøgersen, H. & Sørensen, O. W. (1995). Doubling the sensitivity of INADEQUATE for tracing out the carbon skeleton of molecules by NMR. *J. Am. chem. Soc.* **117**, 11365–11366.

Nieto, R., Cruz, F., Tejedor, J. M., Barroso, G. & Cerdan, S. (1992). Origin of the ammonia used for mitochondrial citrulline synthesis as revealed by ^{13}C–^{15}N spin coupling patterns observed by ^{13}C NMR. Biochimie **74**, 903–911.

Ogino, T., Garner, C., Markley, J. & Hermann, K. M. (1982). Biosynthesis of aromatic compounds: ^{13}C NMR spectroscopy of whole *Escherichia coli* cells. *Proc. natn. Acad. Sci* **79**, 5828–5832.

Otting, G. & Wüthrich, K. (1988). Efficient purging scheme for proton-detected heteronuclear two-dimensional NMR. *J. magn. Reson.* **76**, 569–574.

Ovådi, J. & Srere, P. A. (1992). Channel your energies. *Trends biochem. Sci.* **17**, 445–447.

Pahl-Wostl, C. & Seelig, J. (1986). Metabolic pathways for ketone body production. ^{13}C NMR spectroscopy of rat liver using ^{13}C-multilabelled fatty acids. *Biochemistry* **25**, 6799–6807.

Palmer, A. G., Cavanagh, J. Wright, P. E. & Rance, M. (1991). Sensitivity improvement in proton-detected two-dimensional heteronuclear correlation NMR spectroscopy. *J. magn. Reson.* **93**, 151–170.

Palsson, B. O. (1997). What lies beyond bioinformatics. *Nature Biotechnol.* **15**, 3–4.

Papoutsakis, E. T. (1984). Equations and calculations for fermentations of butyric acid bacteria. *Biotechnol. Bioeng.* **26**, 174–187.

Parella, T., Sánchez-Ferrando, F. & Virgili, A. (1997). Improved sensitivity in gradient-based and 2D multiplicity-edited HSQC experiments. *J. magn. Reson.* **126**, 274–277.

Park, S. S., Ryu, C. J., Gripon, P., Guguen-Guillouzo, C. & Hong, H. J. (1996). Generation and characterization of a humanized antibody with specificity for preS2 surface antigen of hepatitis B virus. *Hybridoma* **15**, 435–441.

Park, S. M., Shaw-Reid, C., Sinskey, A. J. & Stephanopoulos, G. (1997a). Elucidation of anaplerotic pathways in *Corynebacterium glutamicum* via ^{13}C-NMR spectroscopy and GC-MS. *Appl. Microbiol. Biotechnol.* **47**, 430–440.

Park, S. M., Sinskey, A. J. & Stephanopoulos, G. (1997b). Metabolic and physiological studies of *Corynebacterium glutamicum* mutants. *Biotechnol. Bioeng.* **55**, 864–879.

Parker, R. S., Brenna, J. T., Swanson, J. E., Goodman, K. J. & Marmor, B. (1997). Assessing metabolism of β-[^{13}C] carotene using high precision isotope ratio mass spectrometry. *Meth. Emzymol.* **282**, 131–140.

Pasternack, L. B., Laude, D. A. & Appling, D. R. (1994). ^{13}C NMR analysis of intercompartmental flow of one-carbon units to choline and purines in *Saccharomyces cerevisiae*. *Biochemistry* **33**, 74–82.

Pasternack, L. B., Littlepage, L. E., Laude, D. A. & Appling, D. R. (1996). ^{13}C NMR analysis of the use of alternative donors to the tetrahydrofolate-dependent one-carbon pools in *Saccharomyces cerevisiae*. *Arch. Biochem. Biophys.* **326**, 158–165.

Patniak, R., Roof, W. D., Young, R. F. & Liao, J. C. (1992). Stimulation of glucose catabolism in *Escherichia coli* by a potential futile cycle. *J. Bacteriol.* **174**, 7527–7532.

Pennisi, E. (1996). From genes to genome biology. *Science* **272**, 1736–1737.

Perkins, J. B., Pero, J. G. & Sloma, A. (1991). Riboflavin overproducing strains of bacteria. *Europ. Pat. Appl.* o 405 370 A1.

Perrin, A., Gout, E., Chambaz, E. M. & Defaye(1994). Metabolism of malate in bovine adrenocortical mitochondria studied by ^{13}C-NMR spectroscopy. *Eur. J. Biochem.* **223**, 51–59.

Pickett, M. W., Williamson, M. P. & Kelly, D. J. (1994). An enzyme and ^{13}C-NMR study of carbon metabolism in *heliobacteria*. *Photosyn. Res.* **41**, 75–88.

Pissarra, P. N. & Nielsen, J. (1997). Thermodynamics of metabolic pathways for penicillin production: analysis of thermodynamic feasibility and free energy changes during fed-batch cultivation. *Biotechnol. Prog.* **13**, 156–165.

Portais, J. -C., Portais, R., Schuster, R., Merle, M. & Canioni, P. (1993). Metabolic flux determination of C6 glioma cells using carbon-13 distribution upon [1-^{13}C] glucose incubation. *Eur. J. Biochem.* **217**, 457–468.

Pramanik, J. & Keasling, J. D. (1997). Stoichiometric model of *Escherichia coli* metabolism: incorporation of growth-rate dependent biomass composition and mechanistic energy requirements. *Biotechnol. Bioeng.* **56**, 398–421.

Pratum, T. K. & Moore, B. S. (1993). Inverse detection of ^{13}C multiple-quantum coherence for biosynthetic studies. *J. magn. Reson. B* **102**, 91–97.

Pratum, T. K. (1995). A proton-detected HMQC-INADEQUATE with a carbon–carbon display. *J. magn. Reson. A* **117**, 132–136.

Pratum, T. K. (1996). Comparison of a proton-detected-carbon-displayed HSQC-INADEQUATE with a carbon-detected INADEQUATE data on a natural product. *J. magn. Reson. A* **113**, 76–82.

Quant, P. A. (1993). Experimental application of top-down control analysis to metabolic systems. *Trends biochem. Sci.* **18**, 26–30.

Quistorff, B., Frye, J. S. & Bock, K. (1993). Methods for liquid- and solid-state CP-MAS NMR spectroscopy of untreated tissue biopsies. *Anal. Biochem.* **213**, 68–74.

Reich, J. G. & Sel'kov, E. E. (1981). *Energy Metabolism of the Cell*. New York: Academic Press.

Reif, B., Köck, M., Kerssebaum, R., Kang, H., Fenical, W. & Griesinger, C. (1996). ADEQUATE, a new set of experiments to determine the constitution of small molecules at natural abundance. *J. magn. Reson.* **A 118**, 282–285.

Rinehart, K. L., Potgieter, M. & Wright, D. A. (1982). Use of D-[$^{13}C_6$] glucose with ^{13}C-depleted glucose and homonuclear ^{13}C decoupling to identify the labelling pattern by this precursor of the '*m*-C_7N' unit of geldanamycin. *J. Am. chem. Soc.* **104**, 2649–2652.

Robitaille, P. L., Rath, D., Abduljalil, A. M., O'Donnell, J. M., Jiang, Z., Zhang, H. & Hamlin, R. L. (1993). Dynamic ^{13}C NMR analysis of oxidative metabolism in the *in vivo* canine myocardium. *J. biol. Chem.* **268**, 26296–26301.

Rognstad, R. (1995). Models of the liver pentose cycle. *J. theor. Biol.* **173**, 195–206.

Rollin, C., Morgant, V., Guyonyarch, A. & Guerquin-Kern, J.-L. (1995). ^{13}C-NMR studies of *Corynebacterium melassecola* metabolite pathways. *Eur. J. Biochem.* **227**, 488–493.

Rosenblatt, J., Chinkes, D., Wolfe, M. & Wolfe, R. R. (1992). Stable isotope tracer analysis by GC-MS, including quantification of isotopomer effects. *Am. J. Physiol.* **263**, E584–E596.

Ross, A., Czisch, M., Cieslar, C. & Holak, T. A. (1993). Efficient methods for obtaining phase-sensitive gradient-enhanced HMQC spectra. *J. biomol. NMR* **3**, 215–224.

Ross, B. D., Kingsley, P. B. & Ben-Yoseph, O. (1994). Measurement of the pentose phosphate-pathway activity in a single incubation with [1,6-$^{13}C_2$, 6,6-$^{2}H_2$]glucose. *Biochem. J.* **302**, 31–38.

Rowen, L., Mahairas, G. & Hood, L. (1997). Sequencing the human genome. *Science* **278**, 605–607.

Saito, T. & Rinaldi, P. L. (1996). An improved 3D ^{1}H-detected PFG ^{13}C–^{13}C correlation experiment (PFG-HCCH). *J. magn. Reson.* **A 118**, 136–139.

Santoro, J. & King, G. C. (1992). A constant-time Overbodenhausen experiment for inverse correlatin of isotopically enriched species. *J. magn. Reson.* **97**, 202–207.

Sasajima, K.-I. & Yoneda, M. (1984). Production of pentoses by micro-organisms. *Biotechnol. genet. Eng. Rev.* **2**, 175–213.

Sasikala, C. & Ramana, C. V. (1995). Biotechnological potentials of anoxygenic phototrophic bacteria. II. Biopolymers, biopesticides, biofuel, and biofertilizer. *Adv. appl. Microbiol.* **41**, 227–278.

Sauer, U., Cameron, D. C. & Bailey, J. E. (1998). Metabolic capacities of *Bacillus subtilis* for the production of purine nucleosides, riboflavin, and folic acid. *Biotechnol. Bioeng.*, in press.

Sauer. U., Hatzimanikatis, V., Bailey, J. E., Hochuli, M., Szyperski, T. & Wüthrich, K. (1997). Metabolic fluxes in riboflavin-producing *Bacillus subtilis*. *Nature Biotechnol.* **15**, 448–452.

Sauer, U., Hatzimanikatis, V., Hohmann, H.-P., Manneberg, M., Van Loon, A. P. G. M. & Bailey, J. E. (1996). Physiology and metabolic fluxes of wild-type and riboflavin-producing *Bacillus subtilis*. *Appl. environ. Microbiol.* **62**, 3687–3696.

Savageau, M. A. (1969). Biochemical systems analysis. Parts I & II. *J. theor. Biol.* **25**, 365–379.

Savageau, M. A. (1970). Biochemical systems analysis. Part III. *J. theor. Biol.* **26**, 215–226.

Savageau, M. A., Voit, E. O. & Irvine, D. H. (1987). Biochemical systems theory and metabolic control theory: 1. fundamental similarities and differences. *Math. Biosci.* **86**, 127–145.

Savinell, J. M. & Palsson, B. O. (1992). Optimal selection of metabolic fluxes for in vivo measurement. I. Development of mathematical models. *J. theor. Biol.* **155**, 201–214.

Schäefer, J. & Stejskal, E. O. (1976). Carbon-13 nuclear magnetic resonance of polymers spinning at the magic angle. *J. Am. chem. Soc.* **98**, 1031–1032.

Schäefer, J., McKay, R. A. & Stejskal, E. O. (1979). Double-cross-polarization NMR of solids. *J. magn. Reson.* **34**, 443–447.

Schäfer, S., Paalme, T., Vilu, R. & Fuchs, G. (1989). ^{13}C-NMR study of acetate assimilation in *Thermoproteus neutrophilus*. *Eur. J. Biochem.* **186**, 695–700.

Schleucher, J., Schwendinger, M., Sattler, M., Schmidt, P., Schedletzky, O., Glaser, S. J., Sørensen, O. W. & Griesinger, C. (1994). A general enhancement scheme in heteronuclear multidimensional NMR employing pulsed field gradients. *J. biomol. NMR* **4**, 301–306.

Schmidt, K. Carlsen, M., Nielsen, J. & Villadsen, J. (1997). Modeling isotopomer distributions in biochemical networks using isotopomer matrices. *Biotechnol. Bioeng.* **55**, 831–840.

Schrader, M. C., Eskey, C. J., Simplaceanu, V. & Ho, C. (1993). A carbon-13 nuclear magnetic resonance investigation associated with glucose metabolism in human erythrocytes. *Biochim. Biophys. Acta* **1182**, 162–178.

Schügerl, K. (ed.) (1991). *Biotechnology. Measuring, Modelling and Control*, vol 4. Weinheim: VCH.

Schuster, R., Holzhütter, H. & Schuster, S. (1992). Simplification of complex kinetic models used for the quantitative analysis of nuclear magnetic resonance and radioactive tracer. *J. chem. Soc. Faraday Trans.* **88**, 2837–2844.

Sel'kov, E. E. (1979). The oscillatory basis of cell energy metabolism. In *Pattern Formation by Dynamic Systems and Pattern Recognition* (ed. H. Haken), pp. 166–174. New York: Springer Verlag.

Senn, H., Weber, C., Köbel, H. & Traber, R. (1991). Selective ^{13}C-labelling of cyclosporin A. *Eur. J. Biochem.* **199**, 653–658.

Senn, H., Werner, B., Messerle, B. A., Weber, C., Traber, R. & Wüthrich, K. (1989). Stereospecific assignment of the methyl ^{1}H NMR lines of valine and leucine in polypeptides by nonrandom ^{13}C labelling. *FEBS Lett.* **249**, 113–118.

Seto, H., Sato, T. & Yonchara, H. (1973). Utilization of carbon-13 carbon-13 coupling in structural and biosynthetic studies. An alternate double labelling method. *J. Am. chem. Soc.* **95**, 8461–8462.

Shaka, A. J., Keeler, J. & Freeman, R. (1983). Evaluation of a new broadband decoupling sequence: WALTZ-16. *J. magn. Reson.* **53**, 313–340.

Sharfstein, S. T., Tucker, S. N., Mancuso, A., Blanch, H. W. & Clark, D. S. (1994). Quantitative *in vivo* nuclear magnetic resonance studies of hybridoma metabolism. *Biotechnol. Bioeng.* **43**, 1059–1074.

Sherry, A. D., Sumegi, B., Miller, B., Cottam, G. L., Gavva, S., Jones, J. G. & Malloy, C. R. (1994). Orientation-conserved transfer of symmetric Krebs cycle intermediates in mammalian tissue. *Biochemistry* **33**, 6268–6275.

Sherry, A. D. & Malloy, C. R. (1996). Isotopic methods for probing organization of cellular metabolism. *Cell biochem. Func.* **14**, 259–268.

Shulman, R. G. & Rothman, D. L. (1996). Enzymatic phosphorylation of muscle glycogen synthase: a mechanism for maintenance of metabolic homeostasis. *Proc. natn. Acad. Sci. U.S.A.* **93**, 7491–7495.

Sonenshein, A. L., Hoch, J. A. & Losick, R. (eds.) (1993). *Bacillus subtilis*. Washington: American Society for Microbiology.

Sonnewald, U., Westergaard, N., Petersen, S. B., Unsgard, G. & Schousboe(1993). Metabolism of [U-^{13}C] glutamate in astrocytes studied by ^{13}C NMR spectroscopy: incorporation of more label into lactate than into glutamine demonstrates the importance of the tricarboxylic acid cycle. *J. Neurochem.* **61**, 1179–1182.

Sonntag, K., Eggeling, L., De Graaf, A. A. & Sahm, H. (1993). Flux partitioning in the split pathway of lysine synthesis in *Corynebacterium glutamicum*. *Eur. J. Biochem.* **213**, 1325–1331.

Spraul, M., Hofmann, M., Dvortsak, P., Nicholson, J. K. & Wilson, I. D. (1993). High-performance liquid chromatography coupled to high-field proton nuclear magnetic resonance spectroscopy: application to the urinary metabolites of ibuprofen. *Anal. Chem.* **65**, 327–330.

Stejskal, E. O. & Memory, J. D. (1994). *High Resolution NMR in the Solid State. Fundamentals of CP/MAS*. New York: Oxford University Press.

Stephanopoulos, G. & Sinskey, A. J. (1993). Metabolic engineering – methodologies and future prospects. *Trends Biotechnol.* **11**, 392–396.

Stephanopoulos, G. & Yallino, J. J. (1991). Network rigidity and metabolic engineering in metabolite overproduction. *Science* **252**, 1675–1681.

Stevenson, S. & Dorn, H. C. (1994). ^{13}C dynamic nuclear polarization: a detector for continuous-flow, on-line chromatography. *Anal. Chem.* **66**, 2993–2999.

Stoll, T. S., Muhlethaler, K., Von Stockar, U. & Marison, I. W. (1996). Systematic improvement of a chemically-defined protein-free medium for hybridoma growth and monoclonal antibody production. *J. Biotechnol.* **45**, 111–123.

Strohman, R. C. (1997). The coming Kuhnian revolution in biology. *Nature Biotechnol.* **15**, 194–200.

Stryer, L. (1994). *Biochemistry*. New York: Freeman.

Sun, B. -Q., Rienstra, C. M., Costa, P. R., Williamson, J. R. & Griffin, R. G. (1997). 3D ^{15}N-^{13}C-^{13}C chemical shift correlation spectroscopy in rotating solids. *J. Am. chem. Soc.* **119**, 8540–8546.

Szyperski, T. (1995). Biosynthetically directed fractional ^{13}C-labelling of proteinogenic amino acids. An efficient analytical tool to investigate intermediary metabolism. *Eur. J. Biochem.* **232**, 433–448.

Szyperski, T., Neri, D., Leiting, B., Otting, G. & Wüthrich, K. (1992). Support of ^{1}H-NMR assignments in proteins by biosynthetically directed fractional ^{13}C-labelling. *J. biomol. NMR.* **2**, 323–334.

Szyperski, T., Wider, G., Bushweller, J. H. & Wüthrich, K. (1993*a*). 3D ^{13}C–^{15}N heteronuclear two-spin coherence spectroscopy for polypeptide backbone assignments in ^{13}C–^{15}N-double labelled proteins. *J. biomol. NMR* **3**, 127–132.

Szyperski, T., Wider, G., Bushweller, J. H. & Wüthrich, K. (1993*b*). Reduced dimensionality in triple resonance experiments. *J. Am. chem. Soc.* **115**, 9307–9308.

Szyperski, T., Bailey, J. E. & Wüthrich, K. (1996*a*). Detecting and dissecting metabolic fluxes using biosynthetic fractional ^{13}C labelling and two-dimensional NMR spectroscopy. *Trends Biotechnol.* **14**, 453–459.

Szyperski, T., Braun, D., Banecki, B. & Wüthrich, K. (1996*b*). Useful information from axial magnetization in projected NMR experiments. *J. Am. chem. Soc.* **118**, 4147–4148.

Szyperski, T., Fernández, C. & Wüthrich, K. (1997). Two dimensional *ct*-HC(C)H-COSY for resonance assignments of smaller ^{13}C-labelled biomolecules. *J. magn. Reson.* **128**, 228–232.

Szyperski, T., Fernández, C., Ono, A., Kainosho, M. & Wüthrich, K. (1998*a*). Measurement of deoxyribose $^{3}J_{HH}$ scalar couplings reveals protein binding-induced changes in the sugar puckers of the DNA. *J. Am. chem. Soc.* **120**, 821–822.

Szyperski, T., Banecki, B., Braun, D. & Glaser, R. W. (1998*b*). Sequential resonance assignment of medium-sized $^{15}N/^{13}C$-labelled proteins with projected 4D triple resonance experiments. *J. biomol. NMR* **10**, in press.

Takahashi, S., Uchida, K., Nakagawa, A., Miyake, Y., Kainosho, M., Matsuzuki, K. & Omura, S. (1995). Biosynthesis of lactacystin. *J. Antibiotics* (*Tokyo*). **48**, 1015–1020.

Torres, A. M., Nakashima, T. T. & McClung, R. E. D. (1992). Improvement of INADEQUATE using compensated delays and pulses. *J. magn. Reson.* **99**, 99–117.

Torres, A. M., Nakashima, T. T. & McClung, R. E. D. (1993). J-compensated proton-detected heteronuclear shift-correlation experiments. *J. magn. Reson. A* **102**, 219–227.

Tran-Dinh, S., Hervé, M., Lebourguais, O., Jerome, M. & Wietzerbin, J. (1991). Effects of amphoterin B on the glucose metabolism in *Saccharomyces cerevisiae* cells. *Eur. J. Biochem.* **197**, 271–279.

Tsai, C. S., Ye, H. G. & Shi, J. L. (1995). Carbon-13 NMR studies and purification of gluconate pathway enzymes from *Schizosaccharomyces pombe*. *Arch. Biochem. Biophys.* **316**, 155–162.

Tsai, P., Hatzimanikatis, V. & Bailey, J. E. (1996). Effect of *Vitreoscilla* hemoglobin dosage on microaerobic *Escherichia coli* carbon and energy metabolism. *Biotechnol. Bioeng.* **49**, 139–150.

Tycko, R. & Dabbagh, G. (1990). Measurement of nuclear magnetic dipole-dipole couplings in magic-angle-spinning NMR. *Chem. Phys. Lett.* **173**, 461–465.

Ugurbil, K., Brown, T. R., Den Hollander, J. A., Glynn, P. & Shulman, R. G. (1978). High-resolution ^{13}C nuclear magnetic resonance studies of glucose metabolism in *Escherichia coli*. *Proc. natn. Acad. Sci. U.S.A.* **75**, 3742–3746.

Valentin, H. E. & Dennis, D. (1997). Production of poly(3-hydroxybutyrate-co-4-hydroxybutyrate) in recombinant *Escherichia coli* grown on glucose. *J. Biotechnol.* **58**, 33–38.

Vallino, J. J. & Stephanopoulos, G. (1990). Flux determination in cellular bioreaction networks: application to lysine fermentations. In *Frontiers in Bioprocessing* (eds S. K. Sikdar, M. Bier & P. Todd), pp. 205–219. Boca Raton: CRC press.

Vallino, J. J. & Stephanopoulos, G. (1993). Metabolic flux distribution *in Corynebacterium glutamicum* during growth and lysine overproduction. *Biotechnol. Bioeng.* **41**, 633–646.

Van Gulik, W. M. & Heijnen, J. J. (1995). A metabolic network stoichiometry analysis of microbial growth and product formation. *Biotechnol. Bioeng.* **48**, 681–698.

Varma, A., Boesch, B. W. & Palsson, B. O. (1993*a*). Biochemical production capabilities of *Escherichia coli*. *Biotechnol. Bioeng.* **42**, 59–73.

Varma, A., Boesch, B. W. & Palsson, B. O. (1993*b*). Stoichiometric interpretation of *Escherichia coli* glucose catabolism under various oxygenation rates. *Appl. environ. Microbiol.* **59**, 2465–2473.

Varma, A. & Palsson, B. O. (1993) Metabolic capabilities of *Escherichia coli*: I. synthesis of biosynthetic precursors and cofactors. *J. theor. Biol.* **165**, 477–502.

Varma, A. & Palsson, B. O. (1994) Metabolic flux balancing: basic concepts, scientific and practical use. *Bio/Technology* **12**, 994–998.

Yélot, C., Mixon, M. B., Teige, M. & Srere, P. A. (1997). Model of a quinary structure between Krebs TCA cycle enzymes: a model for the metabolon. *Biochemistry* **36**, 14271–14276.

Verhoff, F. H. & Spradlin, J. E. (1976). Mass and energy balance analysis of metabolic pathways applied to citric acid production by *Aspergillus niger*. *Biotechnol. Bioeng.* **18**, 425–432.

Volk, R. & Bacher, A. (1991). Biosynthesis of riboflavin. *J. biol. Chem.* **266**, 20610–20618.

Volschenk, H., Viljoen, M., Grobler, J., Petzold, B., Bauer, F., Subden, R. E., Young, R. A., Lonvaud, A., Dena Yrolles, M. & Van Vuuren, H. J. J. (1997). Engineering pathways for malate degradation in *Saccharomyces cerevisiae*. *Nature Biotechnol.* **15**, 253–257.

Vos, J.-M. H. (1997). The simplicity of complex MACs. *Nature Biotechnol.* **15**, 1257–1260.

Yuister, G. W. & Bax, A. (1992). Resolution enhancement and spectral editing of uniformly ^{13}C-enriched proteins by homonuclear broadband ^{13}C-decoupling. *J. magn. Reson.* **98**, 428–435.

Walker, T. E., Kollman, V. H., London, R. E. & Matwiyoff, N. A. (1982). ^{13}C nuclear magnetic resonance studies of the biosynthesis by *Microbacterium ammoniaphilum* of L-glutamate selectively enriched with carbon-13. *J. biol. Chem.* **257**, 1189–1195.

Walsh, K. & Koshland, D. E. (1984). Determination of flux through the branch point of two metabolic cycles. *J. biol. Chem.* **259**, 9646–9654.

Walsh, K. & Koshland, D. E. (1985). Branch point control by the phosphorylation state of isocitrate dehydrogenase. *J. biol. Chem.* **260**, 8430–8437.

Warshel, A. (1997). *Modelling Enzyme Reactions*. New York: Wiley.

Weigelt, J. & Otting, G. (1995*a*). ^{1}H-detected INEPT-INADEQUATE at natural ^{13}C abundance. *J. magn. Reson.* **A 113**, 128–130.

Weigelt, J. & Otting, G. (1995*b*). ^{13}C-relayed ^{13}C-HSQC at natural isotopic abundance. *J. magn. Reson. A* **116**, 133–134.

Werner, I., Bacher, A. & Eisenreich, W. (1997). Retrobiosynthetic NMR studies with ^{13}C-labelled glucose. Formation of gallic acid in plants and fungi. *J. biol. Chem.* **272**, 25474–25482.

Westerhoff, H. V. & Kell, D. B. (1996). What biotechnologists knew all along ...? *J. theor. Biol.* **182**, 411–420.

Weuster-Botz, D. & De Graaf, A. A. (1996). Reaction engineering methods to study intracellular metabolite concentrations. In *Adv. Biochem. Eng. Biotechnol.* **54** (ed. T. Scheper), pp. 75–108. New York: Springer.

Wider, G., Dötsch, V. & Wüthrich, K. (1994). Self-compensating pulsed field gradients for short recovery times. *J. magn. Reson. A* **108**, 255–258.

Wider, G. & Wüthrich, K. (1993). A simple experimental scheme using pulsed field gradients for coherence pathway rejection and solvent suppression in phase-sensitive heteronuclear correlation spectra. *J. magn. Reson. B* **102**, 239–241.

Wiechert, W. W. & De Graaf, A. A. (1996). *In vivo* stationary flux analysis by ^{13}C labelling experiments. In *Adv. Biochem. Eng. Biotechnol.* **54** (ed. T. Scheper), pp. 111–154. New York: Springer.

Wiechert, W. & De Graaf, A. A. (1997). Bidirectional reaction steps in metabolic networks: I. modeling and simulation of carbon isotope labelling experiments. *Biotechnol. Bioeng.* **55**, 118–135.

Wiechert, W., Siefke, C., De Graaf, A. A. & Marx, A. (1997). Bidirectional reaction steps in metabolic networks. II. flux estimation and statistical analysis. *Biotechnol. Bioeng.* **55**, 118–135.

Wilkens, M. R., Sanchez, J.-C., Gooley, A. A. Appel, R. D., Humphrey-Smith, I., Hochstrasser, D. F. & Williams, K. L. (1995). Progress with proteome projects: why all proteins expressed by a genome should be identified and how to do it. *Biotech. Gen. Eng. Rev.* **13**, 19–50.

Willker, W., Flögel, U. & Leibfritz, D. (1997). Ultra-high-resolved HSQC spectra of multiple-^{13}C-labelled biofluids. *J. magn. Reson.* **125**, 216–219.

Wolfe, R. R. (1992). *Radioactive and Stable Isotope Tracers*. New York: John Wiley.

Wu, D., Chen, A. & Johnson, C. S. (1995). An improved diffusion-ordered

spectroscopy experiment incorporating bipolar-gradient pulses. *J. magn. Reson. A* **115**, 260–264.

Wu, D., Chen, A. & Johnson, C. S. (1996*a*). Heteronuclear-detected diffusion-ordered NMR spectroscopy through coherence transfer. *J. magn. Reson. A* **123**, 215–218.

Wu, D., Chen, A. & Johnson, C. S. (1996*b*). Three-dimensional diffusion-ordered NMR spectroscopy: the homonuclear COSY-DOSY experiment. *J. magn. Reson. A* **121**, 88–91.

Wüthrich, K. (1976). *NMR in Biological Research*: *Peptides and Proteins*. Amsterdam: North Holland.

Wüthrich, K, Szyperski, T., Leiting, B. & Otting, G. (1992). Biosynthetic pathways of the common proteinogenic amino acids investigated by fractional ^{13}C labelling and NMR spectroscopy. In *Frontiers and New Horizons in Amino Acid Research* (ed. K. Takai), pp. 41–48. Amsterdam: Elsevier.

Yamaguchi, K., Ishino, S., Araki, K. & Shirahata, K. (1986). ^{13}C NMR studies of lysine fermentation with a *Corynebacterium glutamicum* mutant. *Agric. biol. Chem.* **50**, 2453–2459.

Yarmush, M. L. & Berthiaume, F. (1997). Metabolic engineering and human disease. *Nature Biotechnol.* **15**, 525–528.

Yu, L., Goldman, R., Sullivan, P., Walker, G. F. & Fesik, S. W. (1993). Heteronuclear NMR studies of ^{13}C-labelled yeast cell wall β-glucan oligosaccharides. *J. biomol. NMR* **3**, 429–441.

Zabriskie, D. W. (1996). Biochemical Engineering. *Cur. Opin. Biotechnol.* **7**, 187–189.

Zangger, K. & Sterk, H. (1996). ^{1}H-detected 2D J-resolved INEPT-INADEQUATE. *J. magn. Reson. A* **121**, 56–59.

Zerbe, O., Szyperski, T., Ottiger, M. & Wüthrich, K. (1996). Three-dimensional ^{1}H-TOCSY relayed ct-[^{13}C,^{1}H]-HMQC for aromatic spin system identification in uniformly ^{13}C-labelled proteins. *J. biomol. NMR* **7**, 99–106.

Zupke, C. & Stephanopoulos, G. (1994). Modeling of isotope distributions and intracellular fluxes in metabolic networks using atom mapping matrices. *Biotech. Prog.* **10**, 489–498.

Zupke, C. & Stephanopoulos, G. (1995). Intracellular flux analysis in hybridomas using mass balances and *in vitro* ^{13}C NMR. *Biotechnol. Bioeng.* **45**, 292–303.